# Function of the Zinc-Finger Repressor NLZ in the Developing Zebrafish Hindbrain: a Dissertation

# FUNCTION OF THE ZINC-FINGER REPRESSOR NLZ IN THE DEVELOPING ZEBRAFISH HINDBRAIN

A Dissertation Presented

By

**ALEXANDER PETER RUNKO**

Submitted to the Faculty of the
University of Massachusetts Graduate School of Biomedical Sciences, Worcester
in partial fulfillment of the requirements for the degree of

**DOCTOR OF PHILOSOPHY**

In

**BIOCHEMISTRY AND MOLECULAR PHARMACOLOGY**

OCTOBER 6, 2003

**DEVELOPMENTAL NEUROSCIENCE**

Parts of this dissertation have appeared in separate publications:

Runko, A.P., and Sagerström, C. G. (2003). Nlz belongs to a family of zinc-finger-containing repressors and controls segmental gene expression in the zebrafish hindbrain. *Dev Biol* **262,** 254-67.

Lane, M.E., Runko, A.P., Roy, N.M., and Sagerström, C.G. (2002). Dynamic expression and regulation by Fgf8 and Pou2 of the zebrafish LIM-only gene, *lmo4*. *Gene Expr Patterns* **2,** 207-11.

**FUNCTION OF THE ZINC-FINGER REPRESSOR NLZ IN THE DEVELOPING ZEBRAFISH HINDBRAIN**

A Dissertation Presented

By

**ALEXANDER PETER RUNKO**

Approved as to the style and content by:

**Dr. Kendall L. Knight, Ph.D., Chair of Committee**

**Dr. Stephen H. Devoto, Ph.D., Member of Committee**

**Dr. Y. Tony Ip, Ph.D., Member of Committee**

**Dr. Stephen N. Jones, Ph.D., Member of Committee**

**Dr. Kai Lin, Ph.D., Member of Committee**

**Dr. Charles G. Sagerstrom, Ph.D., Dissertation Mentor**

**Dr. Anthony Carruthers, Ph.D., Dean of the Graduate School of Biomedical Sciences**

**Department of Biochemistry and Molecular Pharmacology**

**October 6, 2003**

## ACKNOWLEDGMENTS

I would like to thank my graduate advisor Dr. Charles G. Sagerström for his reliable guidance and help throughout my thesis research. His support was key for the acceptance of my publications and successful completion of my thesis project.

I would also like to thank the members of my thesis committee: Dr. Kendall L. Knight, Dr. Stephen H. Devoto, Dr. Y. Tony Ip, Dr. Stephen N. Jones and Dr. Kai Lin for their helpful comments and suggestions.

I would like to thank all members of the Sagerström laboratory for their helpful discussions and collaborations that contributed to my graduate thesis work.

I would also like to thank my fellow colleagues and friends at the University of Massachusetts Graduate School, especially Madathia Sarkissian, for their support and camaraderie during my graduate school career.

Lastly, I would like to thank my parents, Milan and Dionora, my grandparents, Donato and Lucia, and especially my brother, Erik, for their unconditional support and encouragement that was vital for the successful completion of my graduate school career and thesis project.

## ABSTRACT

Generation of the primitive neuroectoderm into specialized brain subdivisions, such as the hindbrain primordium, involves the regulated coordination of complex morphogenetic and molecular mechanisms. These processes are evident in the segregation of the zebrafish hindbrain into seven distinct lineage-restricted compartments, termed rhombomeres (r), which are established by the interplay of several spatially-restricted expressed genes. These include transcription factors, members of specific signaling pathways and specialized molecules that mediate cell adhesion and identity. Despite their extensive characterization, it is evident that other genes are involved to mediate the proper specification and segregation of individual rhombomeres. One candidate that likely fits this role is related to the *no ocelli/l(2)35Ba* gene in *Drosophila*, termed *nlz* (*nocA*-like zinc-finger). Nlz-related proteins behave as transcriptional repressors and are related to the vertebrate Sp1-like family of transcription factors. *nlz* is dynamically expressed in the zebrafish hindbrain, residing in the caudal hindbrain at gastrula stages and rostrally expanding from presumptive r3/r4 boundary to encompass r3 and r2 at segmentation stages. Nlz localizes to the nucleus and associates with the co-repressors Groucho and histone deacetylases, suggesting that Nlz acts as a repressor. Consistent with this, misexpression of *nlz* into zebrafish embryos results in a loss of gene expression in the rostral hindbrain (r1-r3). Taken together, the findings in this thesis suggest that Nlz functions as a transcriptional repressor to control segmental gene expression in the rostral hindbrain.

## TABLE OF CONTENTS

## LIST OF TABLES

### Chapter I



### Chapter II

## LIST OF FIGURES

### INTRODUCTION



### CHAPTER I

**CHAPTER II**



**CONCLUSION**

## APPENDIX

# INTRODUCTION

Development of the vertebrate hindbrain is a highly coordinated process that utilizes a vast score of complex cellular and molecular mechanisms underlying the basic principles of morphogenesis. Events in the early differentiating embryo are organized and programmed to induce an undifferentiated group of cells into a presumptive hindbrain domain. Description of this progression is highlighted by the examination of a model vertebrate, the teleost zebrafish (*Danio rerio*) (Kimmel et al., 1995). Since zebrafish embryos are transparent and develop rapidly, this organism is well suited for this analysis. In the adjoining sections, I will broadly discuss the embryonic stages of the zebrafish with particular emphasis on the mechanisms and genes involved for proper formation of the nervous system.

## Morphology of the developing zebrafish hindbrain

*Development of an undifferentiated single-cell embryo to an embryo defined with distinct germ layers*

After fertilization of the zebrafish egg, contractile movements force non-yolky cytoplasm to segregate from yolk vesicles toward the animal pole and form the blastodisc (Fig. 1A). Rapid, synchronous cell divisions (at 15 minute intervals) result in a meroblastic division of the blastodisc into an array of blastomeres residing on top of a large non-dividing yolk

mass (yolk sac) (Fig. 1B-F) (Kimmel and Law, 1985a; Langeland and Kimmel, 1997). By the 64-cell stage and throughout the 256-cell stage (2 - 2.25 hours post fertilization, hpf), blastomeres that are present on the upper, superficial layer are termed the enveloping layer (EVL), while cells that reside on the lower, enclosed layer are termed the deep cells (Fig. 1G). By the tenth zygotic cell cycle (512-cell stage, 2.75 hpf), lengthened, asynchronous cell cycles and the initiation of zygotic transcription marks the beginning of the mid-blastula transition (MBT), and deep blastomere cells that lie marginally to the yolk cell form the yolk syncytial layer (YSL) (Kimmel and Law, 1985b). The MBT also marks the onset of cell motility in which both the blastodisc and the YSL begins to thin and spread out over the yolk sac (akin to pulling a cap over a round head) in a process termed epiboly (4.3 hpf) (Kane and Kimmel, 1993). During the early stages of epiboly, the blastodisc flattens around the yolk and the YSL contracts, allowing for the deep cells to stream outward and repack by radial intercalation, filling the area between the EVL and the YSL throughout its extension over the yolk (Fig. 1H) (Keller, 1980). These radial intercalations do not affect the EVL, which remains a compartmentalized monolayer and eventually forms the periderm, a protective outer layer that covers the entire embryo (Kimmel et al., 1990). As epiboly progresses, cells of the blastodisc form a blastoderm, which proceeds to expand and engulf the yolk cell completely (Fig. 1I). The cellular movements that occur during epiboly are dependent on a network array of microtubules and early-acting transcription factors (Schulte-Merker et al., 1992; Solnica-Krezel and Driever, 1994; Stachel et al., 1993; Strahle and Jesuthasan, 1993).

**Figure 1**

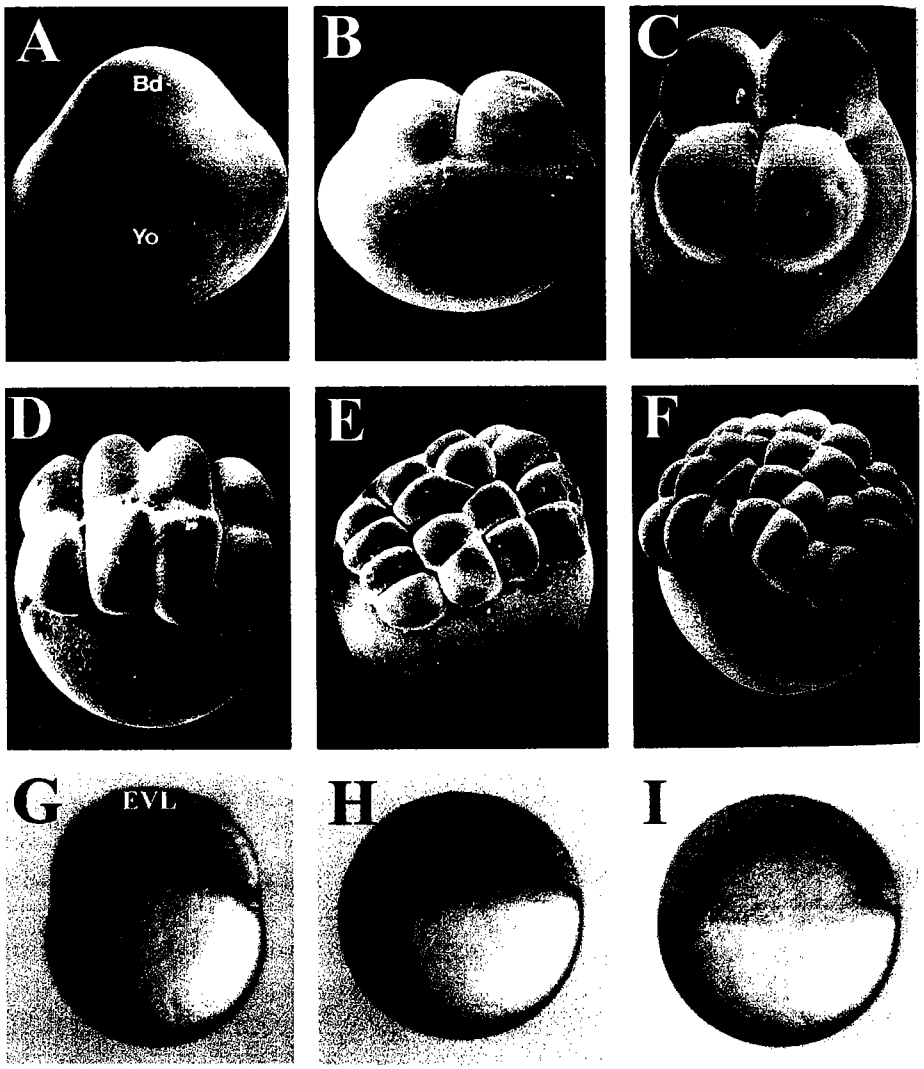


**Figure 1.** Zebrafish embryonic development throughout blastula stages. (A-F) Scanning electron micrographs of early stage zebrafish embryos. (A) 1-cell (0.2 hpf). (B) 2-cell (0.75 hpf). (C) 4-cell (1 hpf). (D) 8-cell (1.25 hpf). (E) 16-cell (1.5 hpf). (F) 32-cell (1.75 hpf). (G) 256-cell (2.25 hpf). (H) 30% epiboly (4.75 hpf). (I). 50% epiboly (5.25 hpf). Embryos are shown at dorsal views with anterior to the top. Abbreviations: Bd, blastodisc; Yo, yolk; EVL, enveloping layer; hpf, hours post fertilization. (Adapted from Langeland and Kimmel, 1997).

In addition to the continuance of epiboly, morphogenetic movements of involution, convergence and extension occur, producing the three distinctive germ layers and defining the primary embryonic axis (Schoenwolf and Smith, 2000; Solnica-Krezel et al., 1995). At the onset of this stage, termed gastrulation (Fig. 1I) (50% epiboly, 5.25 hpf), cells are first specified and committed to a particular embryonic fate (Fig. 2) (Ho and Kimmel, 1993). Only deep cells of the blastoderm contribute to a definitive fate, while yolk cells, including the YSL, have not been shown to contribute to embryonic fate and EVL cells impend exclusively to formation of the periderm (Kimmel et al., 1990). The injection of dye molecules into individual cells, in order to trace cell lineage and examine the particular tissues to where the labeled descendents of the injected cell lie, proved to be valuable for establishing a fate map for the differentiating embryo (summarized in (Ho and Kimmel, 1993; Kimmel and Warga, 1987; Kimmel et al., 1990; Woo and Fraser, 1995; Woo et al., 1995)). Fate mapping indicate that cells located nearest the animal pole will produce ectodermal fates (Fig. 2). This includes the epidermis, sensory organs such as the nose and eyes, the neural crest and central nervous system derivatives such as the brain and spinal cord. A broad ring of cells located near the margin produces mesodermal derivatives such as the notochord, blood and heart, head and somite muscle, the kidney and fins (Fig. 2). Lastly, cells overlapping the blastoderm margin, occupying closest to the yolk cell at the vegetal pole, will give rise to endodermal tissues (Fig. 2). This includes epithelial cells that make up the pharynx, liver and intestines.

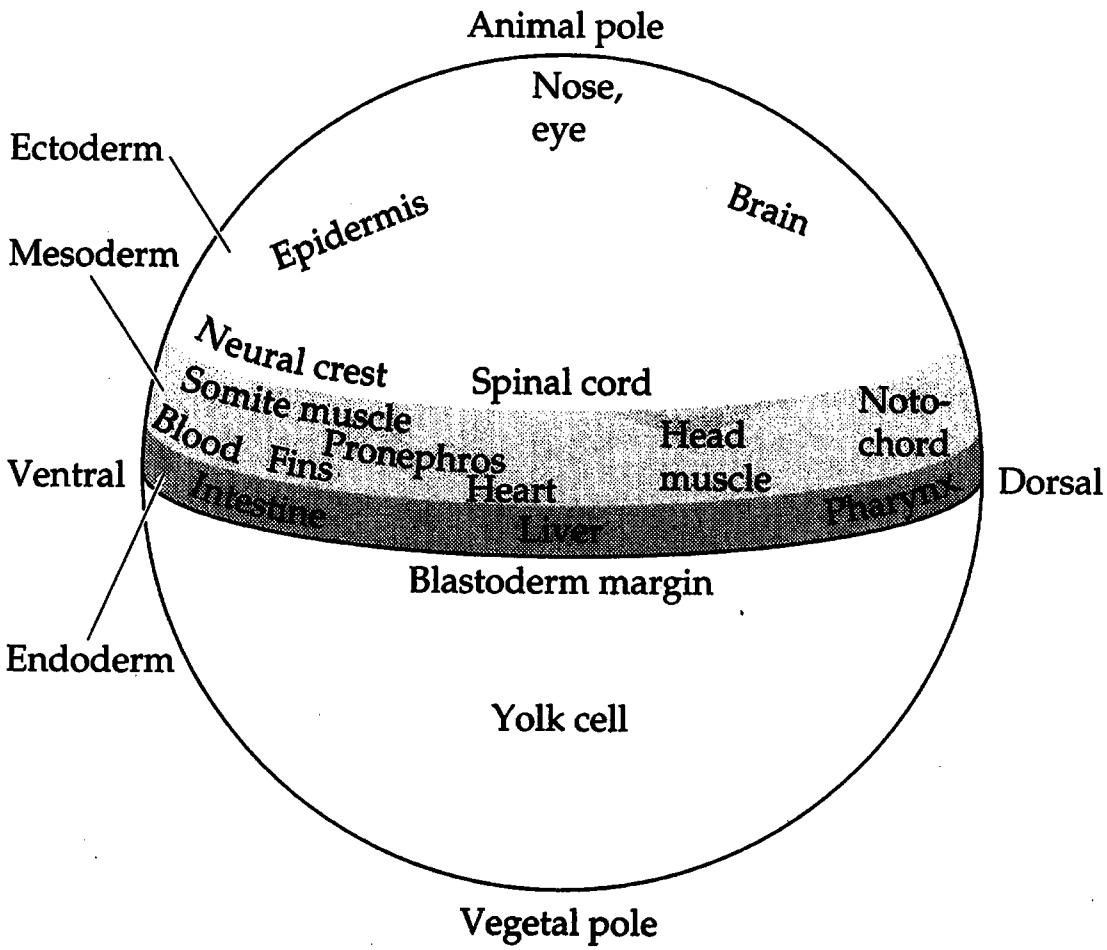


**Figure 2.** Fate map of the deep cell layer of an early gastrula-stage zebrafish embryo. Lateral view of embryo showing cell postition in relation to the prospective tissue or organ rudiment. Ectodermal fates map nearest to the animal pole, mesodermal fates map to a broad marginal ring and endodermal fates map nearest to the blastoderm margin. (From Langeland and Kimmel, 1997).

Transplantation experiments, in which a single labeled cell is transplanted from one particular region in an early gastrula-stage embryo (donor) into a different region in another early gastrula-stage embryo (recipient), have shown that the relocated donor cell will differentiate according to the recipient environment it now occupies (Ho and Kimmel, 1993; Woo and Fraser, 1998). This indicates that cells at this stage have not yet commit to a certain fate and remain plastic, regardless how they are specified. For example, transplant of a cell located near the blastoderm margin, normally fated to become endodermal, to near the animal pole, will result in the cell transforming into an ectodermal fate (Schulte-Merker et al., 1992). However, if a donor cell is from a late gastrula-stage embryo, the transplanted cell will instead migrate to a region within the recipient from which the donor cell was originally specified to be and remain committed to that original fate (Ho and Kimmel, 1993; Woo and Fraser, 1998). This suggests that while cells are specified, they are capable of exhibiting plasticity and differentiating into other fates during early gastrula and only are committed after mid-gastrula.

As epiboly progresses and the blastoderm continues to envelope over the yolk, cells of the blastoderm begin to involute near the margin, forming a germ ring (5.75 hpf) (Cooper and D'Amico, 1996). This thickened region circumscribes the entire width of the blastoderm margin and is composed of two distinct layers - the outer layer (termed the epiblast), whose cells migrate into the lower layer (termed the hypoblast), toward the animal pole (Warga and Kimmel, 1990). Convergence movements (Fig. 3) then bring cells from both the hypoblast and the epiblast toward the dorsal side of the embryo, forming an embryonic shield (6 hpf) (Warga and Kimmel, 1990). This region is

**Figure 3**

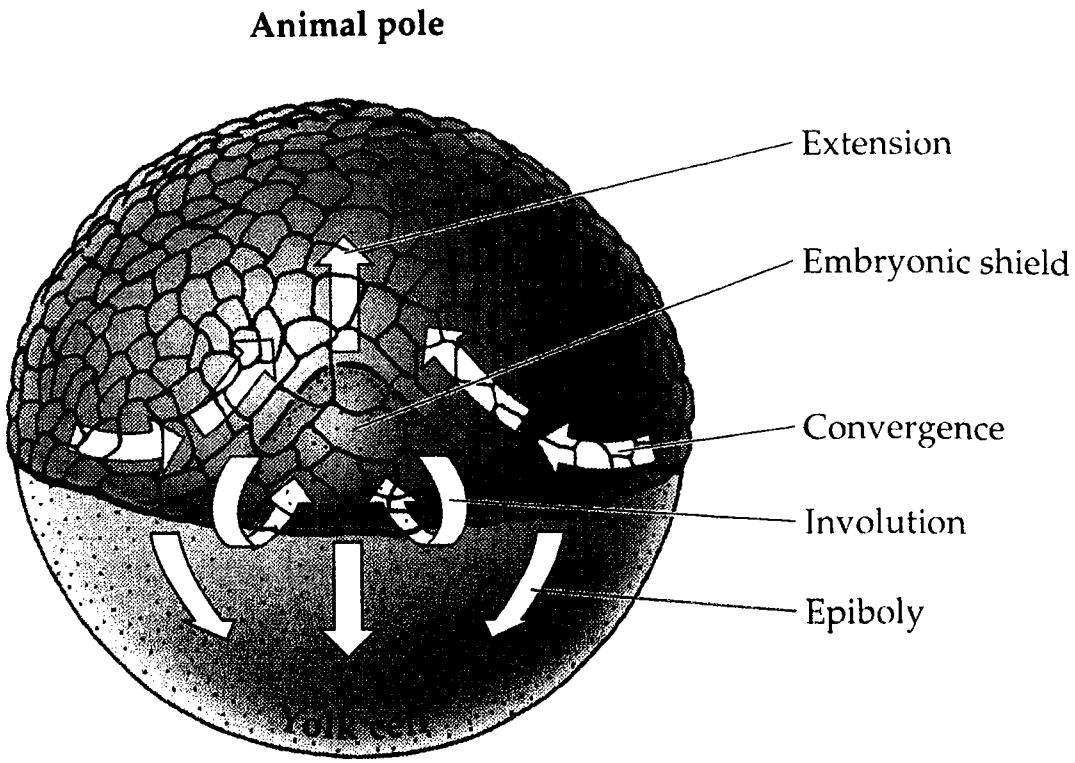


**Figure 3.** Involution, convergence and extension in a gastrula-stage zebrafish embryo. Arrows indicate cellular movements. (From Langeland and Kimmel, 1997).

equivalent to Spemann's organizer in the amphibian (Harland and Gerhart, 1997; Spemann and Mangold, 1924) or Hensen's node in the chick (Boettger et al., 2001; Joubin and Stern, 1999), due to its ability to produce a secondary embryonic axis in transplantation experiments (Saude et al., 2000). Mediolateral intercalations among the cells in the embryonic shield then narrow and extend (Fig. 3) in order to produce the primary embryonic axis (Warga and Kimmel, 1990). The earliest cells involuting at the embryonic shield (Fig. 3) give rise to the axial hypoblast (marked by the expression of *goosecoid*) (Stachel et al., 1993) and the most anterior cells that progresses toward the animal plate will develop as the prechordal plate (Fig. 4A) (70% epiboly, ~7.5 hpf) (Warga and Kimmel, 1990). Later involuting cells give rise to the chorda mesoderm, which forms the notochord (marked by the expression of *no tail*) (Schulte-Merker et al., 1992). At 80% epiboly (8.5 hpf), the paraxial hypoblast begins to segregate from the axial hypoblast, which will give rise to mesodermal derivatives that are located anteriorly such as muscle tissue (which are involved controlling head and mouth movement) (Fig. 4B) (Durbin et al., 1998) or those which are located posteriorly such as the somites (which control tail movement) (Thisse et al., 1993). These processes during gastrulation – involution, convergence and extension, function in properly orientating the anterior-posterior axis and thus establishing the rudiment specified body plan for the developing embryo.

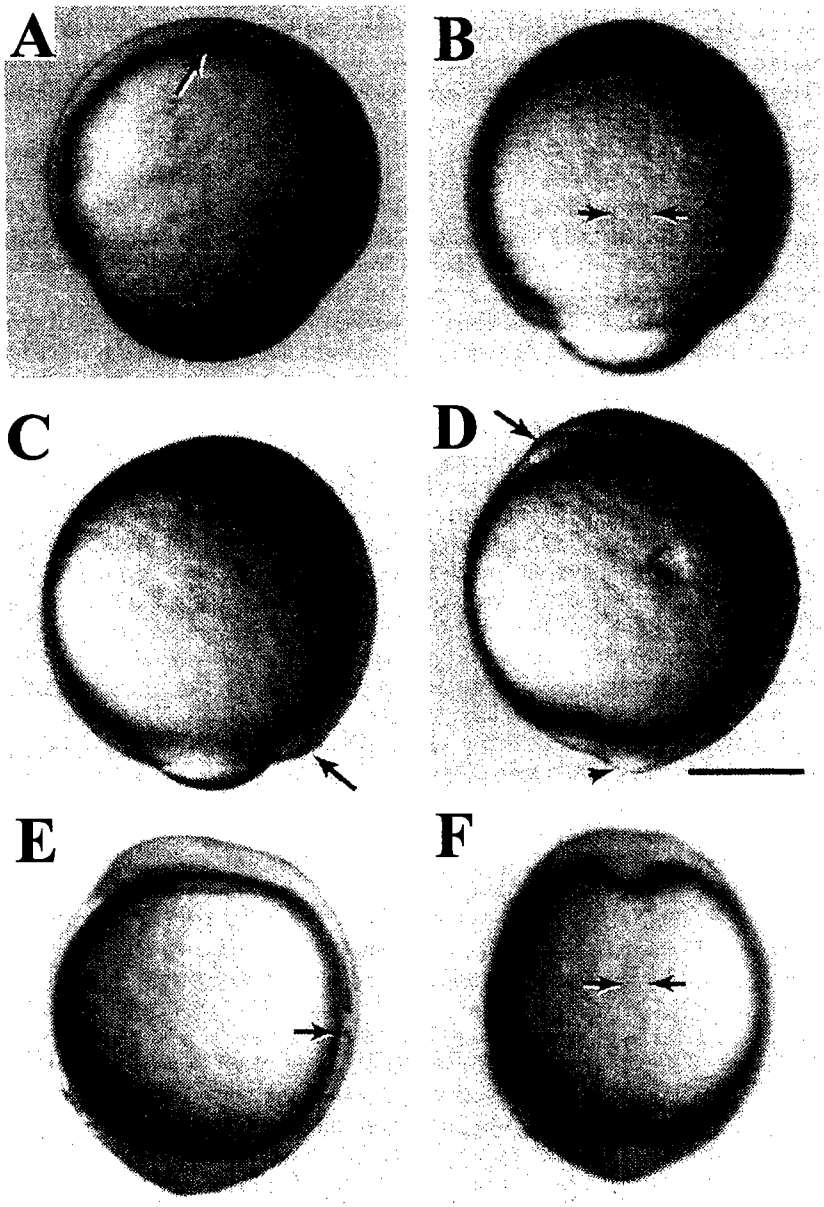


**Figure 4.** Zebrafish embryonic development through late gastrula and early segmentation stages. (A) 70% epiboly (7.5 hpf). Arrow denotes the hypoblast of the prechordal plate. (B) 80% epiboly (8.5 hpf). Arrows denote boundaries between the axial mesoderm in the midline and the paraxial mesoderm. (C) 90% epiboly (9 hpf). Arrow denotes tail bud. (D) 100% epiboly (10 hpf). Arrow indicates the polster and arrowhead denotes the yolk plug closure site. (E) 2-somite (10.7 hpf). Arrow denotes boundary of second somite. (F) 2-somite (10.7 hpf). Arrows indicate notochord rudiment. (A,C) Ventral views. (B,F) Dorsal views. (D,E) Lateral views. Abbbreviations: hpf, hours post fertilization. (Adapted from Kimmel et al., 1995).

*Signaling molecules pattern the anterior-posterior axis of the gastrulating embryo*

The anteroposterior patterning of the central nervous system is induced by a proposed two-signal model (Nieuwkoop, 1952; Nieuwkoop and Weijer, 1978). The first signal (termed the activation signal) induces the formation of neural tissue through the production of BMP (bone morphogenetic proteins) antagonists such as Noggin (Lamb et al., 1993; Zimmerman et al., 1996), Follistatin (Hemmati-Brivanlou et al., 1994) and Chordin (Piccolo et al., 1996; Sasai et al., 1995). The second signal (termed the posteriorizing signal or transformer), which further specifies the neuroectoderm into distinct fates such as the hindbrain, include the Wnts (McGrew et al., 1995), fibroblast growth factors (FGFs) (Kengaku and Okamoto, 1995; Lamb and Harland, 1995) and retinoic acid (RA) (Durston et al., 1989; Papalopulu and Kintner, 1996).

Members of the Wnt family, a group of secreted cysteine-rich glycoproteins, are candidates for transforming signals (Lee and Jessell, 1999). The misexpression of Wnts or its downstream signaling components result in the loss of anterior fates (forebrain) and a posteriorization of the embryo (Nordstrom et al., 2002). Genetic mutants that encode for repressors of the Wnt signaling pathway also exhibit a similar phenotype (Heisenberg et al., 2001; Kim et al., 2000). However, the interference of Wnt signaling, through the misexpression of dominant negative constructs or antisense oligonucleotides, result in a loss of hindbrain markers and an expansion of forebrain markers (Erter et al., 2001; Lekven et al., 2001). The misexpression of Wnt signaling inhibitors, including *dickkopf1* (*dkk1*) in zebrafish (Shinya et al., 2000) and *cerberus* in the mouse (Biben et al., 1998) and *Xenopus* (Glinka et al., 1997), results in anteriorization of the embryo. Additionally,

Wnt signals are expressed in the lateral germ ring at the onset of gastrulation (Schneider et al., 1996) and cells transplanted from the lateral germ ring to the animal pole can induce hindbrain fates, while cells transplanted from the shield (dorsal organizer) cannot (Woo and Fraser, 1997; Woo and Fraser, 1998). These results suggest that Wnt signals specify posterior neural fates.

FGF signals also have a distinct role in the promotion of posterior fates in the neuroectoderm (Storey et al., 1998). Loss of function analysis, through the disruption of FGF signaling, results in a loss of posterior structures in the caudal part of the embryo, while more anterior regions are unaffected (Griffin et al., 1995; Pownall et al., 1996). Gain of function analysis, through misexpression, results in the development of caudal (posterior) structures at the expense of anterior derivatives (Griffin et al., 1995) or an anterior shift of posterior gene expression into the hindbrain (Pownall et al., 1996). These studies reveal that FGF signaling is an important contributor for posteriorization of the embryo.

Retinoic acid (RA) signaling has been suggested to play a pivotal role in promoting posterior fates within the neural ectoderm (Durston et al., 1989; Durston et al., 1998). Misexpression of RA results in a loss of the anterior hindbrain, while the posterior hindbrain is not affected (Godsave et al., 1998; Hill et al., 1995; Holder and Hill, 1991) and an anterior to posterior transformation of the rostral hindbrain is apparent (Hauptmann and Gerster, 1995; Marshall et al., 1992). Loss of RA function studies reveals an opposite phenotype to that of exogenous RA treatment. The use of dominant negative RA receptors resulted in the anteriorization of the caudal hindbrain (van der

Wees et al., 1998) while treatment with a RA receptor antagonist resulted in a similar phenotype (caudal hindbrain assuming a more rostral-like state) (Dupe and Lumsden, 2001). Interestingly, a zebrafish mutant for an enzyme in the RA biosynthesis pathway exhibited a truncation of the posterior hindbrain (Begemann et al., 2001). Other candidates that participate in posteriorizing the embryo include downstream repressors of the Nodal-signaling pathway. The misexpression of an Nodal antagonist (*antivin*) or genetic mutants that have disrupted Nodal signaling (such as *cyclops* and *squint*) leads to an elimination of posterior fates within the neuroectoderm (Feldman et al., 1998; Gritsman et al., 2000; Thisse et al., 2000). Zebrafish embryos, mutant in the Mix homeodomain gene *bonnie and clyde* (*bon*) (which functions downstream of Nodal signaling), exhibit a reduction in the anterior neuroectoderm (Trinh le et al., 2003). Taken together, these studies indicate that posterior specification of the neuroectoderm involves the collective activity of multiple pathways including components of the Wnt, FGF and RA signaling cascades.

*The end of gastrulating movements within the embryo coincides with the formation of the prospective neuroectoderm and subsequent segmentation of the hindbrain*

Towards the end of gastrulation (90% epiboly, ~9 hpf), only the vegetal pole of the yolk (termed the yolk plug) is left uncovered by the enveloping blastoderm (Fig. 4C). At this stage, the epiblast layer begins to thicken anteriorly, at the dorsal midline, in order to form the neural plate at the prospective head region (Driever et al., 1997). Unlike the more lateral and ventral epiblast cells that remain cuboidal, cells that form the neural

plate adopt a more columnar shape (Fig. 5A) (Concha and Adams, 1998). This region represents the first morphological indication of the rudiment central nervous system. The anterior prechordal plate is also apparent, as it enlarges prominently and forms a bulge which gives rise to the hatching gland (termed polster) (Fig. 4C) (Shih and Fraser, 1996). At bud stage (100% epiboly, 10 hpf), the blastoderm completely covers the yolk, marking the end of gastrulation. Morphogenetic movements that occur during gastrulation (involution, convergence and extension) commences, except for a distinct region located at the yolk plug closure site (termed the tail bud), which will begin to enlarge and extend in order to give rise to the posterior trunk and the embryonic tail (Fig. 4D) (Solnica-Krezel et al., 1995).

After gastrulation establishes the primary germ layers and the embryonic axis, a series of concurrent morphogenetic processes take place in order to designate and define distinct visible rudiment body derivatives (termed the segmentation period, after 10 hpf). One such event, which is used as a staging index for zebrafish development, is the appearance of somites (Fig. 4E) (Kanki and Ho, 1997). These undifferentiated mesodermal components develop bilaterally and sequentially arise in the trunk and tail. Somites consist of a lateral dermamyotome, which gives rise to chevron-shaped myotomes and develop as muscle segments, and a medial sclerotome, which gives rise to the vertebral cartilage (Bernhardt et al., 1998; Stickney et al., 2000). A second differentiating structure that is apparent during segmentation is the notochord (Fig. 4F). These cells transiently appear as a column of coin-like units then, as some cells swell and

**Figure 5**

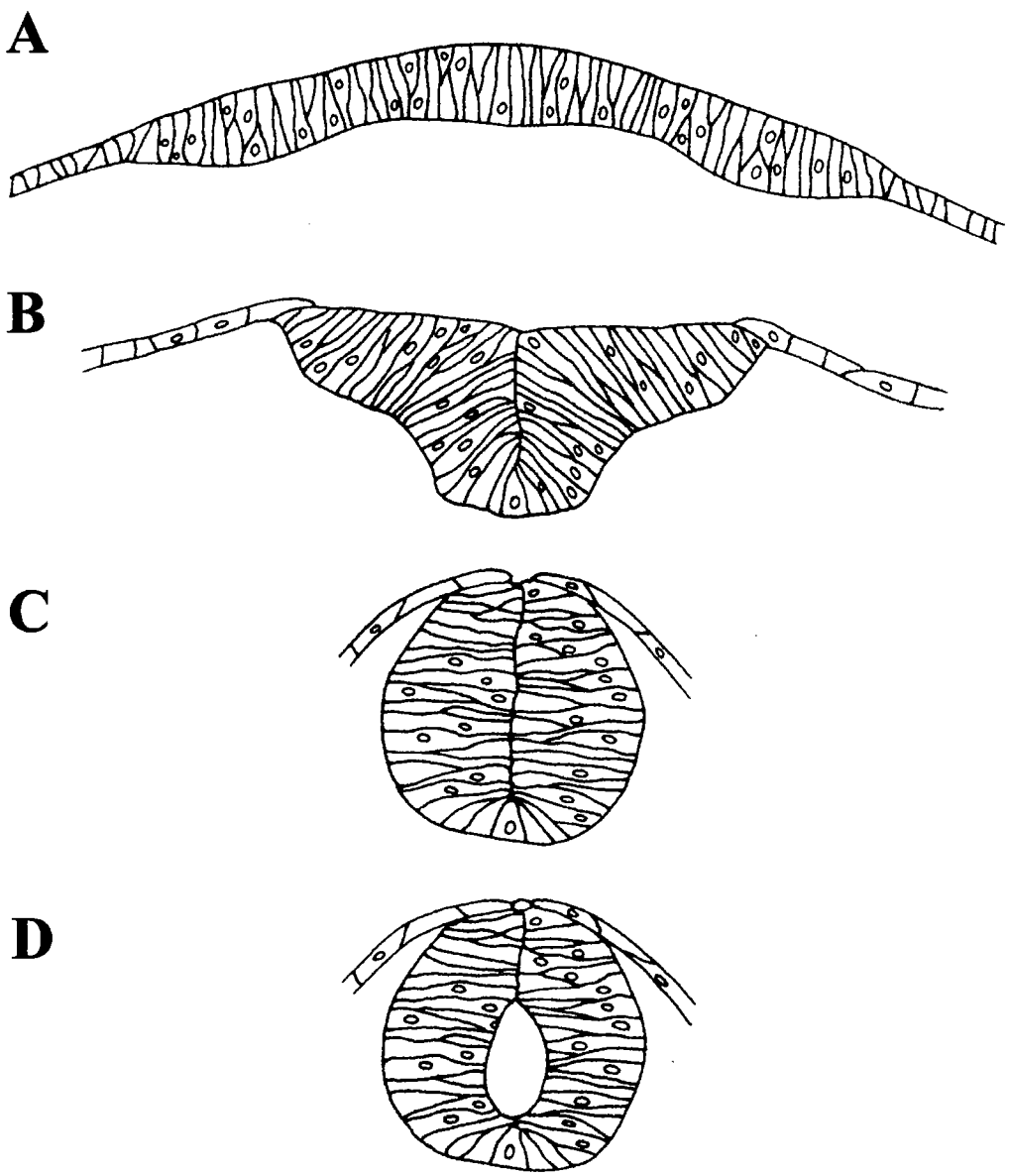


**Figure 5.** Neurulation in the zebrafish embryo. (A) Presumptive neuroectoderm condenses to form the neural plate at late gastrula . (B) Neural plate condenses and infolds to form the neural keel during segmentation stages. (C) Neural keel then infolds and rounds up into a cylindrical neural rod. (D) Neural rod is then formed by cavitation. (Adapted from Langeland and Kimmel, 1997).

become vacuolated in an anterior to posterior manner, elongate to form a rod surrounded by an epithelial sheath (Kimmel et al., 1995).

At the onset of segmentation, the neuroectodermal primordium undergoes a series of highly defined transformations in order to properly form the central nervous system (CNS). The thickened neural plate of columnar cells begins to condense and infold at the midline (13 hpf), causing epithelial cells that were originally at the outermost side of the neural plate (apical cells) to meet and form the neural keel (Fig. 5A,B) (Strahle and Blader, 1994). Even though the neural keel is uniform in length, extensive morphogenesis is apparent such that the anterior region, which will give rise to the brain rudiment, enlarges in comparison to the more posterior region, which will develop into the spinal cord rudiment (Fig. 6A) (Lumsden and Krumlauf, 1996). As the neural keel continues to infold, a solid cylindrical neural rod is formed (16 hpf) which then subsequently hollows out to form the neural tube (Fig. 5C,D) (Strahle and Blader, 1994). This process is termed 'secondary' neurulation, due to the fact that in 'primary' neurulation (as with most vertebrates including amphibians), the neural plate infolds directly to form a hollow neural rod rather than undergoing an intermediate stage where a transient neural keel forms into a solid rod that is not hollowed out yet (Concha and Adams, 1998; Kimmel et al., 1995; Wilson and Hemmati-Brivanlou, 1997). Shortly after formation of the neural rod (18 hpf), the brain rudiment is partitioned into about ten distinct swellings, termed neuromeres, prominently subdivided by constrictions that appear throughout its length (Fig. 6B) (Kimmel, 1993). These subdivisions mark the morphological appearance of the segmenting central nervous system.

Figure 6

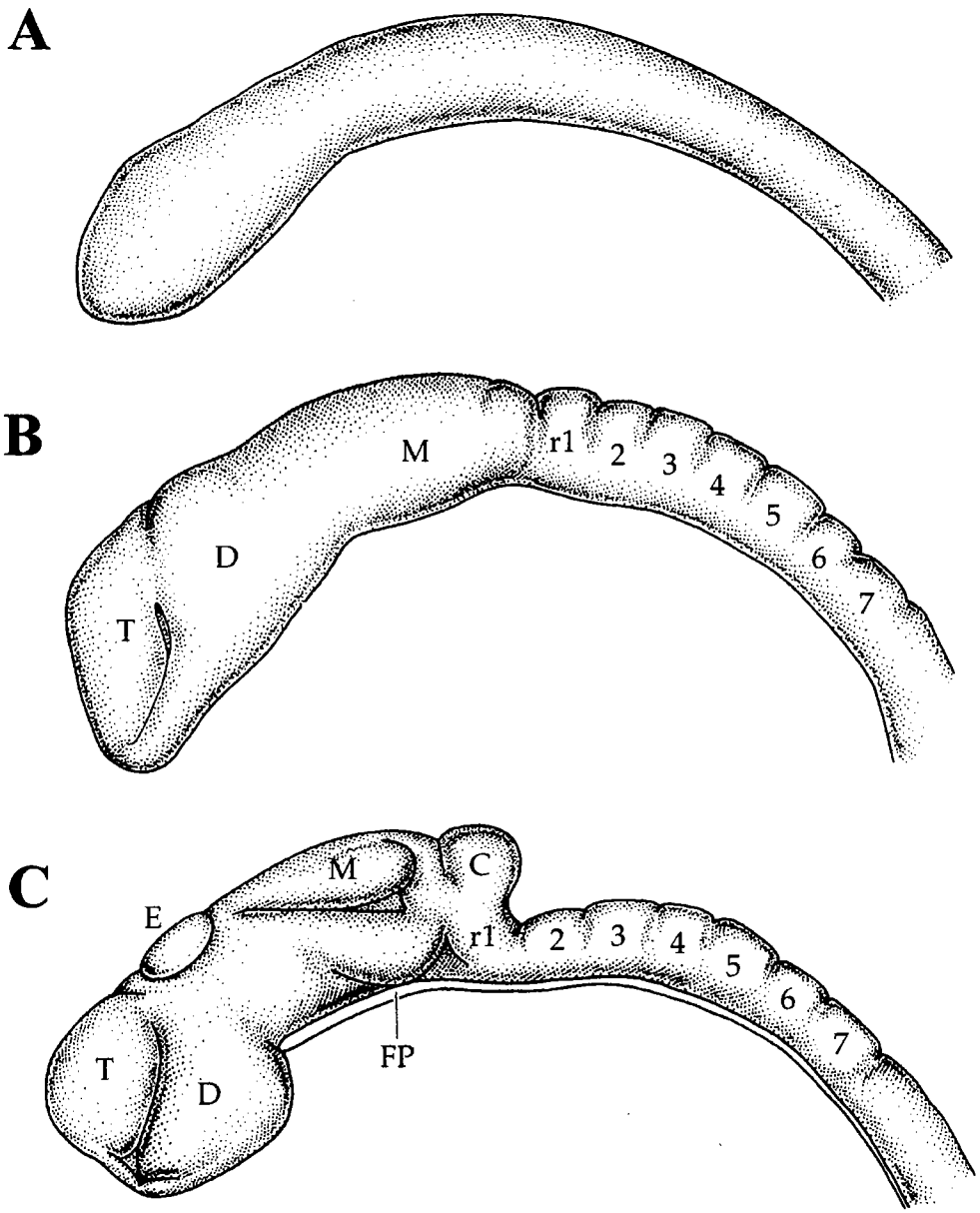


**Figure 6.** The prospective zebrafish brain is partitioned into neuromeres. (A) No morphological subdivisions are evident in the neural analge (12 hpf). (B) Brain is subdivided into ten neuromeres (18 hpf). (C) Brain undergoes distinct morphogenesis (24 hpf). Abbreviations: hpf, hours post fertilization; T, telencephalon; D, diencephalon; M, midbrain; r, rhombomeres; E, epiphysis; C, cerebellum; FP, floor plate. Brain rudiment is shown at lateral views, with anterior to the left. (Adapted from Langeland and Kimmel, 1997).

*Segmentation of the hindbrain reveals the formation of several specialized structures*

The neuromeres consist of three subdivisions located rostrally – the diencephalon and telecephalon, which correspond to the forebrain, and the mesencephalon, which corresponds to the midbrain (Fig. 6B) (Kimmel, 1993). The seven neuromeres that are located caudally are termed rhombomeres (r) and they subdivide the hindbrain (Hanneman et al., 1988). The genes that regulate this process will be discussed in detail in the next few sections. During late stages of the segmentation period (24 hpf), additional sculpturing of the brain rudiment is evident (Fig. 6C). These consist of an expansion of the ventral diencephalon, which will go on to form the hypothalamus (posterior pituitary gland) (Wullimann and Puelles, 1999; Wullimann et al., 1999); a swelling in the midline of the diencephalon roof, which will give rise to the epiphysis (pineal primordium) (Ross et al., 1992); subdivision of the mesencephalon to the dorsal midbrain (optic tectum) (Schmitt and Dowling, 1994) and the ventral midbrain (tegmentum) (Wilson et al., 2002); formation of the cerebellum, arising from the posterior midbrain and anterior hindbrain (Koster and Fraser, 2001); and the floor plate, extending throughout the ventral midline (excluding the forebrain region) (Roelink et al., 1994).

Another group of specialized tissue that is established during segmentation is the formation of sensory placodes (Fig. 7). As mentioned above, the optic primordium arises laterally from the mesencephalon (midbrain) and develops into a two-layered optic cup (11.5 hpf) (Schmitt and Dowling, 1994). The inner layer will then form into the neural

**Figure 7**

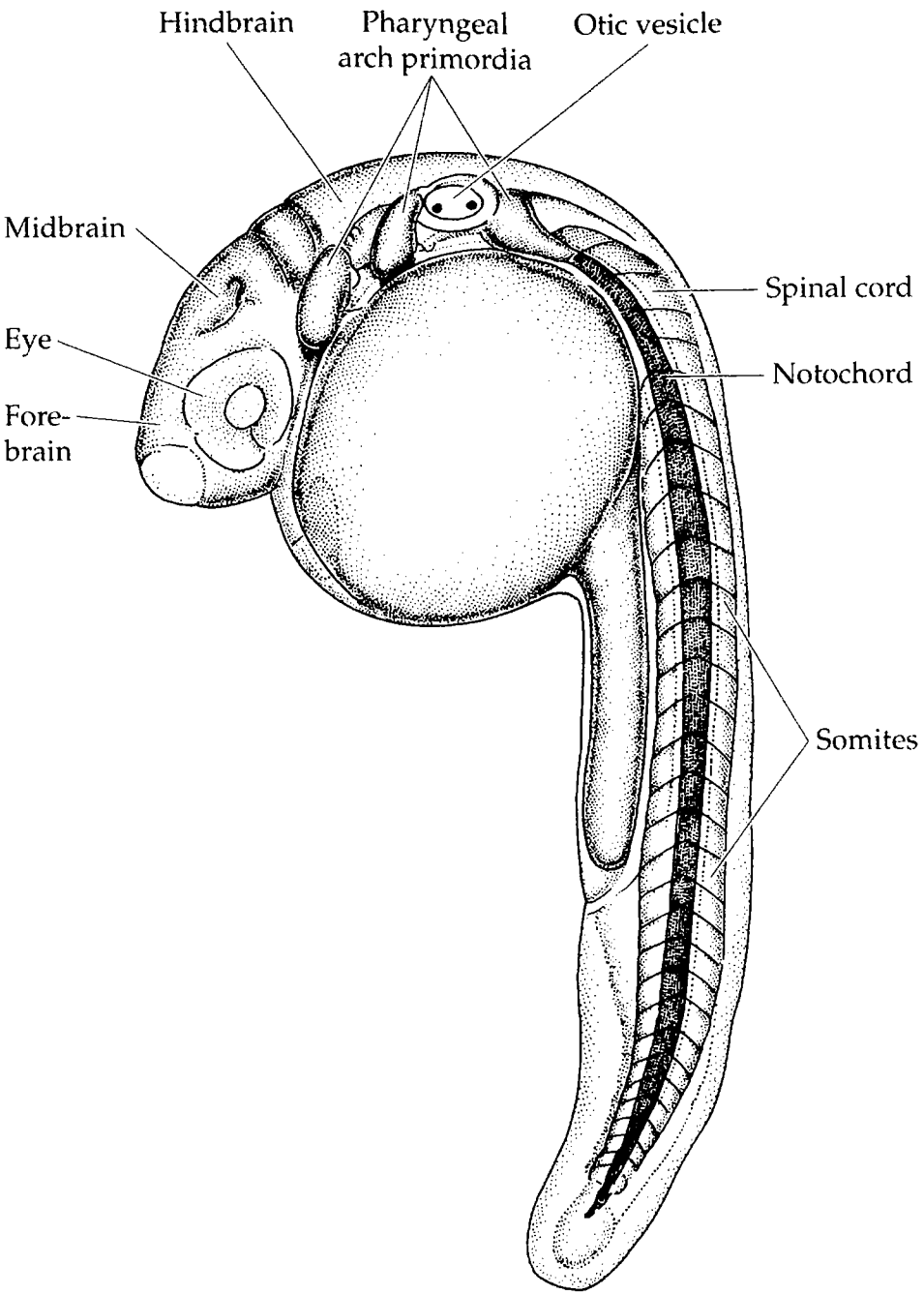


**Figure 7.** Prominent features of a prim-5 stage zebrafish embryo (24 hpf). Various structures are labeled. Sensory organs include the eyes, ears (otic vesicles) and nose (olfactory placodes). Abbreviations; hpf, hours post fertilization. (From Langeland and Kimmel, 1997).

retina while the outer layer develops as the pigmented retina. Positioned at the anterior periphery of the optic primordium are the olfactory placodes, which develop into highly specialized chemosensory cells (Hansen and Zeiske, 1993). At 16 hpf, located between the optic and olfactory placodes are the trigeminal ganglion, a group of differentiated touch-sensory neurons (Metcalfe et al., 1990). Also at this stage, the otic placode is readily distinguishable between the optic vesicle and the first somite (Haddon and Lewis, 1996). The primordium of the ear hollows out and forms the otic vesicle, which lies adjacent to the brain rudiment, level to r5 (Fig. 7). This vesicle contains two small otoliths and develops into the organ necessary for hearing and balance. Lastly, lateral-line placodes form mechanosensory ganglion cells that migrate the length of the embryo and function in detecting water movement (Kuwada et al., 1990).

Concomitant with the partition events of the segmentation period is the appearance and differentiation of primary neurons (Grunwald et al., 1988). These include: motor neurons, which develop adjacent to each somite in the spinal cord and innervate dorsal and ventral body muscle (Eisen et al., 1986; Myers et al., 1986; Westerfield and Eisen, 1988); touch sensory neurons, which are present in the brain (trigeminal ganglion) and dorsal spinal cord (Rohon-Beard neurons) (Metcalfe et al., 1990); and reticulospinal and branchiomotor neurons, whose pattern corresponds to the characteristic segmental organization of the hindbrain (Fig. 8) (Trevarrow et al., 1990).

The hindbrain reticulospinal neurons are organized into seven bilateral groups arranged periodically along the neural axis (Fig. 8A) (Metcalfe et al., 1986). The approximately one-hundred reticulospinal cells are present in three clusters in the rostral

**Figure 8**

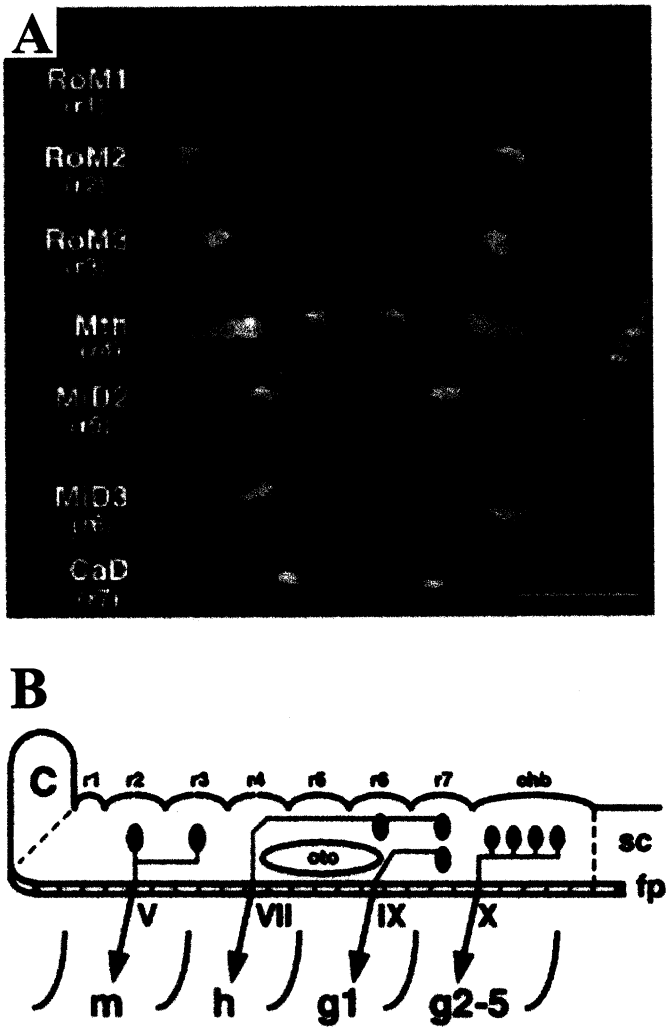


**Figure 8.** Segmental pattern of neurons in the zebrafish hindbrain. (A) Reticulospinal neurons. Conofocal image of a 5-day old zebrafish embryo in which the neurons are visualized by retrograde filling with lysinated rhodamine-dextran. Names of individual neurons and rhombomeres (r) are indicated. Bilateral pair of Mauthner neurons are at r4. Anterior is to the top. (Adapted from Moens et al., 1996). (B) Branchiomotor neurons are shown schematically. Location of branchiomotor nuclei (V, VII, IX and X) and their projections into the pharyngeal arches (m, h, g1 and g2-5) are shown. Anterior is to the left. Abbreviations: C, cerebellum; m, mandibular arch; h, hyoid arch; g1-5, gill arches 1-5; r1-7, rhombomeres 1-7; oto, otocyst; chb, caudalmost hindbrain; sc, spinal cord; fp, floor plate. (Adapted from Chandrasekhar et al., 1997).

region (Ro), three clusters in the middle region (Mi) and at least one cluster in the caudal region (Ca) in the hindbrain (Hanneman et al., 1988). Their respective axons project into the spinal cord along two major routes – the medial longitudinal fascicle (mlf) and the lateral longitudinal fascicle (llf). There are 27 types of reticulospinal neurons and nineteen are present as single identified cells on each side of the midline (Metcalfe et al., 1986). One prominent reticulospinal neuron is the Mauthner cell, residing in rhombomere 4, which is involved in the initiation and control of an escape response from a predator (Foreman and Eaton, 1993; Metcalfe et al., 1986).

The branchiomotor neurons in the hindbrain are present in a segmental pattern that correlates with the organization of rhombomeres (Fig. 8B) (Chandrasekhar et al., 1997). These motor neurons function in innervations of the pharyngeal arch musculature, which contributes to the proper formation of craniofacial structures such as the jaw skeleton, essential mouth supports and the gills (Schilling and Kimmel, 1994). Trigeminal motor neurons (nV), which are located in an anterior cluster in r2 (Va) and a more posterior cluster in r3 (Vp), project their axons out at a common hindbrain exit point, r2, in order to innervate the mandibular arch (Higashijima et al., 2000). Facial neurons (nVII), which are specified in r4, subsequently migrate posteriorly into r5, r6 and r7 before taking up residence in r6 and r7 (Chandrasekhar et al., 1997). Their axons then extend rostrally to exit r4 and innervate the hyoid arch. Glossopharyngeal neurons (nIX) are located in r7 and extend their axons rostrally to exit r6 to innervate the first gill arch (Chandrasekhar et al., 1997). Finally, the vagus motorneurons (nX), which are located in

the caudal-most hindbrain region, extend their axons from the same region to innervate the second to fifth gill arches (Chandrasekhar et al., 1997).

The last major morphogenetic event that occurs during the segmentation period is the formation and differentiation of specialized migrating cells known as the neural crest cells (Bronner-Fraser, 1994; Lumsden et al., 1991). These cells are present at the dorsal-most region of the neural tube and are capable of migrating extensively throughout the embryo via distinct pathways and generate an array of cell types (Le Douarin et al., 1993). Neural crest cells are classified as cranial, hindbrain, vagal or trunk, according to their anterior to posterior location, and give rise to sensory neurons, glia cells, melanocytes (pigment cells), and bones and cartilage of the facial and visceral skeleton (Anderson, 1997; Anderson et al., 1997).

The subdivisions of the rudimentary hindbrain formed during the sementation period underlie the development of three adult hindbrain regions – the pons, cerebellum and medulla oblongata (Fig. 9) (Kandel et al., 1991). The medulla oblongata, which resides directly anterior to the spinal cord, contains a network of cell groups (termed reticular formation) involved in autonomic (involuntary) functions such as respiration, digestion and heart rate control. The pons, which is located anterior to the medulla, transmits movement information from the cerebrum to the cerebellum. These two structures, including the midbrain, form a 'brain stem' involved in conveying signals from the brain to the spinal cord and vice-versa, receiving sensory information from the skin and muscles of the head and control motor movements of the head including the face, neck and eyes. The cerebellum, located besides the pons and medulla, is involved in

**Figure 9**

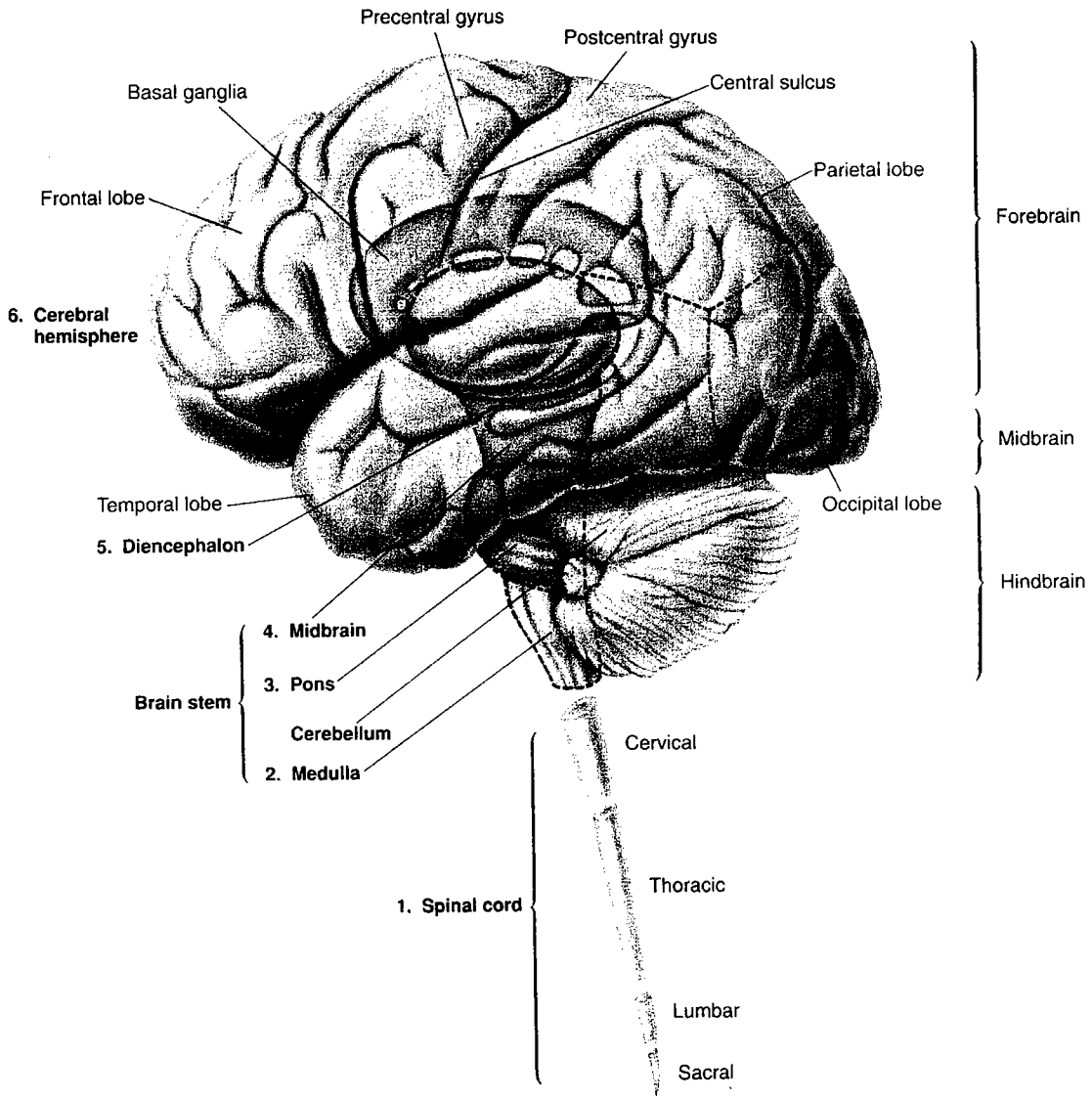


**Figure 9.** Anatomical representation of the human central nervous system. The six main parts are labeled including the major lobes, gooves (gyri and sulci) and ganglia. The brain is also subdivided into the forebrain, midbrain and hindbrain. Brainstem and spinal cord components are labeled. (From Kandel et al., 1991).

the coordination of movement and the learning of motor skills, and is connected to the brain stem through three major fiber tracks termed peduncles.

## Regionalization of the hindbrain

Before rhombomeres are apparent as transient bulges along the anterior to posterior axis of the developing hindbrain, restricted gene expression patterns predict their compartmentalization. These segmentation genes, which include transcription factors and signaling molecules, serve as signals to not only initiate the formation of individual rhombomeres, but also their consequential specification and segmentation. Loss of function analyses of these genes reveals that partial or entire segments of the hindbrain are lost. The mechanisms that determine and regulate cell identity suggest that complex processes synergize to demarcate the presumptive rhombomeres into a progressive, functional hindbrain.

### *FGF signals pattern the anterior and posterior hindbrain*

Time-lapse analyses of zebrafish hindbrain development reveal that r4 is the first rhombomere to form (Maves et al., 2002). The earliest rhombomere boundaries that are morphological distinguishable are the r3/r4 and r4/r5 boundaries, which first appear at the 5-somite stage (~11.6 hpf), with the remaining boundaries forming by the 10-somite stage (14 hpf) (Moens et al., 1998). The primary differentiation of r4 suggests that this

rhombomere may promote the subsequent development of adjacent rhombomeres through secretion of signaling factors. Indeed, the fibroblast growth factors (FGF) 3 and 8 are both expressed in the presumptive r4 at 9 hpf (90% epiboly) and 7.5 hpf (70% epiboly), respectively (Maves et al., 2002; Reifers et al., 1998). Loss of function analyses with FGF3, through the use of an antisense morpholino oligo (Maves et al., 2002), or FGF8, through the use of zebrafish mutant (*acerebellar*) line (Brand et al., 1996; Reifers et al., 1998), reveals no dramatic effects on hindbrain patterning. However, loss of both FGF3 and FGF8 function results in a severe effect - subsequent gene expression is lost in r5 and r6 (and partially in r3) with no effect on r4 (Maves et al., 2002). This indicates that FGF3 and FGF8 signals from r4 normally promote the development of r5 and r6 (Fig. 10).

Transplantation experiments, in which r4 cells from an early 1-somite stage donor embryo are transplanted into the ventral ectoderm of a shield-stage host, revealed that r4 cells are sufficient to induce r5/r6 development (Maves et al., 2002). Mosaic analyses, in which animal pole cells from a donor embryo are transplanted into a host embryo without FGF3 and FGF8 signals, revealed that wild-type cells can partially rescue r5 gene expression (Maves et al., 2002). Gain of function analysis, through the misexpression of *fgf3* and *fgf8*, reveal that these FGF signals can induce the expression of r5 and r6 genes (Maves et al., 2002). Taken together, this indicates that FGF signals, derived from r4, functions as a signaling center in the hindbrain and are necessary for the promotion of r5 and r6 development (Fig. 10).

**Figure 10**

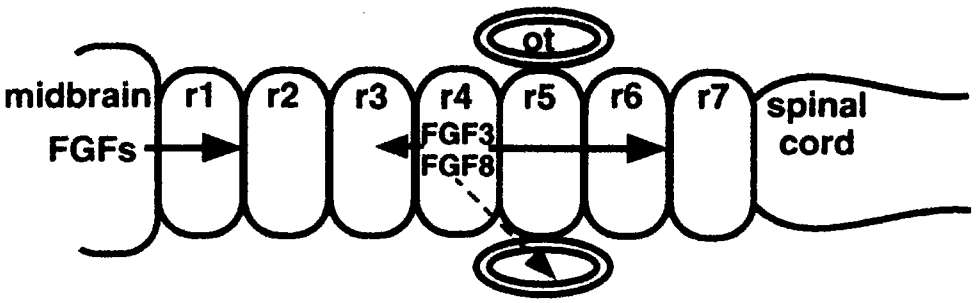


**Figure 10.** Fibroblast growth factors pattern the anterior and posterior hindbrain. Schematic figure of the zebrafish hindbrain illustrating that FGFs signals define the r1 terrritory and promotes the development of r5/r6, r3 and otic vesicle. Abbreviations: FGFs, fibroblast growth signals; r1-7, rhombomeres 1-7; ot, otic vesicle. Anterior is to the left. (Adapted from Maves et al., 2002).

FGF signaling is also involved in patterning the anterior hindbrain through a conserved organizing center, the midbrain-hindbrain boundary (MHB) (Irving and Mason, 2000). Zebrafish mutant embryos, defective in FGF8 (*acerebellar*), lack both the MHB and the cerebellum (Furthauer et al., 1997; Reifers et al., 1998). Fate mapping experiments indicate that r1 contributes to the formation of the cerebellum (Koster and Fraser, 2001) but it has been suggested that r1 is actually composed of two distinct domains – an anterior portion, termed r0, which corresponds to the upper rhombic lip and gives rise to the cerebellum and a thinner posterior portion, and the r1 domain, which gives rise to neurons in the ventral brain stem (Koster and Fraser, 2001; Vaage, 1969; Wingate and Hatten, 1999). In the absence of FGF8 at the MHB in the *acerebellar* mutants, locus coeruleus (LC) noradrenergic neurons, normally present in the anterior region of r1 (or r0, see above), are lost (Guo et al., 1999). These results indicate the FGF8 signaling from the MHB is necessary for the proper formation of the anterior hindbrain (Fig. 10). Additionally, these FGF8 mutants exhibit an expansion of *fgfr3* expression into the midbrain, the MHB and the cerebellum (whereas *fgfr3* expression normally presides in the posterior region of r1, the anterior midbrain and the posterior forebrain) (Sleptsova-Friedrich et al., 2001). This indicates that FGF8 signals may exclusively repress the expression of *fgfr3* from the anterior portion of r1 in order to properly segment the cerebellum from the posterior portion of r1. Further examples of FGF8 involvement in influencing hindbrain patterning include the implantation of beads containing anti-FGF8 antiserum, which resulted in an anterior expansion of r2-gene expression into r1 (Irving and Mason, 2000), and application of a specific FGF receptor inhibitor, which lead to a

strong reduction of r3/r5/r6 gene expression in the hindbrain (Marin and Charnay, 2000). Tissue-specific inactivation of a FGF receptor (*fgfr1*) in mice embryos resulted in severe abnormalities in the cerebellum (r1), in addition to defects in the midbrain (Trokovic et al., 2003). Taken together, these experiments clearly demonstrate that FGF signals play a pivotal role in patterning the anterior hindbrain.

*pou2 controls r2 and r4 development*

Another gene that is expressed in the hindbrain prior to morphologically visible segmentation is *pou2* (Hauptmann and Gerster, 1995; Takeda et al., 1994), a transcription factor that contains a bipartite DNA-binding domain consisting of a homeodomain and a POU-specific domain (Ryan and Rosenfeld, 1997). At the end of gastrulation, *pou2* is expressed as a transverse stripe in the prospective hindbrain that is resolved into two bilateral patches that correspond to the presumptive hindbrain domains r2 and r4 (Hauptmann and Gerster, 1995). Analyses of *spiel-ohne-grenzen* (*spg*) zebrafish mutants, which have lesions in the *pou2* gene, reveal that in addition to defects in the midbrain, these embryos also lack the midbrain-hindbrain boundary and the cerebellum (Belting et al., 2001; Burgess et al., 2002; Hauptmann et al., 2002). The expression of *pou2* in *acerebellar* (*ace*) mutants, which are inactive for FGF8, indicate that the initiation of *pou2* expression in hindbrain occurs independently of FGF8 signaling (Belting et al., 2001). *spg* (*pou2*) mutants were found to have a marked reduction in several genes involved in the initiation of rhombomere formation, such as those expressed from r3 and r5, concomitant with an enlargement of the r2 and r4 gene expression domains (Burgess

et al., 2002; Hauptmann et al., 2002). The size and shape of rhombomeric territories also appear to develop abnormally in *spg* mutants, as indicated by the reduction of r1, r3, r5 and r6 territories, while those of r2 and r4 are enlarged. *spg* mutants also display mispositioned or absent rhombomere boundaries and an alteration in the segmental pattern of reticulospinal neurons. In addition, *pou2* function was found to be important for the expression of *gbx2* in the hindbrain primordium (Reim and Brand, 2002; Rhinn et al., 2003). Morphological analyses of mice homozygous for a deletion allele of *gbx2* reveal that the anterior hindbrain is abnormal and motor neurons which are derived from r1 (locus coeruleus) and r2/3 (Vth motor nucleus) are absent (Wassarman et al., 1997). The *pou2* gene also appears to mediate the competence of neuroectodermal cells to respond to FGF8 signaling (Reim and Brand, 2002). With the finding that *pou2* is expressed in the hindbrain prior the activation of genes that are expressed in the presumptive rhombomeric territories advocates that *pou2* functions as an early essential component of the cascade of regulatory events controlling regionalization of the hindbrain.

*krox20 initiates and maintains the formation of r3 and r5*

The early hindbrain also requires *krox20*, a transcription factor with three $C_2H_2$ type zinc fingers, for the initiation of the presumptive r3 and r5 territories into distinct subdivisions. This gene is expressed in the prospective neuroectoderm at the end of gastrulation (100% epiboly, 10 hpf) first as an anterior stripe, then followed by a second posterior stripe around 11 hpf (Oxtoby and Jowett, 1993). These regions correspond to r3

and r5, before morphological distinguishment of these rhombomeres are apparent. The mouse *krox20* gene was found to be activated early during the $G_0/G_1$ transition in cultured cells, indicating that this factor is likely involved in the control of cell proliferation (Chavrier et al., 1988) and functions as a transcriptional activator (Chavrier et al., 1990). Ectopic expression of *krox20*, through the use of electroporation on the developing chick hindbrain, confers odd-numbered rhombomere identity (r3 and r5) to even-numbered rhombomeres (r2, r4 and r6) (Giudicelli et al., 2001). The change in identity occurs through a cell-autonomous manner since electroporations that were performed after the establishment of cell-lineage restriction compartments resulted in the formation of patches with an r3-like identity in r2. Ectopic *krox20* could also pattern the hindbrain through a non cell-autonomous mechanism since electroporated mouse *krox20* induces the expression of endogenous chick *krox20* in large cell patches throughout the hindbrain (Giudicelli et al., 2001).

Analyses of homozygous *krox20* mice mutants reveal that while segmentation in the hindbrain is maintained, there is a complete disappearance of r3 and r5 (Fig. 11) (Schneider-Maunoury et al., 1997; Schneider-Maunoury et al., 1993; Swiatek and Gridley, 1993; Voiculescu et al., 2001). Cells normally fated to become r3 instead acquire r2 or r4 identity while r5 cells acquire r6 identity. The rhombomere boundaries corresponding to r2/r3, r3/r4 and r4/r5, r5/r6 are no longer visible. The loss of r3 and r5 appear to have a substantional effect on the segmental organization of neurons in the hindbrain (Fig. 11). Trigeminal motor neurons (Vth nerve), which reside in subpopulations form r1 to r3, are reduced and instead of innervating the first branchial

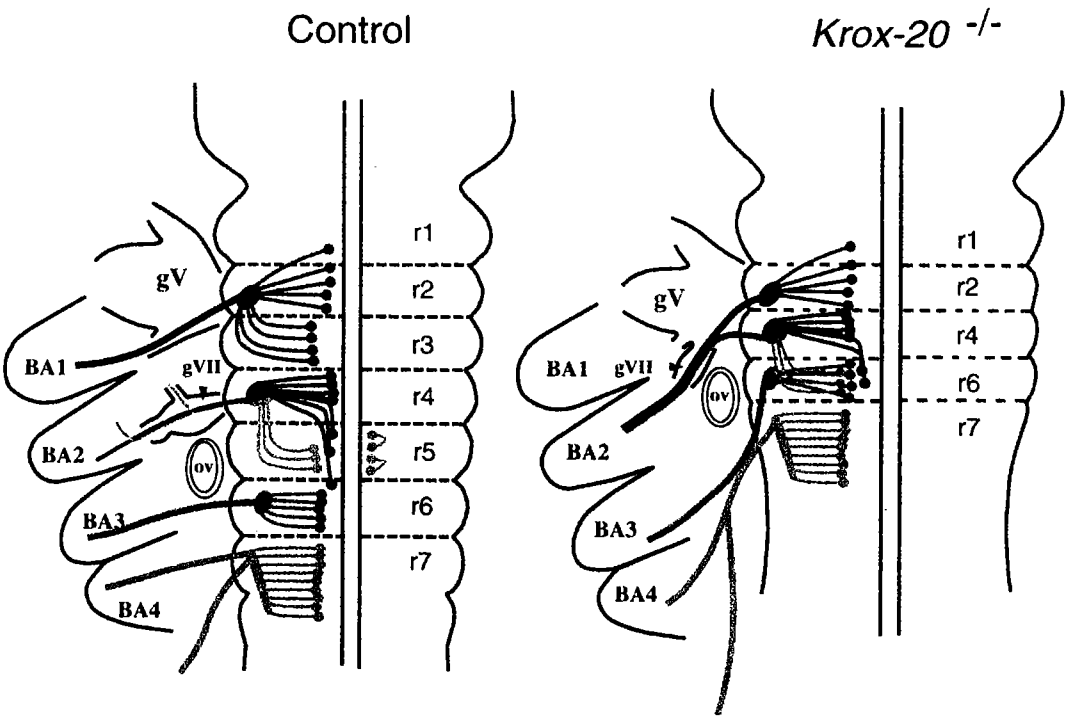


**Figure 11.** Homozygous *krox20* mice mutants display segmental and neuronal hindbrain defects. Schematic representation of branchiomotor neurons in the hindbrain of control and *krox20*$^{-/-}$ mice. Trigeminal (red), facial motor (dark blue), facial (light blue), abducens (orange), r6-derived facial (light purple), glossopharyngeal (green) and vagus (pink) neurons are shown. Abbreviations: r1-7, rhombomeres 1-7; gV, gill innervated by the Vth motor neuron pool; gVII, gill innervated by the facial motor neuron pool; BA1-4, branchial arches 1-4; ov, otic vesicle. Anterior is to the top. (From Schneider-Maunoury et al., 1997).

arch, they fasciculate with facial motor neurons (VIIth) from r4 into the second branchial arch. The abducens nerve (VIth) is absent and a population of facial neurons appears to arise from r6 and innervate the second branchial arch. The glossopharyngeal neurons (IXth) from r6 and the vagus motor neurons (Xth) from r7 appear to be partially fused, but migrate normally to innervate the third and fourth branchial arch, respectively.

Since some r3 and r5 cells persist in homozygous *krox20* mice mutants at an early stage, but then are integrated into neighboring rhombomeres, suggests that *krox20* maintains its own expression in r3 and r5. It has been proposed that *krox20* is first activated in a few cells, in the prospective r3 and r5 regions, and then recruits its own expression in nearby cells by a non cell-autonomous manner. Maintenance and regulation of *krox20* expression is then conferred by an auto-regulatory loop in a cell autonomous process. In addition, *krox20* expression is also mediated by the co-repressors NAB1 and NAB2 in a negative feedback loop (Mechta-Grigoriou et al., 2000; Russo et al., 1995; Svaren et al., 1996). The mouse NAB proteins were found to repress *krox20* transcriptional activity in cultured cells presumably through a transcription repression domain (Russo et al., 1995). The expression patterns of *nab1* and *nab2* closely overlaps with that of *krox20* in the developing mouse hindbrain demonstrating that these genes may regulate each other in vivo. Homozygous *krox20* mice mutants do not express either *nab1* or *nab2*, indicating that these genes are in fact downstream of *krox20* (Mechta-Grigoriou et al., 2000). The ectopic expression of *nab1* or *nab2* resulted in an alteration of r3 and r5 territories in which genes expressed in the r3 and r5 regions were reduced or appeared misshapen and the r4 region was expanded (Mechta-Grigoriou et al., 2000).

These results indicate that the *nab* genes can antagonize *krox20* activity and in turn, *krox20* can control the expression of its own antagonists in a regulated negative feedback manner. Thus, both gain of function and loss of function analyses determine that *krox20* is a key regulator in controlling early regionalization of the hindbrain. In addition, *krox20* is involved in the mediation of numerous specific genes expressed in the developing hindbrain (Nonchev et al., 1996a), and this will be discussed in greater detail in the next section.

*valentino subdivides a proto-segment into the r5 and r6 domains*

Another regulatory gene involved in the establishment and maintenance of a specific territory into distinct rhombomeres is the basic leucine zipper transcription factor *valentino* (or in the mouse, *kreisler*) (Cordes and Barsh, 1994; McKay et al., 1994; Moens et al., 1998; Moens et al., 1996; Prince et al., 1998b). The presumptive r5-r6 domain initially appears as a proto-segment that subsequently subdivides and expands into definitive rhombomeres. Time-lapse observations indicate that the r5/r6 boundary becomes visible after the appearance of the r4/r5 and r6/r7 boundaries (Moens et al., 1998). Analysis of *valentino* mutant embryos reveal that the hindbrain is reduced by the length of one rhombomere and a region, rX, remains and fail to form boundaries, subdivide or develop into r5 and r6 (Moens et al., 1996). Although the primary reticulospinal neurons, characteristic of r5 and r6, are still present in rX (however they are clustered together due to the shortened interval), motor neurons of the abducens cranial nerve (VIth) are almost absent in *valentino* mutant embryos (Moens et al., 1996).

Mosaic analysis demonstrates that *valentino* is required for cells to contribute either to r5 or r6 since the distribution of mutant (*valentino*$^-$) cells in a wild-type host embryo are excluded from r5 and r6 (Moens et al., 1996). These results indicate that the expression of *valentino* in r5 and r6 is required for the proper cell identity and division of the r5-r6 proto-segment into distinct domains. The segmentation gene *valentino* is also likely involved in the regulation (and function upstream) of genes expressed in r5 and r6 since *valentino* mutant embryos exhibit an expansion of r4 genes into the posterior hindbrain (Prince et al., 1998b). This result could be due to either the loss of inhibition for r4 gene expression in the r5-r6 domain or to an absence of the r4/5 boundary (Prince et al., 1998b).

*valentino* appears to be regulated by the homeobox transcription factor *vhnf1* (*variant hepatocyte nuclear factor 1*) since *vhnf1* mutant embryos, similar to *valentino* mutant embryos, exhibit a loss of gene expression in r5 and r6 and a transformation of this region to an r4-like identity (Sun and Hopkins, 2001; Wiellette and Sive, 2003). Since *vhnf1* mutant embryos were found not to express *valentino* and the misexpression of *vhnf1* in wild type embryos resulted in a rostral expansion of r5 genes (including *valentino*), *vhnf1* was suggested to function upstream of *valentino* (Sun and Hopkins, 2001). It is likely that *vhnf1*, synergizing with *fgf3* and *fgf8* signals, promotes the expression of *valentino* and thereby establishing r5 and r6 identity (Wiellette and Sive, 2003). Additionally, *vhnf1* is expressed in the prospective hindbrain during late gastrulation (Sun and Hopkins, 2001), suggesting that this gene can function as an early regulator of segmentation in the hindbrain.

## Specification of rhombomere identity

While the genes discussed in the previous section represent those that are involved for establishing a segmental pattern, factors that mediate the differentiation of individual rhombomeres are classified as segment identity genes. Loss of function analyses of these genes reveals that while individual segments are maintained, the rhombomeres are transformed with an altered identity. Gain of function analyses indicates that these factors can transform the characteristics of one particular segment into another. Thus, segment identity genes function in establishing specification of rhombomere identity and mediation of proper hindbrain segmentation.

*Rhombomere identity is conferred by the hox genes*

The *hox* genes, a conserved family of transcription factors related to the *Drosophila Homeotic* genes, are defined by a 60-amino acid DNA-binding region termed the homeobox (Krumlauf, 1994; McGinnis and Krumlauf, 1992; Scott and Weiner, 1984; Scott et al., 1983). Phylogenetic analysis reveal that zebrafish *hox* genes are organized into seven clusters (Amores et al., 1998), in which each gene is assigned to one of thirteen paralogue groups (Scott, 1992). *hox* genes from paralogue groups 1 through 4 are found to be expressed in the developing hindbrain during late gastrula stages (Prince et al., 1998a; Prince et al., 1998b). *hoxb1a* (functional equivalent to *hoxb1* in mice) and

*hoxb1b* (functional equivalent to *hoxa1* in mice) are both expressed in the presumptive r4 region (Amores et al., 1998; McClintock et al., 2002; Prince et al., 1998b). The expression of *hoxb1b* in r4 is transient – by segmentation stages, *hoxb1b* expression recedes caudally to the trunk of the embryo (Alexandre et al., 1996). While the expression of *hoxb1a* in the caudal hindbrain is also gradually lost (Prince et al., 1998b), an auto-regulatory positive feedback mechanism has been suggested to maintain the expression of *hoxb1a* in r4 (Popperl et al., 1995). Other genes expressed in the hindbrain during late gastrula include *hoxa2* in the presumptive r2/r3 (weakly expressed in the presumptive r4/r5), *hoxb2* in the presumptive r3/r4/r5, *hoxb3* in the presumptive r5/r6 and *hoxd4* (or *hoxb4*) in the presumptive r7 (Fig. 12) (Prince et al., 1998a; Prince et al., 1998b).

In recognition of the similar expression patterns between vertebrates, analysis of homozygous mice with targeted disruptions in the *hox* genes give insight to their counterpart function in the zebrafish hindbrain. Mice mutant in *hoxb1* (*hoxb1a*) exhibit a loss of r4-derived facial (VIIth) motorneurons (Goddard et al., 1996; Studer et al., 1996). This phenotype is similar to *hoxb1a*-deficient zebrafish embryos, in which VIIth nerve cell bodies fail to migrate (McClintock et al., 2002). Ectopic expression of *hoxb1a* in zebrafish reveal that r2 undergoes a r4 transformation – *hoxb1a* expression is apparent in r2, Mauthner neurons that normally reside in r4 are ectopically present from r2 to r4 and ectopic vestibular (nV) neurons form at r2 (McClintock et al., 2001). In addition, localized misexpression of *hoxb1* (*hoxb1a*) in chick embryos resulted in the loss of r2 motor neurons and presence of r4-like motor neurons in r2 (Bell et al., 1999). Mice

**Figure 12**

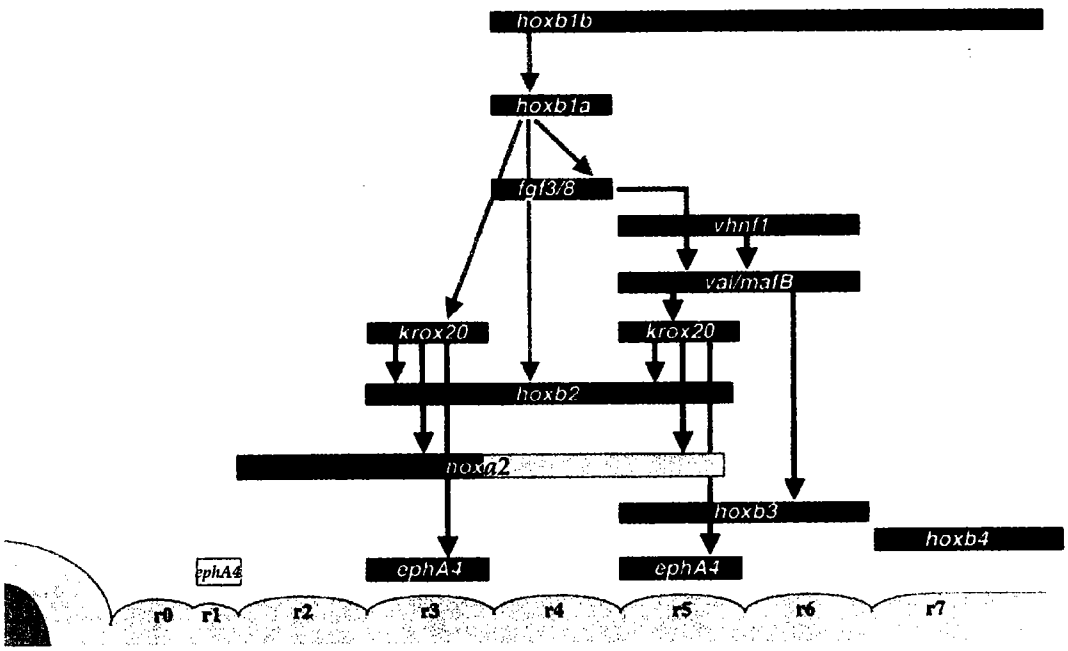


**Figure 12.** Gene regulatory interactions leads to proper segmental hindbrain patterning in the zebrafish embryo. Dark boxes correspond to gene expression domains, with light boxes denoting low expression levels. Arrows indicate regulatory relationships. Hindbrain is depicted with anterior to the left. Abbreviations: r0-7, rhombomeres 0-7. (Adapted from Waskiewicz et al., 2002).

mutant in *hoxa1* (*hoxb1b*) exhibit altered rhombomere compartments in which r5 is lost, r4 appears to be diminished and the r3 region is expanded (Barrow et al., 2000; Carpenter et al., 1993; Mark et al., 1993). Similarly, loss of *hoxb1b* function in zebrafish embryos resulted in an expansion of r3 and a reduction of the r4-r6 domains (McClintock et al., 2002). Transgenic mice ectopically expressing *hoxa1* (*hoxb1b*) exhibit r4-gene expression markers in r2/r3 and r2-derived neurons were transformed into neurons with r4-identity (Zhang et al., 1994). Likewise, ectopic expression of *hoxb1b* in zebrafish embryos resulted in a posterior transformation of r4 to r2 - r4-specific gene expression is present in r2 and r4-characteristic Mauthner neurons and motor neurons of the VIIth nerve form in r2/r3 (Alexandre et al., 1996; McClintock et al., 2001). Mice deficient in the *hoxa2* gene exhibit a transformation of the second pharyngeal arch into first arch identity (Gendron-Maguire et al., 1993; Rijli et al., 1993), while ectopic expression of *hoxa2* in *Xenopus* results in a reversed phenotype to that of the loss of function mutant (Pasqualetti et al., 2000). In all, these gain- and loss- of function phenotypes reveal that *hox* genes facilitate the identity of individual segments into distinct rhombomeres with specific gene expression profiles and neuronal cell sub-types.

The resulting alterations in rhombomere specificity and neuronal differentiation that arise from the disturbance of *hox* function suggest that these genes are tightly regulated (Fig. 12). Double mutants, lacking both *hoxb1* and *hoxa1* function, reveal that *hoxb1* expression in r4 is established and maintained through the presence of both *hoxb1* and *hoxa1* (Gavalas et al., 1998; Rossel and Capecchi, 1999; Studer et al., 1998). Mutants analysis extend these observations to suggest that *hoxb1b* (*hoxa1*) is required for the

initial expression of *hoxb1a* (*hoxb1*) in the anterior region of r4 (Barrow et al., 2000; McClintock et al., 2001) and *hoxb2* in r4 (Maconochie et al., 1997). The segment identity *hox* genes not only regulate their own expression but also are directly affected by the presence of priorly expressed segmentation genes (Fig. 12). *krox20* regulates the expression of *hoxa2* (Maconochie et al., 2001; Nonchev et al., 1996b) and *hoxb2* (Sham et al., 1993) in r4 and *hoxb3* (Seitanidou et al., 1997) in r5. In some cases, the activities of *hox* genes are found to have a synergistic effect on genes involved in segmentation. The phenotypes (see above) of *hoxa1*-deficient mice become more severe with the additional inactivation of one *krox20* allele, suggesting that *hoxa1* signals may synergize with *krox20* to specify and maintain r3-cell identity (Helmbacher et al., 1998). The involvement of segmentation genes regulating segment identity genes (Fig. 12) is further implicated with the finding that *vhnf1* activates *valentino* expression in r5 and r6 (Sun and Hopkins, 2001; Wiellette and Sive, 2003), which in turns regulates the expression of *krox20* and *hoxb3* in r5 (Manzanares et al., 1997; Manzanares et al., 1999b; Prince et al., 1998b) and the expression of *hoxa3* in r5 and r6 (Manzanares et al., 2001; Manzanares et al., 1999a). The gain- and loss- of function phenotypes reveal that *hox* genes not only confer segment identity but also may play a role in the organization of segmentation. The widespread appearance and similar expression patterns of *hox* genes in evolutionary distinct organisms signify their dual functional role and importance for proper development of the hindbrain.

The activity of *hox* genes during hindbrain development is also regulated by their association with the DNA binding-cofactors, Pbx and Meis, which are members of the

TALE (Three Amino acid Loop Extension) homeodomain family (Mann and Affolter, 1998). Elimination of *pbx4* function, through the use of homozygous mutant embryos with a recessive lethal allele (*lazarus*), results in the disruption of segmentation and segment identity in the hindbrain (Popperl et al., 2000). Specifically, *krox20* expression in r3 and r5 is reduced, with r3 failing to maintain its own expression while *hox* gene expression from r3 to the r6/7 boundary also fail to maintain its expression. In addition, motor neurons that originate from r4 fail to migrate posteriorly and r4-specific Mauthner cells are absent. These *pbx* mutants mimic the loss of *hox* function phenotypes in the mouse (see above) suggesting that *pbx*, through their interaction with the *hox* cofactors, is required for the proper coordination of head segmentation. Furthermore, the elimination of *pbx4* and *pbx2* function results in an anterior transformation of cell identities from r2 to r6 to that of r1, revealing that *pbx* activity is essential for specification of segment identity (Waskiewicz et al., 2002). Modulation of *hox* activity is also mediated by the association of *meis* with *pbx* and *hox*, which form a heterotrimeric complex and function in regulating hindbrain patterning (Choe et al., 2002; Vlachakis et al., 2001; Vlachakis et al., 2000; Waskiewicz et al., 2001). Gain of function analysis, through the ectopic expression of the heterotrimeric complex, resulted in an extensive transformation of anterior (forebrain and midbrain) fates to more posterior (hindbrain or spinal cord) fates (Dibner et al., 2001; Vlachakis et al., 2001). Since the misexpression of *meis* and *hox* mutant constructs with reduced *pbx* binding activity resulted in a reduction of the phenotype, this suggests that *pbx* interaction, and thus trimeric association is necessary for the promotion of hindbrain fates (Vlachakis et al., 2001). In addition, the expression

of dominant negative *meis* (removal of the DNA-binding domain) or *pbx* (lacking the nuclear localization motif) constructs resulted in phenotypes similar to mutants that are deficient in *pbx* (*lazarus*) or *hox* function (as stated above) (Choe et al., 2002; Waskiewicz et al., 2001). These results strongly suggest that the heterotrimeric complex of *hox*, *pbx* and *meis* is required for specification of hindbrain fates.

## Restriction of segment identity within the hindbrain

In order to properly establish segmental identity of individual rhombomeres, gene expression must be organized and tightly restricted to defined domains. Mechanisms that underlie these complex functions include plasticity or regulation of cell identity as well as cell sorting events. Both processes are involved in contributing to the gradual sharpening of adjacent rhombomere-restricted gene expression domains and the subsequent maintenance of boundary formation.

### *Cell sorting is mediated by specific gene expression*

The restriction of cell movement across rhombomere boundaries is demonstrated with the finding that alternating cellular properties within the hindbrain causes r3/r5 cells to be immiscible with cells from r2/r4/r6 (Fraser et al., 1990; Guthrie and Lumsden, 1991; Guthrie et al., 1993). This suggests that mechanisms that regulate the repressive interactions that occur between cells expressing different genes are indeed imperative for

conferring segmental specification. For example, explants of r5 cells, but not r3 cells, appear to express *krox20* regardless if they are cultured in the presence or absence of adjoining hindbrain segments (Graham and Lumsden, 1996). Both mutant and wild-type embryo analyses support the suggestion that *krox20* expression in r3 is dependent on neighboring influences (such as signals expressed in r4), while *krox20* expression in r5 appear to be under intrinsic control (Barrow et al., 2000). *hoxa1/hoxb1* double mutants in mice do not express *krox20* in r3, however *krox20* expression is apparent in r4 and r5 despite the absence of *hoxa1* and *hoxb1* (Rossel and Capecchi, 1999). Analysis of wild-type embryos indicate that *krox20* expression is activated just anteriorly (in r3) to the initial expression of *hoxb1a* (*hoxb1*) and *hoxb1b* (*hoxa1*) in r4, and *krox20* expression in r5 is apparent only after the retreat of *hoxb1a* and *hoxb1b* expression in r5 (Barrow et al., 2000; McClintock et al., 2001). Thus, the mechanisms that activate the expression of *krox20* in r3 appear different from those which activate *krox20* expression in r5 (Barrow et al., 2000). Taken together, these findings support a dual role of *hox* gene activity in which their presence from an adjacent rhombomere promotes r3 cell identity while their absence in r5 promotes proper r5 cell identity. More importantly, the mechanisms that regulate these processes serve as an example by which cell identity and sorting are coupled in order to dictate restricted segmental domains in the hindbrain.

*Eph-ephrin signaling restrict sorting of cells*

Candidates for a role in rhombomere-specific cell sorting include the Eph family of receptor tyrosine kinases and their associated ligands, the ephrins (Lumsden, 1999; Xu

and Wilkinson, 1997). The Eph receptors are divided into two subclasses (A and B) on their basis of their comparative sequence homologies and ligand affinity (Holder and Klein, 1999). The Eph receptor (Fig. 13) consists of: an extracellular domain, which is composed of a ligand-binding globular domain, a cysteine-rich region and two fibronectin type II repeats (of which may be involved in Eph receptor clustering); a transmembrane region; and a cytoplasmic domain, which consists of a juxtamembrane region, a kinase domain, and the sterile α–motif (SAM) and PDZ domain (both of which function in mediating protein-protein interactions) (Himanen and Nikolov, 2003; Kullander and Klein, 2002). The ephrin ligands can be classified into two classes on the basis of their membrane attachment - ephrinA proteins, which are tethered through a glycosylphosphatidylinositol (GPI) linkage and ephrinB proteins (Fig. 13), which have a transmembrane domain, followed by a cytoplasmic tail and a PDZ-binding motif (Kullander and Klein, 2002). Eph receptors generally bind to their respective ligand of the same class with the exception of EphA4, which binds to both class A and B ephrins (Flanagan and Vanderhaeghen, 1998).

Eph receptor-ephrin interactions are suggested to participate in boundary formation since their expression patterns fall into complementary domains. In the mouse, *Eph* receptors (*EphA4*, *EphB2* and *EphB3*) are found in r3 and r5 while their ligands (*ephrinB1*, *ephrinB2* and *ephrinB3*) are expressed in r2, r4 and r6 (Becker et al., 1994; Flenniken et al., 1996; Nieto et al., 1992). In the zebrafish, *ephrinB2* is expressed in r1, r4 and r7 while *EphA4* is expressed in r3 and r5 and *EphB4* is expressed in r2, r5 and r6 (Durbin et al., 1998; Xu et al., 1995). Since the interactions of Eph receptor-expressing

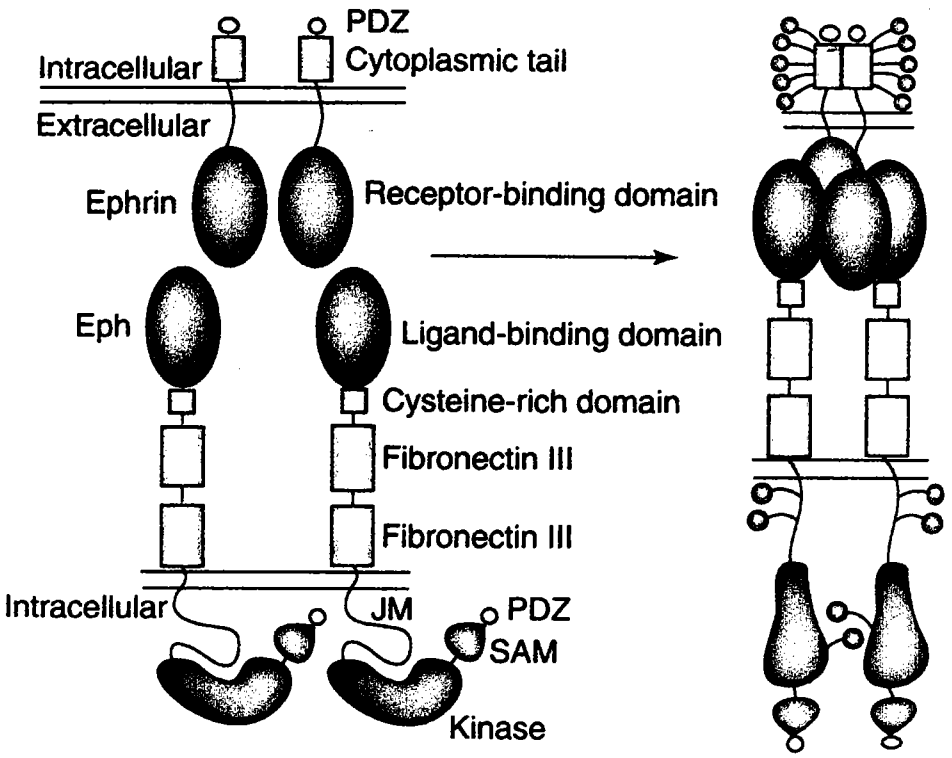


**Figure 13.** Structure of Eph receptors-ephrins and their clustering. Thin lines represent plasma membrane. Class B ephrins are depicted in schematic. Ephrin receptor-binding domain is shown in red, Eph ligand-binding domain is shown in dark blue, phosphate groups are labeled in purple and kinase and SAM domains are shown in light blue. Abbreviations: PDZ, PSD95/Dlg/ZO1 (PDZ)-binding motif; JM, juxtamembrane region; SAM, sterile α-motif. (Adapted from Himanen and Nikolov, 2003).

cells and ephrin-expressing cells occur at the boundaries of rhombomeres, it is likely that their mutual repulsion governs cell sorting and mediate their interface.

Activation of Eph-ephrin signaling occurs through two mechanisms that both involve clustering of Eph receptors (Murai and Pasquale, 2003). A trimer composed of two Eph receptors and one ephrin-ligand is sufficient to bring two intracellular kinase domains (of the Eph receptors) together to initiate unidirectional or 'forward' signaling (Kullander and Klein, 2002). A tetramer composed of two Eph receptors interacting with two ephrin-ligands (Fig. 13) is sufficient to initiate bidirectional ('forward' and 'reverse') signaling through tyrosine phosphorylation of the intracellular domains of ephrinB-ligands upon receptor binding (Kullander and Klein, 2002). Interference of signaling could occur through the generation of truncated receptors or ligands (Cooke and Moens, 2002). The association of an Eph receptor or ephrinB-ligand without an intracellular domain to their respective endogenous receptor/ligand-binding partner results in propagation of a signal in only one direction (through the endogenous receptor or ligand intracellular domain) since the truncated receptor/ligand lacks a kinase domain and cannot transduce a signal back into their own cell (Mellitzer et al., 1999; Xu et al., 1995). Soluble forms of ephrinB-ligands are able to block receptor clustering and competitively inhibit the binding of endogenous ligands to receptors thus blocking bi-directional signaling (Davis et al., 1994; Krull et al., 1997).

Functional studies utilizing these truncated Eph receptor or ephrin-ligand constructs revealed that Eph signaling plays a major role for the propagation of restricted cell sorting. Eph-ephrin interactions are involved in early developmental events such as

the control of cellular movements during gastrula stages (Chan et al., 2001). The expression of soluble forms of *ephA3* or *ephrinA5* in zebrafish embryos result in a perturbance of involution and convergence movements that occur during gastrulation (Oates et al., 1999). The ectopic expression of *ephA4* or *ephrinB1* in Xenopus embryos results in a loss of cell adhesion prior to the onset of gastrulation (Jones et al., 1998; Winning et al., 1996) while mutations in a *C. elegans* Eph receptor disrupt neuroblast movements during closure of the ventral gastrulation cleft (George et al., 1998). More importantly, Eph-ephrin signaling also mediates cell sorting and the subsequent formation of sharply bordered gene expression domains in the hindbrain. The misexpression of a truncated *Eph* receptor in zebrafish and *Xenopus* embryos resulted in the expansion of (or ectopic) gene expression from r3 and r5 into the boundaries of adjacent r2, r4 and r6 domains (Xu et al., 1999; Xu et al., 1995). The misexpression of a full-length *Eph* receptor resulted in a similar phenotype, with ectopically-expressing *Eph* receptor cells localizing to the boundaries of even-number rhombomeres, while contributing to odd-numbered rhombomeres (Cooke et al., 2001). Conversely, the misexpression of truncated or full-length *ephrinB2a* in zebrafish embryos resulted in ectopically expressing *ephrinB2a* cells localizing to the boundaries of r3 and r5, while distributed in a scattered fashion within r2, r4 and r6 (Cooke et al., 2001; Xu et al., 1999).

The involvement of Eph-ephrin signaling in rhombomere-specific cell sorting is also exemplified by mutant analysis of the *valentino* segmentation gene in zebrafish embryos. These mutant embryos fail to subdivide a proto-segment into the r5 and r6 domains and do not exhibit proper formation of the r4/r5 and r6/r7 boundaries (Cooke et

al., 2001; Moens et al., 1996). Specifically, *ephB4* expression is lost in r5 and r6 and *ephrinB2a* expression expands from r4 throughout r7 (Cooke et al., 2001). Using a genetic mosaic approach, *valentino*$^-$ cells (which are *ephB4*$^-$ and *ephrinB2a*$^+$) transplanted into a wild-type host are excluded from r5 and r6 (Cooke et al., 2001; Moens et al., 1996). However, when wild-type cells are transplanted into a *valentino*$^-$ host embryo, an interface is established between the host cells in the proto-segment that express *erphrinB2a* and the transplanted wild-type 'clump' of cells that express *ephB4* (Cooke et al., 2001). Furthermore, while transplanted *valentino*$^-$ cells that were injected with *ephB4a* can partially contribute to r5 and r6 of wild-type hosts, the blocking of EphB signaling (through the injection of soluble *ephrinB2a* ligands) enabled *valentino*$^-$ donor cells to fully contribute to the r5 and r6 domains (Cooke et al., 2001). This suggests that *valentino*, in addition specifying r5 and r6 identity (see above), can control the complementary *eph/ephrin* gene expression domains. Another segmentation gene that functions upstream of Eph signaling is *krox20*, which can regulate the expression of *ephA4* in r3 and r5 (Theil et al., 1998). Taken together, these results indicate that Eph-ephrin signaling is essential for establishing and maintaining segmental integrity and the proper formation of rhombomere boundaries.

*Plasticity in rhombomere boundary formation*

The regulation of cell sorting, as indicated by the repulsive interactions that occur between cells from adjacent rhombomeres and the adhesive interactions that occur between cells from the same rhombomere, is mediated by Eph-ephrin signaling and is an

important contributor for proper rhombomere boundary formation. Another mechanism that can control the sharpening of rhombomere boundaries is cell plasticity, which is the ability for a cell to alter its specific segment identity in response to its environment (Trainor and Krumlauf, 2000b). Transplantation of cells between different hindbrain rhombomeres in the zebrafish or mouse embryo reveal that the donor cells can indeed regulate differential gene expression (such as the *hox* genes) according to their new surroundings (Schilling et al., 2001; Trainor and Krumlauf, 2000a). These set of transpositions also indicate that individual cell transplants are more likely to exhibit plasticity than those which reside in the center of larger cell transplants and transplantation of cells at a later stage of development were likely to remain committed to their original fate (Schilling et al., 2001). These results suggest that cells do have the ability to exhibit plasticity however, they may progressively lose plasticity as their segmental identities become finalized and rhombomere boundaries form. Thus, it is likely that both the mechanisms of cell sorting and plasticity might cooperate in the formation of distinguishable expression domains and maintenance of rhombomere boundaries.

## Identification of novel genes involved in hindbrain development

In spite of the large number of genes identified, they cannot account for all the mechanisms that are responsible for the regionalization, specification and segmentation of the hindbrain. In order to characterize additional genes that may be involved in the

regulation of hindbrain development, the isolation of novel genes that are expressed in the prospective hindbrain must first be undertaken. Utilizing a subtractive hybridization-based screen, candidate novel genes that are expressed in the dorsoposterior region (which are specified to hindbrain fates) of the zebrafish embryo were isolated (Sagerstrom et al., 2001). In short, cDNAs generated from RNAs expressed in the anterior neuroectoderm at mid-gastrula stages were subtracted from cDNAs generated from RNAs expressed in the posterior neuroectoderm (at the same stage). This approach will enrich for genes only expressed in the posterior neuroectoderm of the embryo and subsequently a dozen genes were found to be expressed in the presumptive hindbrain at mid-gastrula stages (Sagerstrom et al., 2001). The expression of five of these posteriorly-restricted genes have been previously reported and include *hoxb1b* (Alexandre et al., 1996), *wnt5* (Blader et al., 1996; Rauch et al., 1997), *caudal* (Joly et al., 1992), *Myf5* (Braun et al., 1989) and *MesP1* (Saga et al., 1996). The remaining seven isolated genes were novel and are suggested to be candidates for specification and segmentation of the hindbrain (Sagerstrom et al., 2001). Characterization of the novel-isolated gene, *meis3*, reveals that it is a multifunctional regulator of *hox* activity and is integral for hindbrain specification (Choe et al., 2002; Vlachakis et al., 2001; Vlachakis et al., 2000; Waskiewicz et al., 2001). The *lmo4* gene, of which I have independently cloned and initially characterized the expression pattern, only represented a minor part of my graduate work and will not be discussed and only included as an appendix. In this thesis, I will describe the characterization of *nlz* and its novel family of zinc-finger containing proteins and their functional role in regulating segmental gene expression in the hindbrain

in chapters I and II. Furthermore, I will broadly describe possible mechanisms underlying *nlz* function in the discussion.

## References


Alexandre, D., Clarke, J. D., Oxtoby, E., Yan, Y. L., Jowett, T., and Holder, N. (1996). Ectopic expression of Hoxa-1 in the zebrafish alters the fate of the mandibular arch neural crest and phenocopies a retinoic acid-induced phenotype. *Development* **122,** 735-746.

Amores, A., Force, A., Yan, Y. L., Joly, L., Amemiya, C., Fritz, A., Ho, R. K., Langeland, J., Prince, V., Wang, Y. L., Westerfield, M., Ekker, M., and Postlethwait, J. H. (1998). Zebrafish hox clusters and vertebrate genome evolution. *Science* **282,** 1711-4.

Anderson, D. J. (1997). Cellular and molecular biology of neural crest cell lineage determination. *Trends Genet* **13,** 276-80.

Anderson, D. J., Groves, A., Lo, L., Ma, Q., Rao, M., Shah, N. M., and Sommer, L. (1997). Cell lineage determination and the control of neuronal identity in the neural crest. *Cold Spring Harb Symp Quant Biol* **62,** 493-504.

Barrow, J. R., Stadler, H. S., and Capecchi, M. R. (2000). Roles of Hoxa1 and Hoxa2 in patterning the early hindbrain of the mouse. *Development* **127,** 933-44.

Becker, N., Seitanidou, T., Murphy, P., Mattei, M.-G., Topilko, P., Nieto, M. A., Wilkinson, D. G., Charnay, P., and Gilardi-Hebenstreit, P. (1994). Several receptor tyrosine kinases of the Eph family are segmentally expressed in the developing hindbrain. *Mech. Dev.* **47,** 3-17.

Begemann, G., Schilling, T. F., Rauch, G. J., Geisler, R., and Ingham, P. W. (2001). The zebrafish neckless mutation reveals a requirement for raldh2 in mesodermal signals that pattern the hindbrain. *Development* **128,** 3081-94.

Bell, E., Wingate, R. J., and Lumsden, A. (1999). Homeotic transformation of rhombomere identity after localized Hoxb1 misexpression. *Science* **284,** 2168-71.

Belting, H. G., Hauptmann, G., Meyer, D., Abdelilah-Seyfried, S., Chitnis, A., Eschbach, C., Soll, I., Thisse, C., Thisse, B., Artinger, K. B., Lunde, K., and Driever, W. (2001). spiel ohne grenzen/pou2 is required during establishment of the zebrafish midbrain-hindbrain boundary organizer. *Development* **128,** 4165-76.

Bernhardt, R. R., Goerlinger, S., Roos, M., and Schachner, M. (1998). Anterior-posterior subdivision of the somite in embryonic zebrafish: implications for motor axon guidance. *Dev Dyn* **213,** 334-47.

Biben, C., Stanley, E., Fabri, L., Kotecha, S., Rhinn, M., Drinkwater, C., Lah, M., Wang, C. C., Nash, A., Hilton, D., Ang, S. L., Mohun, T., and Harvey, R. P. (1998). Murine cerberus homologue mCer-1: a candidate anterior patterning molecule. *Dev Biol* **194,** 135-51.

Blader, P., Strahle, U., and Ingham, P. W. (1996). Three Wnt genes expressed in a wide variety of tissues during development of the zebrafish, Danio rerio: Developmental and evolutionary perspectives. *Dev. Genes Evol.* **206,** 3.

Boettger, T., Knoetgen, H., Wittler, L., and Kessel, M. (2001). The avian organizer. *Int J Dev Biol* **45,** 281-7.

Brand, M., Heisenberg, C. P., Jiang, Y. J., Beuchle, D., Lun, K., Furutani-Seiki, M., Granato, M., Haffter, P., Hammerschmidt, M., Kane, D. A., Kelsh, R. N., Mullins, M. C., Odenthal, J., van Eeden, F. J., and Nusslein-Volhard, C. (1996). Mutations in zebrafish genes affecting the formation of the boundary between midbrain and hindbrain. *Development* **123,** 179-90.

Braun, T., Buschhausen-Denker, G., Bober, E., Tannich, E., and Arnold, H. H. (1989). A novel human muscle factor related to but distinct from MyoD1 induces myogenic conversion in 10T1/2 fibroblasts. *Embo J* **8,** 701-9.

Bronner-Fraser, M. (1994). Neural crest cell formation and migration in the developing embryo. *Faseb J* **8,** 699-706.

Burgess, S., Reim, G., Chen, W., Hopkins, N., and Brand, M. (2002). The zebrafish spiel-ohne-grenzen (spg) gene encodes the POU domain protein Pou2 related to mammalian Oct4 and is essential for formation of the midbrain and hindbrain, and for pre-gastrula morphogenesis. *Development* **129,** 905-16.

Carpenter, E. M., Goddard, J. M., Chisaka, O., Manley, N. R., and Capecchi, M. R. (1993). Loss of Hox-A1 (Hox-1.6) function results in the reorganization of the murine hindbrain. *Development* **118,** 1063-1075.

Chan, J., Mably, J. D., Serluca, F. C., Chen, J. N., Goldstein, N. B., Thomas, M. C., Cleary, J. A., Brennan, C., Fishman, M. C., and Roberts, T. M. (2001). Morphogenesis of prechordal plate and notochord requires intact Eph/ephrin B signaling. *Dev Biol* **234,** 470-82.

Chandrasekhar, A., Moens, C. B., Warren, J. T., Jr., Kimmel, C. B., and Kuwada, J. Y. (1997). Development of branchiomotor neurons in zebrafish. *Development* **124,** 2633-44.

Chavrier, P., Vesque, C., Galliot, B., Vigneron, M., Dolle, P., Duboule, D., and Charnay, P. (1990). The segment-specific gene Krox-20 encodes a transcription factor with binding sites in the promoter region of the Hox-1.4 gene. *Embo J* **9,** 1209-18.

Chavrier, P., Zerial, M., Lemaire, P., Almendral, J., Bravo, R., and Charnay, P. (1988). A gene encoding a protein with zinc fingers is activated during G0/G1 transition in cultured cells. *Embo J* **7,** 29-35.

Choe, S. K., Vlachakis, N., and Sagerstrom, C. G. (2002). Meis family proteins are required for hindbrain development in the zebrafish. *Development* **129,** 585-95.

Concha, M. L., and Adams, R. J. (1998). Oriented cell divisions and cellular morphogenesis in the zebrafish gastrula and neurula: a time-lapse analysis. *Development* **125,** 983-94.

Cooke, J., Moens, C., Roth, L., Durbin, L., Shiomi, K., Brennan, C., Kimmel, C., Wilson, S., and Holder, N. (2001). Eph signalling functions downstream of Val to regulate cell sorting and boundary formation in the caudal hindbrain. *Development* **128,** 571-80.

Cooke, J. E., and Moens, C. B. (2002). Boundary formation in the hindbrain: Eph only it were simple. *Trends Neurosci* **25,** 260-7.

Cooper, M. S., and D'Amico, L. A. (1996). A cluster of noninvoluting endocytic cells at the margin of the zebrafish blastoderm marks the site of embryonic shield formation. *Dev Biol* **180,** 184-98.

Cordes, S. P., and Barsh, G. S. (1994). The mouse segmentation gene kr encodes a novel basic domain-leucine zipper transcription factor. *Cell* **79,** 1025-1034.

Davis, S., Gale, N. W., Aldrich, T. H., Maisonpierre, P. C., Lhotak, V., Pawson, T., Goldfarb, M., and Yancopoulos, G. D. (1994). Ligands for EPH-related receptor tyrosine kinases that require membrane attachment or clustering for activity. *Science* **266,** 816-9.

Dibner, C., Elias, S., and Frank, D. (2001). XMeis3 protein activity is required for proper hindbrain patterning in Xenopus laevis embryos. *Development* **128,** 3415-26.

Driever, W., Solnica-Krezel, L., Abdelilah, S., Meyer, D., and Stemple, D. (1997). Genetic analysis of pattern formation in the zebrafish neural plate. *Cold Spring Harb Symp Quant Biol* **62,** 523-34.

Dupe, V., and Lumsden, A. (2001). Hindbrain patterning involves graded responses to retinoic acid signalling. *Development* **128,** 2199-208.

Durbin, L., Brennan, C., Shiomi, K., Cooke, J., Barrios, A., Shanmugalingam, S., Guthrie, B., Lindberg, R., and Holder, N. (1998). Eph signaling is required for segmentation and differentiation of the somites. *Genes Dev* **12,** 3096-109.

Durston, A., Timmermans, J., Jage, W., Hendricks, H., deVries, N., Heidiveld, M., and Nieuwkoop, P. (1989). Retinoic acid causes an anteroposterior transformation in the developing central nervous system. *Nature* **340,** 140-144.

Durston, A. J., van der Wees, J., Pijnappel, W. W., and Godsave, S. F. (1998). Retinoids and related signals in early development of the vertebrate central nervous system. *Curr Top Dev Biol* **40,** 111-75.

Eisen, J. S., Myers, P. Z., and Westerfield, M. (1986). Pathway selection by growth cones of identified motoneurones in live zebra fish embryos. *Nature* **320,** 269-71.

Erter, C. E., Wilm, T. P., Basler, N., Wright, C. V., and Solnica-Krezel, L. (2001). Wnt8 is required in lateral mesendodermal precursors for neural posteriorization in vivo. *Development* **128,** 3571-83.

Feldman, B., Gates, M. A., Egan, E. S., Dougan, S. T., Rennebeck, G., Sirotkin, H. I., Schier, A. F., and Talbot, W. S. (1998). Zebrafish organizer development and germ-layer formation require nodal-related signals. *Nature* **395,** 181-5.

Flanagan, J. G., and Vanderhaeghen, P. (1998). The ephrins and Eph receptors in neural development. *Annu Rev Neurosci* **21,** 309-45.

Flenniken, A. M., Gale, N. W., Yancopoulos, G. D., and Wilkinson, D. G. (1996). Distinct and overlapping expression of ligands for Eph-related receptor tyrosine kinases during mouse embryogenesis. *Dev. Biol.* **179,** 382-401.

Foreman, M. B., and Eaton, R. C. (1993). The direction change concept for reticulospinal control of goldfish escape. *J Neurosci* **13,** 4101-13.

Fraser, S., Keynes, R., and Lumsden, A. (1990). Segmentation in the chick embryo hindbrain is defined by cell lineage restrictions. *Nature* **344,** 431-5.

Furthauer, M., Thisse, C., and Thisse, B. (1997). A role for FGF-8 in the dorsoventral patterning of the zebrafish gastrula. *Development* **124,** 4253-64.

Gavalas, A., Studer, M., Lumsden, A., Rijli, F. M., Krumlauf, R., and Chambon, P. (1998). Hoxa1 and Hoxb1 synergize in patterning the hindbrain, cranial nerves and second pharyngeal arch. *Development* **125,** 1123-36.

Gendron-Maguire, M., Mallo, M., Zhang, M., and Gridley, T. (1993). Hoxa-2 mutant mice exhibit homeotic transformation of skeletal elements derived from cranial neural crest. *Cell* **75,** 1317-31.

George, S. E., Simokat, K., Hardin, J., and Chisholm, A. D. (1998). The VAB-1 Eph receptor tyrosine kinase functions in neural and epithelial morphogenesis in C. elegans. *Cell* **92,** 633-43.

Giudicelli, F., Taillebourg, E., Charnay, P., and Gilardi-Hebenstreit, P. (2001). Krox-20 patterns the hindbrain through both cell-autonomous and non cell-autonomous mechanisms. *Genes Dev* **15,** 567-80.

Glinka, A., Wu, W., Onichtchouk, D., Blumenstock, C., and Niehrs, C. (1997). Head induction by simultaneous repression of Bmp and Wnt signalling in Xenopus. *Nature* **389,** 517-9.

Goddard, J. M., Rossel, M., Manley, N. R., and Capecchi, M. R. (1996). Mice with targeted disruption of Hoxb-1 fail to form the motor nucleus of the VII nerve. *Development* **122,** 3217-3226.

Godsave, S. F., Koster, C. H., Getahun, A., Mathu, M., Hooiveld, M., van der Wees, J., Hendriks, J., and Durston, A. J. (1998). Graded retinoid responses in the developing hindbrain. *Dev Dyn* **213,** 39-49.

Graham, A., and Lumsden, A. (1996). Interactions between rhombomeres modulate Krox-20 and follistatin expression in the chick embryo hindbrain. *Development* **122,** 473-80.

Griffin, K., Patient, R., and Holder, N. (1995). Analysis of Fgf function in normal and *no tail* zebrafish embryos reveals separate mechanisms for formation of the trunk and the tail. *Development* **121,** 2983-2994.

Gritsman, K., Talbot, W. S., and Schier, A. F. (2000). Nodal signaling patterns the organizer. *Development* **127,** 921-32.

Grunwald, D. J., Kimmel, C. B., Westerfield, M., Walker, C., and Streisinger, G. (1988). A neural degeneration mutation that spares primary neurons in the zebrafish. *Dev Biol* **126,** 115-28.

Guo, S., Brush, J., Teraoka, H., Goddard, A., Wilson, S. W., Mullins, M. C., and Rosenthal, A. (1999). Development of noradrenergic neurons in the zebrafish hindbrain requires BMP, FGF8, and the homeodomain protein soulless/Phox2a. *Neuron* **24,** 555-66.

Guthrie, S., and Lumsden, A. (1991). Formation and regeneration of rhombomere boundaries in the developing chick hindbrain. *Development* **112,** 221-9.

Guthrie, S., Prince, V., and Lumsden, A. (1993). Selective dispersal of avian rhombomere cells in orthotopic and heterotopic grafts. *Development* **118,** 527-38.

Haddon, C., and Lewis, J. (1996). Early ear development in the embryo of the zebrafish, Danio rerio. *J Comp Neurol* **365,** 113-28.

Hanneman, E., Trevarrow, B., Metcalfe, W. K., Kimmel, C. B., and Westerfield, M. (1988). Segmental pattern of development of the hindbrain and spinal cord of the zebrafish embryo. *Development* **103,** 49-58.

Hansen, A., and Zeiske, E. (1993). Development of the olfactory organ in the zebrafish, Brachydanio rerio. *J Comp Neurol* **333,** 289-300.

Harland, R., and Gerhart, J. (1997). Formation and function of Spemann's organizer. *Annu Rev Cell Dev Biol* **13,** 611-67.

Hauptmann, G., Belting, H. G., Wolke, U., Lunde, K., Soll, I., Abdelilah-Seyfried, S., Prince, V., and Driever, W. (2002). spiel ohne grenzen/pou2 is required for zebrafish hindbrain segmentation. *Development* **129,** 1645-55.

Hauptmann, G., and Gerster, T. (1995). Pou-2--a zebrafish gene active during cleavage stages and in the early hindbrain. *Mech Dev* **51,** 127-38.

Heisenberg, C. P., Houart, C., Take-Uchi, M., Rauch, G. J., Young, N., Coutinho, P., Masai, I., Caneparo, L., Concha, M. L., Geisler, R., Dale, T. C., Wilson, S. W., and Stemple, D. L. (2001). A mutation in the Gsk3-binding domain of zebrafish Masterblind/Axin1 leads to a fate transformation of telencephalon and eyes to diencephalon. *Genes Dev* **15,** 1427-34.

Helmbacher, F., Pujades, C., Desmarquet, C., Frain, M., Rijli, F. M., Chambon, P., and Charnay, P. (1998). Hoxa1 and Krox-20 synergize to control the development of rhombomere 3. *Development* **125,** 4739-48.

Hemmati-Brivanlou, A., Kelly, O. G., and Melton, D. A. (1994). Follistatin, an antagonist of activin, is expressed in the Spemann organizer and displays direct neuralizing activity. *Cell* **77,** 283-295.

Higashijima, S., Hotta, Y., and Okamoto, H. (2000). Visualization of cranial motor neurons in live transgenic zebrafish expressing green fluorescent protein under the control of the islet-1 promoter/enhancer. *J Neurosci* **20,** 206-18.

Hill, J., Clarke, D. W. J., Vargesson, L., Jowett, T., and Holder, N. (1995). Exogenous retinoic acid causes specific alterations in the development of the midbrain and hindbrain of the zebrafish embryo including positional respecification of the Mauthner neuron. *Mech. Dev.* **50,** 3-16.

Himanen, J. P., and Nikolov, D. B. (2003). Eph signaling: a structural view. *Trends Neurosci* **26,** 46-51.

Ho, R. K., and Kimmel, C. B. (1993). Commitment of cell fate in the early zebrafish embryo. *Science* **261,** 109-111.

Holder, N., and Hill, J. (1991). Retinoic acid modifies development of the midbrain-hindbrain border and affects cranial ganglion formation in zebrafish embryos. *Development* **113,** 1159-1170.

Holder, N., and Klein, R. (1999). Eph receptors and ephrins: effectors of morphogenesis. *Development* **126,** 2033-44.

Irving, C., and Mason, I. (2000). Signalling by FGF8 from the isthmus patterns anterior hindbrain and establishes the anterior limit of Hox gene expression. *Development* **127,** 177-86.

Joly, J. S., Maury, M., Joly, C., Duprey, P., Boulekbache, H., and Condamine, H. (1992). Expression of a zebrafish caudal homeobox gene correlates with the establishment of posterior cell lineages at gastrulation. *Differentiation* **50,** 75-87.

Jones, T. L., Chong, L. D., Kim, J., Xu, R. H., Kung, H. F., and Daar, I. O. (1998). Loss of cell adhesion in Xenopus laevis embryos mediated by the cytoplasmic domain of XLerk, an erythropoietin-producing hepatocellular ligand. *Proc Natl Acad Sci U S A* **95,** 576-81.

Joubin, K., and Stern, C. D. (1999). Molecular interactions continuously define the organizer during the cell movements of gastrulation. *Cell* **98,** 559-71.

Kandel, E. R., Schwartz, J. H., and Jessell, T. M. (1991). "Principles of Neural Science." Appleton & Lange, Norwalk, Connecticut.

Kane, D. A., and Kimmel, C. B. (1993). The zebrafish midblastula transition. *Development* **119,** 447-56.

Kanki, J. P., and Ho, R. K. (1997). The development of the posterior body in zebrafish. *Development* **124,** 881-93.

Keller, R. E. (1980). The cellular basis of epiboly: an SEM study of deep-cell rearrangement during gastrulation in Xenopus laevis. *J Embryol Exp Morphol* **60,** 201-34.

Kengaku, M., and Okamoto, H. (1995). bFGF as a possible morphogen for the anteroposterior axis of the central nervous system in *Xenopus*. *Development* **121,** 3121-3130.

Kim, C. H., Oda, T., Itoh, M., Jiang, D., Artinger, K. B., Chandrasekharappa, S. C., Driever, W., and Chitnis, A. B. (2000). Repressor activity of Headless/Tcf3 is essential for vertebrate head formation. *Nature* **407,** 913-6.

Kimmel, C. B. (1993). Patterning the brain of the zebrafish embryo. *Annu. Rev. Neurosci.* **16,** 707-732.

Kimmel, C. B., Ballard, W. W., Kimmel, S. R., Ullman, B., and Schilling, T. F. (1995). Stages of embryonic development of the zebrafish. *Dev. Dynamics* **203,** 253-310.

Kimmel, C. B., and Law, R. D. (1985a). Cell lineage of zebrafish blastomeres. I. Cleavage pattern and cytoplasmic bridges between cells. *Dev Biol* **108,** 78-85.

Kimmel, C. B., and Law, R. D. (1985b). Cell lineage of zebrafish blastomeres. II. Formation of the yolk syncytial layer. *Dev Biol* **108,** 86-93.

Kimmel, C. B., and Warga, R. M. (1987). Indeterminate cell lineage of the zebrafish embryo. *Dev. Biol.* **124,** 269-280.

Kimmel, C. B., Warga, R. M., and Schilling, T. F. (1990). Origin and organization of the zebrafish fate map. *Development* **108,** 581-94.

Koster, R. W., and Fraser, S. E. (2001). Direct imaging of in vivo neuronal migration in the developing cerebellum. *Curr Biol* **11,** 1858-63.

Krull, C. E., Lansford, R., Gale, N. W., Collazo, A., Marcelle, C., Yancopoulos, G. D., Fraser, S. E., and Bronner-Fraser, M. (1997). Interactions of Eph-related receptors and ligands confer rostrocaudal pattern to trunk neural crest migration. *Curr Biol* **7,** 571-80.

Krumlauf, R. (1994). Hox genes in vertebrate development. *Cell* **78,** 191-201.

Kullander, K., and Klein, R. (2002). Mechanisms and functions of Eph and ephrin signalling. *Nat Rev Mol Cell Biol* **3,** 475-86.

Kuwada, J. Y., Bernhardt, R. R., and Nguyen, N. (1990). Development of spinal neurons and tracts in the zebrafish embryo. *J Comp Neurol* **302,** 617-28.

Lamb, T. M., and Harland, R. M. (1995). Fibroblast growth factor is a direct neural inducer, which combined with noggin generates anterior-posterior neural pattern. *Development* **121,** 3627-3636.

Lamb, T. M., Knecht, A. K., Smith, W. C., Stachel, S. E., Economides, A. N., Stahl, N., Yancopolous, G. D., and Harlans, R. (1993). Neural induction by the secreted polypeptide noggin. *Science* **262,** 713-718.

Langeland, J. A., and Kimmel, C. B. (1997). "Embryology: Constructing the Organism." Sinauer Associates, Inc., Sunderland, MA.

Le Douarin, N. M., Ziller, C., and Couly, G. F. (1993). Patterning of neural crest derivatives in the avian embryo: in vivo and in vitro studies. *Dev Biol* **159,** 24-49.

Lee, K. J., and Jessell, T. M. (1999). The specification of dorsal cell fates in the vertebrate central nervous system. *Annu Rev Neurosci* **22,** 261-94.

Lekven, A. C., Thorpe, C. J., Waxman, J. S., and Moon, R. T. (2001). Zebrafish wnt8 encodes two wnt8 proteins on a bicistronic transcript and is required for mesoderm and neurectoderm patterning. *Dev Cell* **1,** 103-14.

Lumsden, A. (1999). Closing in on rhombomere boundaries. *Nat Cell Biol* **1,** E83-5.

Lumsden, A., and Krumlauf, R. (1996). Patterning the vertebrate neuraxis. *Science* **274,** 1109-1115.

Lumsden, A., Sprawson, N., and Graham, A. (1991). Segmental origin and migration of neural crest cells in the hindbrain region of the chick embryo. *Development* **113,** 1281-91.

Maconochie, M. K., Nonchev, S., Manzanares, M., Marshall, H., and Krumlauf, R. (2001). Differences in Krox20-dependent regulation of Hoxa2 and Hoxb2 during hindbrain development. *Dev Biol* **233,** 468-81.

Maconochie, M. K., Nonchev, S., Studer, M., Chan, S. K., Popperl, H., Sham, M. H., Mann, R. S., and Krumlauf, R. (1997). Cross-regulation in the mouse HoxB complex: the expression of Hoxb2 in rhombomere 4 is regulated by Hoxb1. *Genes Dev* **11,** 1885-95.

Mann, R. S., and Affolter, M. (1998). Hox proteins meet more partners. *Curr Opin Genet Dev* **8,** 423-9.

Manzanares, M., Bel-Vialar, S., Ariza-McNaughton, L., Ferretti, E., Marshall, H., Maconochie, M. M., Blasi, F., and Krumlauf, R. (2001). Independent regulation of initiation and maintenance phases of Hoxa3 expression in the vertebrate hindbrain involve auto- and cross-regulatory mechanisms. *Development* **128,** 3595-607.

Manzanares, M., Cordes, S., Ariza-McNaughton, L., Sadl, V., Maruthainar, K., Barsh, G., and Krumlauf, R. (1999a). Conserved and distinct roles of kreisler in regulation of the paralogous Hoxa3 and Hoxb3 genes. *Development* **126,** 759-69.

Manzanares, M., Cordes, S., Kwan, C.-T., Sham, M. H., Barsh, G. S., and Krumlauf, R. (1997). Segmental regulation of Hoxb-3 by kreisler. *Nature* **387,** 191-195.

Manzanares, M., Trainor, P. A., Nonchev, S., Ariza-McNaughton, L., Brodie, J., Gould, A., Marshall, H., Morrison, A., Kwan, C. T., Sham, M. H., Wilkinson, D. G., and Krumlauf, R. (1999b). The role of kreisler in segmentation during hindbrain development. *Dev Biol* **211,** 220-37.

Marin, F., and Charnay, P. (2000). Hindbrain patterning: FGFs regulate Krox20 and mafB/kr expression in the otic/preotic region. *Development* **127,** 4925-35.

Mark, M., Lufkin, T., Vonesch, J.-L., Ruberte, E., Olivo, J.-C., Dolle, P., Gorry, P., Lumsden, A., and Chambon, P. (1993). Two rhombomeres are altered in Hoxa-1 mutant mice. *Development* **119,** 319-338.

Marshall, H., Nonchev, S., Sham, M. H., Muchamore, I., Lumsden, A., and Krumlauf, R. (1992). Retinoic acid alters hindbrain Hox code and induces transformation of rhomoneres 2/3 into a 4/5 identity. *Nature* **360,** 737-741.

Maves, L., Jackman, W., and Kimmel, C. B. (2002). FGF3 and FGF8 mediate a rhombomere 4 signaling activity in the zebrafish hindbrain. *Development* **129,** 3825-37.

McClintock, J. M., Carlson, R., Mann, D. M., and Prince, V. E. (2001). Consequences of Hox gene duplication in the vertebrates: an investigation of the zebrafish Hox paralogue group 1 genes. *Development* **128,** 2471-84.

McClintock, J. M., Kheirbek, M. A., and Prince, V. E. (2002). Knockdown of duplicated zebrafish hoxb1 genes reveals distinct roles in hindbrain patterning and a novel mechanism of duplicate gene retention. *Development* **129,** 2339-2354.

McGinnis, W., and Krumlauf, R. (1992). Homeobox genes and axial patterning. *Cell* **68,** 283-302.

McGrew, L., Lai, C., and Moon, R. (1995). Specification of the anteroposterior neural axis through synergistic interaction of the Wnt signalling cascade with noggin and follistatin. *Dev. Biol.* **172,** 337-342.

McKay, I. J., Muchamore, I., Krumlauf, R., Maden, M., Lumsden, A., and Lewis, J. (1994). The kreisler mouse: a hindbrain segmentation mutant that lacks two rhombomeres. *Development* **120,** 2199-2211.

Mechta-Grigoriou, F., Garel, S., and Charnay, P. (2000). Nab proteins mediate a negative feedback loop controlling Krox-20 activity in the developing hindbrain. *Development* **127,** 119-28.

Mellitzer, G., Xu, Q., and Wilkinson, D. G. (1999). Eph receptors and ephrins restrict cell intermingling and communication. *Nature* **400,** 77-81.

Metcalfe, W. K., Mendelson, B., and Kimmel, C. B. (1986). Segmental homologies among reticulospinal neurons in the hindbrain of the zebrafish larva. *J Comp Neurol* **251,** 147-59.

Metcalfe, W. K., Myers, P. Z., Trevarrow, B., Bass, M. B., and Kimmel, C. B. (1990). Primary neurons that express the L2/HNK-1 carbohydrate during early development in the zebrafish. *Development* **110,** 491-504.

Moens, C. B., Cordes, S. P., Giorgianni, M. W., Barsh, G. S., and Kimmel, C. B. (1998). Equivalence in the genetic control of hindbrain segmentation in fish and mouse. *Development* **125,** 381-391.

Moens, C. B., Yan, Y.-L., Appel, B., Force, A. G., and Kimmel, C. B. (1996). valentino: a zebrafish gene required for normal hindbrain segmentation. *Development* **122,** 3981-3990.

Murai, K. K., and Pasquale, E. B. (2003). 'Eph'ective signaling: forward, reverse and crosstalk. *J Cell Sci* **116,** 2823-32.

Myers, P. Z., Eisen, J. S., and Westerfield, M. (1986). Development and axonal outgrowth of identified motoneurons in the zebrafish. *J Neurosci* **6,** 2278-89.

Nieto, M. A., Gilardi-Hebenstreit, P., Charnay, P., and Wilkinson, D. G. (1992). A receptor protein tyrosine kinase implicated in the segmental patterning of the hindbrain and mesoderm. *Development* **116,** 1137-1150.

Nieuwkoop, P. D. (1952). Activation and organization of the central nervous system in amphibians. I. Induction and activation. *J. Exp. Zool.* **120,** 1-30.

Nieuwkoop, P. D., and Weijer, C. J. (1978). Neural induction, a two-way process. *Med Biol* **56,** 366-71.

Nonchev, S., Maconochie, M., Vesque, C., Aparicio, S., Ariza-McNaughton, L., Manzanares, M., Maruthainar, K., Kuroiwa, A., Brenner, S., Charnay, P., and Krumlauf, R. (1996a). The conserved role of Krox-20 in directing Hox gene expression during vertebrate hindbrain segmentation. *Proc Natl Acad Sci U S A* **93,** 9339-45.

Nonchev, S., Vesque, C., Maconochie, M., Seitanidou, T., Ariza-McNaughton, L., Frain, M., Marshall, H., Sham, M. H., Krumlauf, R., and Charnay, P. (1996b).

Segmental expression of Hoxa-2 in the hindbrain is directly regulated by Krox-20. *Development* **122,** 543-554.

Nordstrom, U., Jessell, T. M., and Edlund, T. (2002). Progressive induction of caudal neural character by graded Wnt signaling. *Nat Neurosci* **5,** 525-32.

Oates, A. C., Lackmann, M., Power, M. A., Brennan, C., Down, L. M., Do, C., Evans, B., Holder, N., and Boyd, A. W. (1999). An early developmental role for eph-ephrin interaction during vertebrate gastrulation. *Mech Dev* **83,** 77-94.

Oxtoby, E., and Jowett, T. (1993). Cloning of the zebrafish krox-20 gene (*krx20*) and its expression during development. *Nucl. Acids Res.* **21,** 1087-1095.

Papalopulu, N., and Kintner, C. (1996). A posteriorising factor, retinoic acid, reveals that anteroposterior patterning controls the timing of neuronal differentiation in Xenopus neirectoderm. *Development* **122,** 3409-3418.

Pasqualetti, M., Ori, M., Nardi, I., and Rijli, F. M. (2000). Ectopic Hoxa2 induction after neural crest migration results in homeosis of jaw elements in Xenopus. *Development* **127,** 5367-78.

Piccolo, S., Sasai, Y., Lu, B., and De Robertis, E. M. (1996). Dorsoventral patterning in Xenopus: inhibition of ventral signals by direct binding of chordin to BMP-4. *Cell* **86,** 589-598.

Popperl, H., Bienz, M., Studer, M., Chan, S. K., Aparicio, S., Brenner, S., Mann, R. S., and Krumlauf, R. (1995). Segmental expression of Hoxb-1 is controlled by a highly conserved autoregulatory loop dependent upon exd/pbx. *Cell* **81,** 1031-42.

Popperl, H., Rikhof, H., Chang, H., Haffter, P., Kimmel, C. B., and Moens, C. B. (2000). Iazarus is a novel pbx gene that globally mediates hox gene function in zebrafish [In Process Citation]. *Mol Cell* **6,** 255-67.

Pownall, M. E., Tucker, A. S., Slack, J. M. W., and Isaacs, H. V. (1996). eFGF, Xcad3 and Hox genes form a molecular pathway that establishes the anteroposterior axis in Xenopus. *Development* **122,** 3881-3892.

Prince, V. E., Joly, L., Ekker, M., and Ho, R. K. (1998a). Zebrafish hox genes: genomic organization and modified colinear expression patterns in the trunk. *Development* **125,** 407-420.

Prince, V. E., Moens, C. B., Kimmel, C. B., and Ho, R. K. (1998b). Zebrafish hox genes:expression in the hindbrain region of wild-type and mutants of the segmentation gene valentino. *Development* **125,** 393-406.

Rauch, G. J., Hammerschmidt, M., Blader, P., Schauerte, H. E., Strahle, U., Ingham, P. W., McMahon, A. P., and Haffter, P. (1997). Wnt5 is required for tail formation in the zebrafish embryo. *Cold Spring Harb Symp Quant Biol* **62,** 227-34.

Reifers, F., Bohli, H., Walsh, E. C., Crossley, P. H., Stainier, D. Y., and Brand, M. (1998). Fgf8 is mutated in zebrafish acerebellar (ace) mutants and is required for maintenance of midbrain-hindbrain boundary development and somitogenesis. *Development* **125,** 2381-95.

Reim, G., and Brand, M. (2002). Spiel-ohne-grenzen/pou2 mediates regional competence to respond to Fgf8 during zebrafish early neural development. *Development* **129,** 917-33.

Rhinn, M., Lun, K., Amores, A., Yan, Y. L., Postlethwait, J. H., and Brand, M. (2003). Cloning, expression and relationship of zebrafish gbx1 and gbx2 genes to Fgf signaling. *Mech Dev* **120,** 919-36.

Rijli, F. M., Mark, M., Lakkaraju, S., Dierich, A., Dolle, P., and Chambon, P. (1993). A homeotic transformation is generated in the rostral branchial region of the head by disruption of Hoxa-2, which acts as a selector gene. *Cell* **75,** 1333-49.

Roelink, H., Augsburger, A., Heemskerk, J., Korzh, V., Norlin, S., Ruiz i Altaba, A., Tanabe, Y., Placzek, M., Edlund, T., Jessell, T. M., and Dodd, J. (1994). *Cell* **76,** 761-775.

Ross, L. S., Parrett, T., and Easter, S. S., Jr. (1992). Axonogenesis and morphogenesis in the embryonic zebrafish brain. *J Neurosci* **12,** 467-82.

Rossel, M., and Capecchi, M. R. (1999). Mice mutant for both Hoxa1 and Hoxb1 show extensive remodeling of the hindbrain and defects in craniofacial development. *Development* **126,** 5027-40.

Russo, M. W., Sevetson, B. R., and Milbrandt, J. (1995). Identification of NAB1, a repressor of NGFI-A- and Krox20-mediated transcription. *Proc Natl Acad Sci U S A* **92,** 6873-7.

Ryan, A. K., and Rosenfeld, M. G. (1997). POU domain family values: flexibility, partnerships, and developmental codes. *Genes Dev* **11,** 1207-25.

Saga, Y., Hata, N., Kobayashi, S., Magnuson, T., Seldin, M. F., and Taketo, M. M. (1996). MesP1: a novel basic helix-loop-helix protein expressed in the nascent mesodermal cells during gastrulation. *Development* **122,** 2769-2778.

Sagerstrom, C. G., Kao, B. A., Lane, M. E., and Sive, H. (2001). Isolation and characterization of posteriorly restricted genes in the zebrafish gastrula. *Dev Dyn* **220,** 402-8.

Sasai, Y., Lu, B., Steinbeisser, H., and De Robertis, E. M. (1995). Regulation of neural induction by the Chd and Bmp-4 antagonistic patterning signals in *Xenopus*. *Nature* **376,** 333-336.

Saude, L., Woolley, K., Martin, P., Driever, W., and Stemple, D. L. (2000). Axis-inducing activities and cell fates of the zebrafish organizer. *Development* **127,** 3407-17.

Schilling, T. F., and Kimmel, C. B. (1994). Segment and cell type lineage restrictions during pharyngeal arch development in the zebrafish embryo. *Development* **120,** 483-94.

Schilling, T. F., Prince, V., and Ingham, P. W. (2001). Plasticity in zebrafish hox expression in the hindbrain and cranial neural crest. *Dev Biol* **231,** 201-16.

Schmitt, E. A., and Dowling, J. E. (1994). Early eye morphogenesis in the zebrafish, Brachydanio rerio. *J Comp Neurol* **344,** 532-42.

Schneider, S., Steinbeisser, H., Warga, R. M., and Hausen, P. (1996). Beta-catenin translocation into nuclei demarcates the dorsalizing centers in frog and fish embryos. *Mech Dev* **57,** 191-8.

Schneider-Maunoury, S., Seitanidou, T., Charnay, P., and Lumsden, A. (1997). Segmental and neuronal architecture of the hindbrain of Krox-20 mouse mutants. *Development* **124,** 1215-26.

Schneider-Maunoury, S., Topilko, P., Seitandou, T., Levi, G., Cohen-Tannoudji, M., Pournin, S., Babinet, C., and Charnay, P. (1993). Disruption of krox-20 results in alteration of rhombomeres 3 and 5 in the developing hindbrain. *Cell* **75,** 1199-1214.

Schoenwolf, G. C., and Smith, J. L. (2000). Gastrulation and early mesodermal patterning in vertebrates. *Methods Mol Biol* **135,** 113-25.

Schulte-Merker, S., Ho, R. K., Herrmann, B. G., and Nusslein-Volhard, C. (1992). The protein product of the zebrafish homologue of the mouse T gene is expressed in nuclei of the germ ring and the notochord of the early embryo. *Development* **116,** 1021-1032.

Scott, M. P. (1992). Vertebrate homeobox gene nomenclature. *Cell* **71,** 551-3.

Scott, M. P., and Weiner, A. J. (1984). Structural relationships among genes that control development: sequence homology between the Antennapedia, Ultrabithorax, and fushi tarazu loci of Drosophila. *Proc Natl Acad Sci U S A* **81,** 4115-9.

Scott, M. P., Weiner, A. J., Hazelrigg, T. I., Polisky, B. A., Pirrotta, V., Scalenghe, F., and Kaufman, T. C. (1983). The molecular organization of the Antennapedia locus of Drosophila. *Cell* **35,** 763-76.

Seitanidou, T., Schneider-Maunoury, S., Desmarquet, C., Wilkinson, D. G., and Charnay, P. (1997). Krox-20 is a key regulator of rhombomere-specific gene expression in the developing hindbrain. *Mech Dev* **65,** 31-42.

Sham, M. H., Vesque, C., Nonchev, S., Marshall, H., Frain, M., Gupta, R. D., Whiting, J., Wilkinson, D., Charnay, P., and Krumlauf, R. (1993). The zinc finger gene

Krox20 regulates HoxB2 (Hox2.8) during hindbrain segmentation. *Cell* **72,** 183-96.

Shih, J., and Fraser, S. E. (1996). Characterizing the zebrafish organizer: microsurgical analysis at the early shield stage. *Development* **122,** 1313-1322.

Shinya, M., Eschbach, C., Clark, M., Lehrach, H., and Furutani-Seiki, M. (2000). Zebrafish Dkk1, induced by the pre-MBT Wnt signaling, is secreted from the prechordal plate and patterns the anterior neural plate. *Mech Dev* **98,** 3-17.

Sleptsova-Friedrich, I., Li, Y., Emelyanov, A., Ekker, M., Korzh, V., and Ge, R. (2001). fgfr3 and regionalization of anterior neural tube in zebrafish. *Mech Dev* **102,** 213-7.

Solnica-Krezel, L., and Driever, W. (1994). Microtubule arrays of the zebrafish yolk cell: organization and function during epiboly. *Development* **120,** 2443-55.

Solnica-Krezel, L., Stemple, D. L., and Driever, W. (1995). Transparent things: cell fates and cell movements during early embryogenesis of zebrafish. *Bioessays* **17,** 931-9.

Spemann, H., and Mangold, H. (1924). Uber Induktion von Embryonanlagen durch Implantation Artfremder Organis Atoren. *Roux's Arch. Dev. Biol.* **100,** 599-638.

Stachel, S. E., Grunwald, D. J., and Myers, P. Z. (1993). Litium perturbation and goosecoid expression identify a dorsal specification pathway in the pregastrula zebrafish. *Development* **117,** 1261-1274.

Stickney, H. L., Barresi, M. J., and Devoto, S. H. (2000). Somite development in zebrafish. *Dev Dyn* **219,** 287-303.

Storey, K. G., Goriely, A., Sargent, C. M., Brown, J. M., Burns, H. D., Abud, H. M., and Heath, J. K. (1998). Early posterior neural tissue is induced by FGF in the chick embryo. *Development* **125,** 473-84.

Strahle, U., and Blader, P. (1994). Early neurogenesis in the zebrafish embryo. *Faseb J* **8,** 692-8.

Strahle, U., and Jesuthasan, S. (1993). Ultraviolet irradiation impairs epiboly in zebrafish embryos: evidence for a microtubule-dependent mechanism of epiboly. *Development* **119,** 909-19.

Studer, M., Gavalas, A., Marshall, H., Ariza-McNaughton, L., Rijli, F. M., Chambon, P., and Krumlauf, R. (1998). Genetic interactions between Hoxa1 and Hoxb1 reveal new roles in regulation of early hindbrain patterning. *Development* **125,** 1025-36.

Studer, M., Lumsden, A., Ariza-McNaughton, L., Bradley, A., and Krumlauf, R. (1996). Altered segmental identity and abnormal migration of motor neurons in mice lacking Hoxb-1. *Nature* **384,** 630-634.

Sun, Z., and Hopkins, N. (2001). vhnf1, the MODY5 and familial GCKD-associated gene, regulates regional specification of the zebrafish gut, pronephros, and hindbrain. *Genes Dev* **15,** 3217-29.

Svaren, J., Sevetson, B. R., Apel, E. D., Zimonjic, D. B., Popescu, N. C., and Milbrandt, J. (1996). NAB2, a corepressor of NGFI-A (Egr-1) and Krox20, is induced by proliferative and differentiative stimuli. *Mol Cell Biol* **16,** 3545-53.

Swiatek, P. J., and Gridley, T. (1993). Perinatal lethality and defects in hindbrain development in mice homozygous for a targeted mutation of the zinc finger gene Krox20. *Genes Dev* **7,** 2071-84.

Takeda, H., Matsuzaki, T., Oki, T., Miyagawa, T., and Amanuma, H. (1994). A novel POU domain gene, zebrafish pou2: expression and roles of two alternatively spliced twin products in early development. *Genes Dev* **8,** 45-59.

Theil, T., Frain, M., Gilardi-Hebenstreit, P., Flenniken, A., Charnay, P., and Wilkinson, D. G. (1998). Segmental expression of the EphA4 (Sek-1) receptor tyrosine kinase in the hindbrain is under direct transcriptional control of Krox-20. *Development* **125,** 443-452.

Thisse, B., Wright, C. V., and Thisse, C. (2000). Activin- and Nodal-related factors control antero-posterior patterning of the zebrafish embryo. *Nature* **403,** 425-8.

Thisse, C., Thisse, B., Schilling, T. F., and Postlethwait, J. H. (1993). Structure of the zebrafish snail1 gene and its expression in wild-type, spadetail and no tail mutant embryos. *Development* **119,** 1203-15.

Trainor, P., and Krumlauf, R. (2000a). Plasticity in mouse neural crest cells reveals a new patterning role for cranial mesoderm. *Nat Cell Biol* **2,** 96-102.

Trainor, P. A., and Krumlauf, R. (2000b). Patterning the cranial neural crest: hindbrain segmentation and Hox gene plasticity. *Nat Rev Neurosci* **1,** 116-24.

Trevarrow, B., Marks, D. L., and Kimmel, C. B. (1990). Organization of hindbrain segments in the zebrafish embryo. *Neuron* **4,** 669-79.

Trinh le, A., Meyer, D., and Stainier, D. Y. (2003). The Mix family homeodomain gene bonnie and clyde functions with other components of the Nodal signaling pathway to regulate neural patterning in zebrafish. *Development* **130,** 4989-98.

Trokovic, R., Trokovic, N., Hernesniemi, S., Pirvola, U., Vogt Weisenhorn, D. M., Rossant, J., McMahon, A. P., Wurst, W., and Partanen, J. (2003). FGFR1 is independently required in both developing mid- and hindbrain for sustained response to isthmic signals. *Embo J* **22,** 1811-23.

Vaage, S. (1969). The segmentation of the primitive neural tube in chick embryos (Gallus domesticus). A morphological, histochemical and autoradiographical investigation. *Ergeb Anat Entwicklungsgesch* **41,** 3-87.

van der Wees, J., Schilthuis, J. G., Koster, C. H., Diesveld-Schipper, H., Folkers, G. E., van der Saag, P. T., Dawson, M. I., Shudo, K., van der Burg, B., and Durston, A. J. (1998). Inhibition of retinoic acid receptor-mediated signalling alters positional identity in the developing hindbrain. *Development* **125,** 545-56.

Vlachakis, N., Choe, S. K., and Sagerstrom, C. G. (2001). Meis3 synergizes with Pbx4 and Hoxb1b in promoting hindbrain fates in the zebrafish. *Development* **128,** 1299-312.

Vlachakis, N., Ellstrom, D. R., and Sagerstrom, C. G. (2000). A novel pbx family member expressed during early zebrafish embryogenesis forms trimeric complexes with Meis3 and Hoxb1b. *Dev Dyn* **217,** 109-19.

Voiculescu, O., Taillebourg, E., Pujades, C., Kress, C., Buart, S., Charnay, P., and Schneider-Maunoury, S. (2001). Hindbrain patterning: Krox20 couples segmentation and specification of regional identity. *Development* **128,** 4967-78.

Warga, R. M., and Kimmel, C. B. (1990). Cell movements during epiboly and gastrulation in zebrafish. *Development* **108,** 569-580.

Waskiewicz, A. J., Rikhof, H. A., Hernandez, R. E., and Moens, C. B. (2001). Zebrafish Meis functions to stabilize Pbx proteins and regulate hindbrain patterning. *Development* **128,** 4139-51.

Waskiewicz, A. J., Rikhof, H. A., and Moens, C. B. (2002). Eliminating zebrafish pbx proteins reveals a hindbrain ground state. *Dev Cell* **3,** 723-33.

Wassarman, K. M., Lewandoski, M., Campbell, K., Joyner, A. L., Rubenstein, J. L., Martinez, S., and Martin, G. R. (1997). Specification of the anterior hindbrain and establishment of a normal mid/hindbrain organizer is dependent on Gbx2 gene function. *Development* **124,** 2923-34.

Westerfield, M., and Eisen, J. S. (1988). Neuromuscular specificity: pathfinding by identified motor growth cones in a vertebrate embryo. *Trends Neurosci* **11,** 18-22.

Wiellette, E. L., and Sive, H. (2003). vhnf1 and Fgf signals synergize to specify rhombomere identity in the zebrafish hindbrain. *Development* **130,** 3821-9.

Wilson, P. A., and Hemmati-Brivanlou, A. (1997). Vertebrate neural induction: inducers, inhibitors, and a new synthesis. *Neuron* **18,** 699-710.

Wilson, S. W., Brand, M., and Eisen, J. S. (2002). Patterning the zebrafish central nervous system. *Results Probl Cell Differ* **40,** 181-215.

Wingate, R. J., and Hatten, M. E. (1999). The role of the rhombic lip in avian cerebellum development. *Development* **126,** 4395-404.

Winning, R. S., Scales, J. B., and Sargent, T. D. (1996). Disruption of cell adhesion in Xenopus embryos by Pagliaccio, an Eph-class receptor tyrosine kinase. *Dev Biol* **179,** 309-19.

Woo, K., and Fraser, S. E. (1995). Order and coherence in the fate map of the zebrafish nervous system. *Development* **121,** 2595-2609.

Woo, K., and Fraser, S. E. (1997). Specification of the zebrafish nervous system by nonaxial signals. *Science* **277,** 254-257.

Woo, K., and Fraser, S. E. (1998). Specification of the hindbrain fate in the zebrafish. *Dev. Biol.* **197,** 283-296.

Woo, K., Shih, J., and Fraser, S. E. (1995). Fate maps of the zebrafish embryo. *Curr Opin Genet Dev* **5,** 439-43.

Wullimann, M. F., and Puelles, L. (1999). Postembryonic neural proliferation in the zebrafish forebrain and its relationship to prosomeric domains. *Anat Embryol (Berl)* **199,** 329-48.

Wullimann, M. F., Puelles, L., and Wicht, H. (1999). Early postembryonic neural development in the zebrafish: a 3-D reconstruction of forebrain proliferation zones shows their relation to prosomeres. *Eur J Morphol* **37,** 117-21.

Xu, L., Glass, C. K., and Rosenfeld, M. G. (1999). Coactivator and corepressor complexes in nuclear receptor function. *Curr Opin Genet Dev* **9,** 140-7.

Xu, Q., Alldus, G., Holder, N., and Wilkinson, D. G. (1995). Expression of truncated Sek-1 receptor tyrosine kinase disrupts the segmental restriction of gene expression in the Xenopus and zebrafish hindbrain. *Development* **121,** 4005-16.

Xu, Q., and Wilkinson, D. G. (1997). Eph-related receptors and their ligands: mediators of contact dependent cell interactions. *J Mol Med* **75,** 576-86.

Zhang, M., Kim, H.-J., Marshall, H., Gendron-Maguire, M., Lucas, A. D., Baron, A., Gudas, L. J., Gridley, T., Krumlauf, R., and Grippo, J. F. (1994). Ectopic Hoxa-1 induces rhombomere transformation in mouse hindbrain. *Development* **120,** 2431-2442.

Zimmerman, L., De Jesus-Escobar, J., and Harland, R. (1996). The Spemann organizer signal noggin binds and inactivates bone morphogenetic protein 4. *Cell* **86,** 599-606.

# CHAPTER I

## NLZ BELONGS TO A FAMILY OF ZINC-FINGER CONTAINING REPRESSORS AND CONTROLS SEGMENTAL GENE EXPRESSION IN THE ZEBRAFISH HINDBRAIN

Alexander P. Runko and Charles G. Sagerström*
Department of Biochemistry and Molecular Pharmacology, and Program in Neuroscience, University of Massachusetts Medical School, Worcester, MA

*To whom correspondence should be addressed:
Department of Biochemistry and Molecular Pharmacology
364 Plantation Street/LRB 822
Worcester MA 01605
Phone: (508) 856 8006
Fax: (508) 856 8007
Email: charles.sagerstrom@umassmed.edu

Runko, A.P., and Sagerström, C.G. (2003). *Dev Biol* **262,** 254-67.

**Abstract**

The zebrafish *nlz* gene has a rostral expression limit at the presumptive rhombomere (r) 3/r4 boundary during gastrula stages and its expression progressively expands rostrally to encompass both r3 and r2 by segmentation stages, suggesting a role for *nlz* in hindbrain development. We find that Nlz is a nuclear protein that associates with the co-repressor Groucho, suggesting that Nlz acts to repress transcription. Consistent with a role as a repressor, misexpression of *nlz* causes a loss of gene expression in the rostral hindbrain, likely due to ectopic *nlz* acting prematurely in this domain, and this repression is accompanied by a partial expansion in the expression domains of r4-specific genes. To interfere with endogenous *nlz* function, we generated a form of *nlz* that lacks the Groucho binding site and demonstrate that this construct has a dominant negative effect. We find that interfering with endogenous Nlz function promotes the expansion of r5 and, to a lesser extent, r3 gene expression into r4, leading to a reduction in the size of r4. We conclude that Nlz is a transcriptional repressor that controls segmental gene expression in the hindbrain. Lastly, we identify additional *nlz*-related genes, suggesting that Nlz belongs to a family of zinc-finger proteins.

*Key words:* Co-repressor; Groucho; Hindbrain; Patterning; Repressor; Rhombomere; Segmentation; Transcription; Zebrafish; Zinc-Finger.

## Introduction

The vertebrate embryonic hindbrain gives rise to the cerebellum and brainstem of the adult organism. During its development, the hindbrain transiently possesses seven cell lineage restricted compartments termed rhombomeres (r). These metameric units play an essential role in establishing proper hindbrain segmentation and craniofacial organization. For instance, formation of the rhombomeres underlies the segment specific pattern of primary reticulospinal neurons, cranial neural crest cells that migrate to the pharyngeal arches, branchiomotor neurons, and sensory ganglia (reviewed in (Lumsden and Krumlauf, 1996).

Specific genes mediate the formation of rhombomeres. For instance, *krox20* is expressed in r3 and r5 (Oxtoby and Jowett, 1993) and is required for the formation and maintaince of these rhombomeres – a loss of *krox20* leads to a progressive disappearance of r3 and r5 (Schneider-Maunoury et al., 1997). *krox20* is also a determinant in anterior-posterior positional identity because of its regulatory relationship with the *hox* family of transcription factors (Krumlauf, 1994; Prince et al., 1998a) - *krox20* regulates *hoxa2* (Nonchev et al., 1996), *hoxb2* (Sham et al., 1993) and *ephA4* (Theil et al., 1998) expression in r3 and r5 and *hoxb3* expression in r5 (Seitanidou et al., 1997). Similarly, *kreisler/valentino* and *vhnf1* are expressed in r5 and r6 (Cordes and Barsh, 1994; Moens et al., 1998; Sun and Hopkins, 2001) and are required for r5/r6 development - *kreisler/valentino* and *vhnf1* mutants have hindbrain defects in r5 and r6 (McKay et al., 1994; Moens et al., 1996; Sun and Hopkins, 2001). It is hypothesized that *vhnf1* regulates

hindbrain patterning by activating *valentino* expression in r5/r6, which in turn regulates *krox20* and *hoxb3* expression in r5 and *hoxa3* expression in r5 and r6 (Manzanares et al., 1999; Manzanares et al., 1997; Prince et al., 1998b; Sun and Hopkins, 2001; Theil et al., 2002). Furthermore, *hoxb1* (equivalent to *hoxb1a* in zebrafish (Amores et al., 1998)) and *hoxa1* (equivalent to *hoxb1b* in zebrafish (Amores et al., 1998)) are both expressed in presumptive r4, where *hoxa1/hoxb1b* regulates the expression of both *hoxb1/hoxb1a* and *hoxb2* (Barrow et al., 2000; Maconochie et al., 1997; McClintock et al., 2001). The loss of *hoxa1/hoxb1b* leads to a loss of r5, a partial loss of r4 and an increase in the size of r3 (Barrow et al., 2000; McClintock et al., 2002; Rossel and Capecchi, 1999) while the ectopic expression of *hoxa1/hoxb1b* leads to a transformation of r2 towards a r4 fate in both mice (Zhang et al., 1994) and fish (Alexandre et al., 1996; McClintock et al., 2001; Vlachakis et al., 2001). Loss of *hoxb1/hoxb1a* function results in a loss of normal VIIth cranial nerve patterning (McClintock et al., 2002; Studer et al., 1998; Studer et al., 1996) and mis-expression of *hoxb1a* causes a posterior transformation of r2 and more anterior structures (McClintock et al., 2001). Additionally, hindbrain development is regulated by signaling centers at the midbrain-hindbrain boundary (MHB), which promotes development of rostral rhombomeres (r1-3) (Irving and Mason, 2000), and at rhombomere 4, which secretes fibroblast growth factor (FGF)3 and FGF8 that in turn promote development of r5 and r6 (Maves et al., 2002).

For proper segmentation of the hindbrain, the expression and function of these various genes must be restricted to individual rhombomeres. This involves a dynamic regulation of cell identity as well as a restriction of cell sorting between adjacent

segments (Cooke and Moens, 2002). The restriction of cell movement is exemplified by the finding that r3/r5 cells are immiscible with r2/r4/r6 cells (Fraser et al., 1990; Guthrie et al., 1993). Members of the *Eph* family of tyrosine kinase receptors and their cognate *ephrin* ligands are dynamically expressed in various rhombomeres (Flanagan and Vanderhaeghen, 1998) and have been implicated in regulating sorting between rhombomeres (Lumsden, 1999; Xu et al., 1999) as well as in the control of cell migration (Holder and Klein, 1999). In particular, disruption of *Eph* signaling via a dominant negative approach in zebrafish and *Xenopus* resulted in cell mixing between rhombomeres (Xu et al., 1995; Xu et al., 1996) as well as in a disruption of convergence movement during gastrulation (Oates et al., 1999). The dynamic regulation of cell identity is exemplified by repressive interactions that occur between *krox20* and the *hox1* paralogs (*hoxa1* and *hoxb1*) to control specification of rhombomeres 3, 4 and 5. For instance, when the anterior limit of *hoxa1* and *hoxb1* expression is shifted caudally, *krox20* expression in r3 also expands caudally, consistent with *hoxa1* and *hoxb1* repressing *krox20* (Barrow et al., 2000).

It is likely that additional genes are involved in regulating cell fate and/or cell sorting during rhombomere formation. One candidate is the zebrafish *nlz* gene (Andreazzoli et al., 2001; Sagerstrom et al., 2001), which is related to the *Drosophila nocA* and *elbow* genes (Cheah et al., 1994; Dorfman et al., 2002) and encodes a zinc-finger protein. Hypomorphic (reduced function) mutations in *nocA* exhibit complete or partial loss of the ocelli (adult photosensory organs located between the compound eyes) and associated bristles, while loss of function mutations exhibit hypertrophy and

mislocation of the embryonic supraesophageal ganglion (Cheah et al., 1994). This suggests a role for *nocA* in cell fate determination and/or patterning of *Drosophila* neural structures and raises the possibility that *nlz* may regulate similar processes in zebrafish. In order to test this, we first characterized the expression pattern of *nlz* during hindbrain development in detail. We confirm that *nlz* is initially expressed in the hindbrain up to the r3/r4 boundary and also demonstrate that *nlz* expression progressively expands to encompass r3 and r2 by somitogenesis stages. Misexpression of *nlz* in the developing embryo causes a distinct disruption in hindbrain patterning. Specifically, we observe a loss of gene expression in the rostral hindbrain (r1-r3), likely due to ectopic *nlz* acting prematurely in this region, as well as a partial expansion of r4-specific gene expression into r3. We find that Nlz is a nuclear protein that associates with the co-repressor Groucho, suggesting that Nlz acts as a repressor, and we demonstrate that misexpression of an Nlz construct lacking the Groucho binding-site interferes with Nlz function, thus acting as a dominant negative. Expression of this dominant negative construct (dnNlz) induces an expansion of gene expression from r5 and, to a lesser extent, r3 into r4. The effect of dnNlz can be mimicked by fusing the VP16 activation domain to full-length Nlz, suggesting that dnNlz promotes activation of target genes normally repressed by Nlz. Our data is consistent with Nlz being a transcriptional repressor involved in the regulation of segmental gene expression during hindbrain development. We also identify additional Nlz-related genes in the zebrafish, mouse and human, thereby defining a family of zinc-finger proteins.

## Materials and Methods

*Cloning*

All constructs (see Fig. 3F for list) were generated by utilizing standard molecular biology cloning techniques (details available upon request), cloned into the pCS2+ or pCS2+MT vectors and verified by sequencing. Oligos 5'-CTATGCACTCTCTCCCAGCC-3' and 5'-AGAGGGGAATCCTGCTTGTT-3' were used to map *nlz* on radiation hybrid panels (Geisler et al., 1999; Hukriede et al., 1999).

*Synthesis and injection of RNA*

Capped mRNAs were synthesized using the SP6 mMessage mMachine kit (Ambion) with *Not*I-linearized pCS2+MT derived plasmids, or for *βgal*, *Xho*I-linearized pSP6-*nucβ-gal*. The capped mRNAs were purified with the RNeasy mini kit (Qiagen), quantified by UV absorbance and gel electrophoresis, and diluted in water and 0.5% phenol red. For in situ analysis, 400 pg of capped mRNA was injected with the exception of the VP16Nlz fusion construct (25 pg). To reduce pigmentation, injected embryos that were analyzed after 24 hours post fertilization (hpf) were transferred to fish water containing 0.003% of phenylthiourea (PTU) between 14 and 16 hpf. For immunostaining with the anti-c-myc antibody, 800 pg of capped mRNA was injected. All injections were performed at the 1- to 2- cell stage.

*In situ hybridization and immunostaining*

Whole mount in situ hybridizations using digoxigenin or fluorescein labeled antisense RNA probes was performed as described (Sagerström et al., 1996) and the following genes were used: *nlz* (Sagerstrom et al., 2001); *krox20* (Oxtoby and Jowett, 1993); *pax2.1* (Krauss et al., 1991); *ephA4* (Macdonald et al., 1994; Xu et al., 1994); *ephB4a* (Cooke et al., 2001); *gbx1*, *iro1* (Itoh et al., 2002); *mariposa* (Moens et al., 1996); *ephrinB2a* (Durbin et al., 1998); *val* (Moens et al., 1998); *hoxa2*, *hoxb1a*, *hoxb3*, *hoxd4* (Prince et al., 1998b); *otx2* (Mori et al., 1994); *ephrinA2* (C. Brennan, personal communication); *myoD* (Weinberg et al., 1996); *ntl* (Schulte-Merker et al., 1992); and *caudal* (Joly et al., 1992). After color development, the embryos were washed with PBT, placed in 90% glycerol and flat-mounted. X-gal staining was performed as described (Blader et al., 1997). Immunostaining with anti-c-myc (clone 9E10) and the islet-1 antibody (39.4D5, (Korzh et al., 1993)) was performed as described (Hatta, 1992) and HRP was detected using either the TSA-direct kit (Dupont Biotechnology Systems) or DAB (Vector Laboratories). Immunostaining with the RMO-44 antibody (Zymed Labs, Inc.) was performed using the Vectastain ABC kit (Vector Laboratories). Protein localization was performed by immunostaining with the anti-c-myc antibody and incubation of the embryos with a 1:1000 dilution of DAPI (Sigma) at room temperature for 10 minutes.

*Western Analysis and GST pull-down*

For western blot analysis, lysates of 3 gastrula stage embryos were used per lane. Samples were resolved on a 10% polyacrylamide gel by SDS-PAGE, western blotted, probed with a 1:1000 dilution of the anti-c-myc (clone 9E10) antibody and detected utilizing chemiluminescence. All GST fusion constructs (Groucho, HDAC1 and HDAC2) were purified on Glutathione Sepharose 4B beads (Amersham) by standard procedures. Nlz constructs were in vitro labeled with $^{35}$S-methionine by utilizing the Promega TnT SP6 Coupled Reticulocyte Lysate System. GST pull-downs were performed in 10 mM Tris (pH 7.6), 600 mM NaCl, 1 mM EDTA, 1 mM DTT, 1 mM $MgCl_2$, 1% NP-40 and 1% BSA. After overnight binding at 4°C, beads were washed four times with the binding buffer (excluding BSA) for 5 minutes each at 4°C. Samples were resolved on a 10% polyacrylamide gel by SDS-PAGE, fixed, washed, dried to Whatman paper and exposed to film by standard procedures.

## Results

*nlz is dynamically expressed during development of the midbrain and hindbrain*

To begin exploring Nlz function, we first expanded on previous reports (Andreazzoli et al., 2001; Sagerstrom et al., 2001) by undertaking a detailed analysis of neural *nlz* expression during early development. Starting at early gastrula stages, *nlz* expression is found in a broad caudal domain that includes both neural and non-neural ectoderm, as well as the underlying mesoderm and endoderm (Andreazzoli et al., 2001; Sagerstrom et al., 2001). By bud stage (10 hpf), *nlz* expression extends from the caudal end of the embryo to the rhombomere (r) 3/r4 border in the hindbrain (delineated by *krox20* expression in r3 (Fig. 1A,B). During early segmentation stages, expression of *nlz* remains in the hindbrain primordium and expands into r3 (10.5 hpf; Fig. 1C,D) such that *nlz* is detectable throughout r3 by the 3- and 6-somite stages (Fig. 1E,G). *nlz* expression expands rostral to r3 by the 8-somite stage (Fig. 1I) and includes r2 by the 14-somite stage (Fig. 1K). By 20 hpf, *nlz* expression persists in r3 while expression in r2 and r4/r5 subsides (Fig. 1M). These results indicate that *nlz* is expressed in a dynamic caudal domain whose anterior boundary expands from the r3/r4 boundary during late gastrulation to r2 during somitogenesis stages.

Double in situ hybridizations also revealed that *nlz* becomes expressed at the midbrain-hindbrain boundary (MHB; delineated by *pax2.1* expression) by the 3-somite stage (Fig. 1F). Expression of *nlz* at the MHB intensifies by the 6-somite stage (Fig. 1H), but gradually diminishes during the 8-somite stage (Fig. 1J) and is lost by the 14-somite (Fig. 1L) and 20 hpf stages (Fig. 1M), while *pax2.1* expression persists. Notably, *nlz*

expression is not significantly affected (not shown) in *acerebellar* zebrafish embryos that carry a mutation in the Fgf8 gene and have defects in the MHB and rostral hindbrain (Reifers et al., 1998). Taken together, our expression analysis suggests a potential role for *nlz* in development of the zebrafish MHB and hindbrain.

*Ectopic expression of nlz disrupts gene expression in the rostral hindbrain*

We first used a zebrafish radiation hybrid panel to place *nlz* onto the zebrafish genetic map. We find that *nlz* maps to an interval between 38.1 and 44 cM from the top of zebrafish linkage group (LG) 5, but this location does not coincide with known zebrafish mutations or deletions.

To explore the function of *nlz*, we ectopically expressed Nlz by injecting *nlz* mRNA into 1-2 cell stage zebrafish embryos. When *nlz*-injected embryos were analyzed at the 10-14 somite stage, pronounced defects were observed in the rostral hindbrain (Table 1). In particular, ~60% of embryos injected with *nlz* demonstrate a severe reduction in *krox20* and *ephA4* expression in r3 (arrows in Fig. 2A,C,K,S,U,W; Table 1) as well as a loss of *hoxa2* and *ephB4a* expression in r2 and r3 (arrows in Fig. 2E,G,I; Table 1). Misexpression of *nlz* frequently leads to loss of r2/r3 expression on only one side of the embryo, which correlates with the distribution of the injected mRNA (detected by co-injection with *lacZ* mRNA; Fig. 2K). We conclude that the ectopic expression of *nlz* disrupts r2 and r3 gene expression.

Examination of *nlz*-injected embryos at an earlier stage (1-2 somite), when *krox20* and *hoxb1a* expression has just been initiated, revealed that 74% (14/20) of embryos

injected with *nlz* exhibit a loss of *krox20* gene expression in r3 (arrow in Fig. 2M) suggesting that ectopic *nlz* may act already at gastrula stages. To examine this further, we examined *nlz*-injected embryos for expression of *gbx1* and *iro1*, the earliest genes expressed in the rostral hindbrain primordium (Itoh et al., 2002), at mid-gastrula stages. We find that expression of *gbx1* (from r1 to the r3/r4 boundary) is reduced (arrow in Fig. 2O, Table 1), while *iro1* expression in the rostral hindbrain is unaffected (not shown, Table 1). This suggests that ectopically expressed *nlz* acts already at late gastrula stages to disrupt genes expressed in the rostral hindbrain primordium.

We next assayed expression of *mariposa*, a marker of rhombomere boundaries, at the 24 hour stage (Fig. 2Q,R). We find that 38% (11/29) of embryos injected with *nlz* exhibit disruption of the boundary separating r3 and r4 (arrow in Fig. 2Q) as well as disorganized boundaries between r1/r2 and r2/r3 (asterisks in Fig. 2Q) while boundaries in the caudal hindbrain are normal (arrowheads in Fig. 2Q). This effect on rhombomere boundaries is consistent with the observed disruption of gene expression in the rostral hindbrain.

Notably, *hoxb1a* and *ephrinB2a* expression in r4 (asterisks in Fig. 2G,I,S,U; Table 1) is also affected in *nlz*-injected embryos. These gene expression domains appear to expand, at least partially, into the region normally occupied by r2- and r3-specific gene expression and this may represent a secondary effect to the loss of r2/r3-specific gene expression. There is a lesser effect in r1, where *ephA4* expression may partially extend caudally (asterisk in Fig. 2W). The effect of ectopic *nlz* does not extend beyond r1-r4 of the hindbrain since gene expression at the MHB (*pax2.1* and *ephB4a*; Fig. 2G,I), in r5

(*krox20* and *ephA4*; Fig. 2A,C,E,K,S,U,W) in r5/r6 (*ephB4a*, *hoxb3* and *valentino*; Fig. 2I and not shown) and in r7 (*hoxd4*, not shown) is unaffected (Table 1). In addition, markers for regions outside the hindbrain, such as the forebrain (*otx2*), midbrain (*ephrinA2*), somites (*myoD*), notochord (*ntl*) and other caudal domains (*caudal*) are unaffected (not shown, Table 1). We conclude that misexpression of *nlz* disrupts normal gene expression in r1-r4. Misexpression of *nlz* also affects neuronal differentiation in the rostral hindbrain, but this effect is comparatively mild. In particular, branchiomotor and reticulospinal neurons residing in r2 and r3 are lost in ~11% of embryos (not shown; 48/438).

*Nlz is a nuclear protein that associates with the Groucho co-repressor*

Since *nlz* disrupts gene expression in the rostral hindbrain, we reasoned that Nlz may act as a repressor. Since repressors would be expected to function in the nucleus, we next determined the subcellular distribution of Nlz. Embryos were injected with mRNA encoding a Myc epitope tagged Nlz protein at the 1-2 cell stage, flat mounted at early gastrulation (5 hpf), and examined for localization of Nlz by fluorescent immunohistochemistry. We find that Nlz primarily localizes in a punctuate pattern (Fig. 3A). Treatment of the injected embryos with DAPI (Fig. 3B), a fluorescent probe that binds DNA (Hajduk, 1976), revealed that DAPI staining and Nlz co-localize (Fig. 3C), demonstrating that Nlz is a nuclear protein.

At least one Nlz-related protein (Elbow) associates with the Groucho co-repressor (Dorfman et al., 2002), although the functional significance of this interaction has not been determined. We therefore tested whether Nlz also interacts with Groucho. Using

GST pull-down assays (Fig. 3D), we find that Nlz interacts efficiently with Groucho (Fig. 3D, lane 1). In order to determine the domain of Nlz required for this association, we generated a series of Nlz deletion constructs (Fig. 3E) and tested them for Groucho binding in the GST pull-down assay (Fig. 3D). Although Nlz contains a putative Groucho binding site (FKPY) at position 149-152, deletions within the N-terminus and up to amino acid 385 have no effect on Groucho interaction (Fig. 3D,E and not shown). However, an Nlz construct lacking the C-terminal 173 amino acids displays significantly weaker association with Groucho (Fig. 3D, lane 2). Deletions within this domain demonstrate that the C-terminal 129 amino acids are not required for Groucho binding (Fig. 3D, lanes 7-9; summarized in Fig. 3E). Instead, deletion of the region between the two zinc fingers (NlzΔ408-460, Fig. 3D, lane 11) severely affects binding to Groucho and, although deletion of the first zinc finger (Z1) alone has no effect (Fig. 4D, lane 6), deleting Z1 together with 408-460 further reduces Groucho binding (Fig. 4D, lane 10). We conclude that the minimal region of Nlz required for interaction with Groucho contains Z1 and the region between the two zinc fingers.

Although the Nlz-related Elbow protein binds Groucho, the functional significance of this interaction has not been explored. To test if Nlz function requires Groucho binding, we tested the in vivo activity of NlzΔ385-460 and NlzΔ408-460. We find that embryos injected with *nlzΔ385-460* do not exhibit loss of rostral gene expression or expansion of r4 gene expression, as compared to injection of *nlz* (3.1% of *nlzΔ385-460*-injected embryos affected vs. 64.9% of *nlz*-injected embryos), although both proteins are expressed at similar levels (Fig. 3F, lanes 1,7). NlzΔ408-460 is also less

active than full-length Nlz, but still affects 25.7% of the injected embryos, consistent with NlzΔ408-460 apparently binding Groucho slightly better than NlzΔ385-460 (Fig. 3D, compare lane 11 to lane 10). This demonstrates that the interaction with Groucho is required for *nlz* to have an effect in vivo.

*Deleting the Groucho binding site generates a dominant negative form of Nlz*

To further understand the role of Nlz, we next set out to interfere with endogenous Nlz function. Since two different sets of antisense morpholino oligos do not repress Nlz function (not shown), we instead turned our attention to generating a dominant negative construct. In particular, we reasoned that a form of Nlz lacking the Groucho interaction domain might substitute for endogenous Nlz, but since it would be unable to recruit Groucho, it might interfere with the repressor activity of Nlz. To determine if NlzΔ385-460 interferes with the function of wild type Nlz, we co-injected *nlz* with either *nlzΔ385-460* or control (*βgal*) mRNA (Table 2). We find that *nlzΔ385-460* reduces *nlz* activity ten-fold. Specifically, *nlz* + *βgal* disrupts rostral gene expression in 21.6% of injected embryos, while *nlz* + *nlzΔ385-460* disrupts rostral gene expression in only 2.1% of embryos (Table 2). This demonstrates that *nlzΔ385-460* interferes with the function of wild-type Nlz. We conclude that NlzΔ385-460 acts as a dominant negative and henceforth refer to it as dnNlz.

*Disrupting endogenous Nlz function leads to an expansion of r5-specific gene expression into r4*

To examine the role of Nlz during hindbrain development, we next expressed dnNlz in developing zebrafish embryos by mRNA injection and assayed for phenotypic changes in hindbrain gene expression. We find that *dnNlz* promotes rostral expansion of r5-specific gene expression, leading to an overlap between r4- and r5-specific gene expression (120/300, 40.0%) and a shortening of r4 (Fig. 4A-D,G). In some instances, the overlap is detected as a localized expansion of *krox20* expression into the *hoxb1a* territory (dashed line in Fig. 4A). In other instances, *krox20* expression is mixed with *hoxb1a* expression along the entire length of the rhombomere boundary (dashed lines in Fig. 4B-D). A less pronounced overlap effect is observed at the r3/r4 (Fig. 4B-D) and the r6/r7 boundaries (not shown). We also find that *dnNlz*-injected embryos display a lateral widening of *krox20* and *hoxb1a* expression, occasionally associated with twisted, kinked and/or shortened notochords (Fig. 4G,I). In most cases, this effect is moderate (Fig. 4G) but in some instances, the widened gene expression encircles the entire width of the embryo (Fig. 4I). Extensive overlap in rhombomere-specific gene expression is seen in embryos both with and without this lateral widening, suggesting that the two phenotypes are not directly related. As observed for ectopic expression of full-length Nlz, dnNlz also has a mild effect on neuronal differentiation. Specifically, migration of nVII branchiomotor neurons from r4 to r5/r6 is incomplete in ~12% of embryos (15/127, not shown) and the axons of reticulospinal neurons appear defasiculated in ~14% of embryos

(43/306, not shown). We conclude that Nlz is required for the proper segregation of r4- and r5-specific gene expression domains.

*A VP16Nlz fusion construct mimics the effect of dnNlz*

We reasoned that dnNlz might lead to an activation of target genes normally repressed by Nlz. To test this, we fused the VP16 transcriptional activation domain to the N-terminus of full-length Nlz (VP16Nlz) and expressed this construct in developing zebrafish embryos by mRNA injection. Indeed, we find that *VP16Nlz*-injected embryos exhibit the same phenotype as *dnNlz*-injected embryos (Fig. 4E) suggesting that dnNlz promotes activation of gene expression. This effect is not due to the VP16 activation domain affecting functions at the insertion site, since placing the VP16 domain internally, in place of amino acids # 237-275, has the same effect (not shown).

*nlz belongs to a novel family of zinc-finger proteins*

We and others (Andreazzoli et al., 2001; Sagerstrom et al., 2001) have previously noted that zebrafish Nlz is related to *Drosophila* NocA (Cheah et al., 1994) as well as to an uncharacterized human protein. Upon renewed BLAST analysis, we find that Nlz is also related to second zebrafish protein (herein referred to as Nlz2; sequence compiled from EST contigs wz1906.2 and wz1906.1), as well as to a second *Drosophila* protein (Elbow (Dorfman et al., 2002)), two hypothetical human proteins (FLJ14299 and MGC2555) and two hypothetical mouse proteins (NM_145459 and XM_146263) (Fig. 5). Several domains are conserved within this group of proteins, including an N-terminal

domain (termed the 'SP motif') that is also found in the Sp1 family of zinc finger transcription factors (Philipsen and Suske, 1999), a zinc-finger motif (Z1) that has one histidine surrounded by four cysteines and may fall into the $C_2HC$ or $CHC_2$ class (Klug and Rhodes, 1987) and a second zinc-finger motif (Z2) which is of the $C_2H_2$ type (Berg, 1990; Laity et al., 2001). Sequence alignment (Fig. 5A) and phylogenetic analysis (Fig. 5B) indicate that the vertebrate proteins fall into two groups with one mouse and one human protein related to each of Nlz and Nlz2, while NocA and Elbow are more divergent. Our finding that more than one Nlz-like protein exists in several organisms suggests that Nlz belongs to a family of related zinc-finger proteins. Since NocA and Elbow regulate neural and tracheal development in *Drosophila*, while Nlz regulates hindbrain development in zebrafish, members of this family may regulate various aspects of vertebrate development.

## Discussion

In this report we address the possibility that *nlz* functions in hindbrain development, as suggested by the initial characterization of this gene (Andreazzoli et al., 2001; Sagerstrom et al., 2001). A detailed expression analysis revealed that while *nlz* is expressed caudal to the r3/r4 boundary during gastrulation, *nlz* expression progresses rostrally during segmentation stages to encompass both r3 and r2, while expression caudal to r5 is reduced. We have demonstrated that Nlz is a nuclear protein that associates with the co-repressor Groucho, suggesting that Nlz may repress transcription. Consistent with a role as a repressor, we find that misexpression of *nlz* disrupts expression of *gbx1*, *hoxa2*, *ephB4a*, *krox20* and *ephA4* in the rostral hindbrain, concomitant with a partial expansion of genes expressed in r4 (*hoxb1a* and *ephrinB2a*) into r3 and a disruption of *mariposa* expression at rhombomere boundaries from r1 to r4. In further support of Nlz acting as a repressor, a form of Nlz unable to bind Groucho does not repress gene expression in the rostral hindbrain. Since endogenous *nlz* is not expressed in the rostral hindbrain until segmentation stages (Sagerstrom et al., 2001), we propose that the premature presence of ectopic *nlz* in this region represses rostral gene expression and, perhaps, indirectly promotes the expansion of adjacent gene expression domains. We also find that a dominant negative form of Nlz leads to an expansion of r5-specific gene expression and induces an overlap of gene expression at the r4/r5 boundary. We conclude that Nlz is required for segmental gene expression, particularly in r4, during hindbrain development.

*Nlz belongs to a novel family of zinc finger proteins that act as transcriptional repressors*

We find that Nlz belongs to a growing family of zinc-fingers proteins that also includes zebrafish Nlz2, *Drosophila* NocA and Elbow, two human proteins and two mouse proteins (Fig. 5). We propose that this family encodes transcriptional repressors based on several observations.

First, Elbow and Nlz associate with the Groucho co-repressor. Elb apparently binds Groucho via an FKPY motif, but while this motif is conserved in Nlz, Nlz instead interacts with Groucho via amino acids #385-460. Although it is not clear if binding to Groucho is essential for Elbow function (Dorfman et al., 2002), we have found that removal of the Groucho interaction domain creates a dominant negative form of Nlz, indicating that Groucho interaction is necessary for Nlz's ability to function as a repressor. Interestingly, we have found that Nlz also binds two class I histone deacetylases (HDAC1 and HDAC2) apparently via the same region used to bind Groucho (not shown). Since Groucho reportedly acts as a co-repressor, at least in part, by interacting with class I histone deacetylases (related to the yeast *rpd3* gene) (Chen et al., 1999), it is possible that Nlz binds HDACs indirectly via Groucho.

Second, misexpression of Nlz-family proteins leads to loss of gene expression. Elbow misexpression abolishes the expression of tracheal genes (Dorfman et al., 2002) and Nlz misexpression results in the loss of gene expression within the rostral hindbrain. Conversely, *elb* and *noc* mutants exhibit an expansion in the expression of tracheal branch-specific genes (Dorfman et al., 2002) and expression of a dominant negative form

of Nlz leads to expansion of r5-specific gene expression. Since a VP16Nlz fusion construct mimics the effect of dnNlz, it is likely that dnNlz leads to activation of gene expression. We hypothesize that the dnNlz construct acts by de-repressing target genes normally repressed by Nlz, but we cannot exclude the possibility that deleting the Groucho interaction domain generates an 'activator form' of Nlz. Lastly, both Nlz and Elb are nuclear proteins, as expected for a protein involved in transcriptional regulation, and share a domain with the Sp1 family of transcription factors (which we termed the SP motif) (Philipsen and Suske, 1999).

In spite of these features, it is not clear if Nlz-family proteins bind DNA directly. In particular, zinc-finger proteins that bind DNA often contain several $C_2H_2$ fingers (Iuchi, 2001) while the Nlz-related proteins (Fig. 5) contain only one $C_2H_2$ zinc-finger motif. However, we have found that the Nlz proteins form a homodimeric complex (not shown), and this homodimer may provide the suitable number of zinc fingers obligatory for DNA binding.

*nlz regulates segmental hindbrain gene expression*

We find that ectopic *nlz* represses genes expressed in r1-r3 and that disruption of endogenous Nlz function (misexpression of *dnNlz*) results in an overlap of gene expression between r4 and r5, with r5 expanding into r4. While this is consistent with Nlz being required for proper formation of r4 by repressing non-r4 gene expression, it is interesting that ectopic Nlz and dnNlz affect different regions (r1-r3 vs. r5). We note that ectopic Nlz affects only the rostral hindbrain (r1-r3), which coincides with the expression

domain of *grg3*, one of the zebrafish Groucho family genes (Runko & Sagerstrom, not shown) (Kobayashi et al., 2001). In contrast, *grg3* is not expressed in r5, perhaps explaining why ectopic Nlz affects r3, but not r5. Furthermore, dnNlz has an effect only in a small portion of its expression domain (r4/r5), suggesting that Nlz is inactive, or has a redundant function, further caudally. Strikingly, our preliminary results indicate that *nlz2* is expressed in r5-r7, but not in r4 (not shown), suggesting that *nlz* and *nlz2* may act redundantly caudal to r4.

Hindbrain segmentation defects may be caused by inappropriate cell sorting or cell fate decisions. For instance, expression of truncated EphA4, which blocks EphA4 intracellular signaling, leads to a disruption in cell sorting such that r3/r5 cells are intermingled with r2/r4/r6 cells (Xu et al., 1995; Xu et al., 1999), and misexpression of soluble forms of *ephrinA5* and *EphA3*, which block signaling through both Eph receptors and ephrins (Oates et al., 1999), gives rise to a lateral expansion of cells expressing MHB and hindbrain genes. While these phenotypes share similarities with *nlz*- and *dnNlz*-induced phenotypes, r4- and r5-gene expression appears to overlap in *dnNlz*-injected embryos, suggesting a role for Nlz in regulating cell fate. Furthermore, the number of cells expressing r3-genes in *nlz*-injected embryos is reduced, but we do not find a change in the number of apoptotic cells (detected by acridine orange staining) or dividing cells (detected with antiserum against phosphorylated histone H3) in this region (not shown), also suggesting that Nlz affects cell fate. We propose that Nlz acts early in development to repress non-r4 gene expression, leading to cells taking on an r4-fate. This effect may be mediated, for instance, by Nlz repressing an early acting gene such as *gbx1* or *krox20*.

The absence of these genes in the rostral hindbrain may subsequently allow an anterior shift of *hoxb1a* expression from r4, since the anterior limit of *hoxb1a* will no longer be repressed by *krox20*. Interestingly, ectopic expression of the *nab* genes (which repress *krox20*) yields a phenotype similar to *nlz* misexpression (Mechta-Grigoriou et al., 2000). We also note that while ectopic *nlz* represses *krox20* in r3 during gastrula stages, endogenous *krox20* expression co-exists with *nlz* in r3 at later stages. This may be due to initiation, but not maintaince, of r3 *krox20* expression being *nlz*-sensitive.

**Acknowledgments**

We thank members of the Sagerström lab for helpful discussions, Albert Courey and Robert Goldstein for the GST:Groucho fusion construct, and Caroline Brennan, Ajay Chitnis, Julie Cooke, Lisa Maves and Vicky Prince for providing plasmids to construct in situ probes. This work was supported by NIH grants NS38183 and HD39156 to CGS.

## References


Alexandre, D., Clarke, J. D., Oxtoby, E., Yan, Y. L., Jowett, T., and Holder, N. (1996). Ectopic expression of Hoxa-1 in the zebrafish alters the fate of the mandibular arch neural crest and phenocopies a retinoic acid-induced phenotype. *Development* **122,** 735-746.

Amores, A., Force, A., Yan, Y. L., Joly, L., Amemiya, C., Fritz, A., Ho, R. K., Langeland, J., Prince, V., Wang, Y. L., Westerfield, M., Ekker, M., and Postlethwait, J. H. (1998). Zebrafish hox clusters and vertebrate genome evolution. *Science* **282,** 1711-4.

Andreazzoli, M., Broccoli, V., and Dawid, I. B. (2001). Cloning and expression of noz1, a zebrafish zinc finger gene related to Drosophila nocA. *Mech Dev* **104,** 117-20.

Barrow, J. R., Stadler, H. S., and Capecchi, M. R. (2000). Roles of Hoxa1 and Hoxa2 in patterning the early hindbrain of the mouse. *Development* **127,** 933-44.

Berg, J. M. (1990). Zinc fingers and other metal-binding domains. Elements for interactions between macromolecules. *J Biol Chem* **265,** 6513-6.

Blader, P., Fischer, N., Gradwohl, G., Guillemont, F., and Strahle, U. (1997). The activity of neurogenin1 is controlled by local cues in the zebrafish embryo. *Development* **124,** 4557-69.

Cheah, P. Y., Meng, Y. B., Yang, X., Kimbrell, D., Ashburner, M., and Chia, W. (1994). The Drosophila l(2)35Ba/nocA gene encodes a putative Zn finger protein

involved in the development of the embryonic brain and the adult ocellar structures. *Molecular and Cellular Biology* **14,** 1487-1499.

Chen, G., Fernandez, J., Mische, S., and Courey, A. J. (1999). A functional interaction between the histone deacetylase Rpd3 and the corepressor groucho in Drosophila development. *Genes Dev* **13,** 2218-30.

Cooke, J., Moens, C., Roth, L., Durbin, L., Shiomi, K., Brennan, C., Kimmel, C., Wilson, S., and Holder, N. (2001). Eph signalling functions downstream of Val to regulate cell sorting and boundary formation in the caudal hindbrain. *Development* **128,** 571-80.

Cooke, J. E., and Moens, C. B. (2002). Boundary formation in the hindbrain: Eph only it were simple. *Trends Neurosci* **25,** 260-7.

Cordes, S. P., and Barsh, G. S. (1994). The mouse segmentation gene kr encodes a novel basic domain-leucine zipper transcription factor. *Cell* **79,** 1025-1034.

Dorfman, R., Glazer, L., Weihe, U., Wernet, M. F., and Shilo, B. Z. (2002). Elbow and Noc define a family of zinc finger proteins controlling morphogenesis of specific tracheal branches. *Development* **129,** 3585-96.

Durbin, L., Brennan, C., Shiomi, K., Cooke, J., Barrios, A., Shanmugalingam, S., Guthrie, B., Lindberg, R., and Holder, N. (1998). Eph signaling is required for segmentation and differentiation of the somites. *Genes Dev* **12,** 3096-109.

Flanagan, J. G., and Vanderhaeghen, P. (1998). The ephrins and Eph receptors in neural development. *Annu Rev Neurosci* **21,** 309-45.

Fraser, S., Keynes, R., and Lumsden, A. (1990). Segmentation in the chick embryo hindbrain is defined by cell lineage restrictions. *Nature* **344,** 431-5.

Geisler, R., Rauch, G. J., Baier, H., van Bebber, F., Brobeta, L., Dekens, M. P., Finger, K., Fricke, C., Gates, M. A., Geiger, H., Geiger-Rudolph, S., Gilmour, D., Glaser, S., Gnugge, L., Habeck, H., Hingst, K., Holley, S., Keenan, J., Kirn, A., Knaut, H., Lashkari, D., Maderspacher, F., Martyn, U., Neuhauss, S., Haffter, P., and et al. (1999). A radiation hybrid map of the zebrafish genome. *Nat Genet* **23,** 86-9.

Guthrie, S., Prince, V., and Lumsden, A. (1993). Selective dispersal of avian rhombomere cells in orthotopic and heterotopic grafts. *Development* **118,** 527-38.

Hajduk, S. L. (1976). Demonstration of kinetoplast DNA in dyskinetoplastic strains of Trypanosoma equiperdum. *Science* **191,** 858-9.

Hatta, K. (1992). Role of the floor plate in axonal patterning in the zebrafish CNS. *Neuron* **9,** 629-42.

Holder, N., and Klein, R. (1999). Eph receptors and ephrins: effectors of morphogenesis. *Development* **126,** 2033-44.

Hukriede, N. A., Joly, L., Tsang, M., Miles, J., Tellis, P., Epstein, J. A., Barbazuk, W. B., Li, F. N., Paw, B., Postlethwait, J. H., Hudson, T. J., Zon, L. I., McPherson, J. D., Chevrette, M., Dawid, I. B., Johnson, S. L., and Ekker, M. (1999). Radiation hybrid mapping of the zebrafish genome. *Proc Natl Acad Sci U S A* **96,** 9745-50.

Irving, C., and Mason, I. (2000). Signalling by FGF8 from the isthmus patterns anterior hindbrain and establishes the anterior limit of Hox gene expression. *Development* **127,** 177-86.

Itoh, M., Kudoh, T., Dedekian, M., Kim, C. H., and Chitnis, A. B. (2002). A role for iro1 and iro7 in the establishment of an anteroposterior compartment of the ectoderm adjacent to the midbrain-hindbrain boundary. *Development* **129,** 2317-27.

Iuchi, S. (2001). Three classes of C2H2 zinc finger proteins. *Cell Mol Life Sci* **58,** 625-35.

Joly, J. S., Maury, M., Joly, C., Duprey, P., Boulekbache, H., and Condamine, H. (1992). Expression of a zebrafish caudal homeobox gene correlates with the establishment of posterior cell lineages at gastrulation. *Differentiation* **50,** 75-87.

Klug, A., and Rhodes, D. (1987). Zinc fingers: a novel protein fold for nucleic acid recognition. *Cold Spring Harb Symp Quant Biol* **52,** 473-82.

Kobayashi, M., Nishikawa, K., Suzuki, T., and Yamamoto, M. (2001). The homeobox protein Six3 interacts with the Groucho corepressor and acts as a transcriptional repressor in eye and forebrain formation. *Dev Biol* **232,** 315-26.

Korzh, V., Edlund, T., and Thor, S. (1993). Zebrafish primary neurons initiate expression of the LIM homeodomain protein Isl-1 at the end of gastrulation. *Development* **118,** 417-25.

Krauss, S., Johansen, T., Korzh, V., and Fjose, A. (1991). Expression of the zebrafish paired box gene pax[zf-b] during early neurogenesis. *Development* **113,** 1193-1206.

Krumlauf, R. (1994). Hox genes in vertebrate development. *Cell* **78,** 191-201.

Laity, J. H., Lee, B. M., and Wright, P. E. (2001). Zinc finger proteins: new insights into structural and functional diversity. *Curr Opin Struct Biol* **11,** 39-46.

Lumsden, A. (1999). Closing in on rhombomere boundaries. *Nat Cell Biol* **1,** E83-5.

Lumsden, A., and Krumlauf, R. (1996). Patterning the vertebrate neuraxis. *Science* **274,** 1109-1115.

Macdonald, R., Xu, Q., Barth, K. A., Mikkola, I., Holder, N., Fjose, A., Krauss, S., and Wilson, S. W. (1994). Regulatory gene expression boundaries demarcate sites of neuronal differentiation in the embryonic zebrafish forebrain. *Neuron* **13,** 1039-53.

Maconochie, M. K., Nonchev, S., Studer, M., Chan, S. K., Popperl, H., Sham, M. H., Mann, R. S., and Krumlauf, R. (1997). Cross-regulation in the mouse HoxB complex: the expression of Hoxb2 in rhombomere 4 is regulated by Hoxb1. *Genes Dev* **11,** 1885-95.

Manzanares, M., Cordes, S., Ariza-McNaughton, L., Sadl, V., Maruthainar, K., Barsh, G., and Krumlauf, R. (1999). Conserved and distinct roles of kreisler in regulation of the paralogous Hoxa3 and Hoxb3 genes. *Development* **126,** 759-69.

Manzanares, M., Cordes, S., Kwan, C.-T., Sham, M. H., Barsh, G. S., and Krumlauf, R. (1997). Segmental regulation of Hoxb-3 by kreisler. *Nature* **387,** 191-195.

Maves, L., Jackman, W., and Kimmel, C. B. (2002). FGF3 and FGF8 mediate a rhombomere 4 signaling activity in the zebrafish hindbrain. *Development* **129,** 3825-37.

McClintock, J. M., Carlson, R., Mann, D. M., and Prince, V. E. (2001). Consequences of Hox gene duplication in the vertebrates: an investigation of the zebrafish Hox paralogue group 1 genes. *Development* **128,** 2471-84.

McClintock, J. M., Kheirbek, M. A., and Prince, V. E. (2002). Knockdown of duplicated zebrafish hoxb1 genes reveals distinct roles in hindbrain patterning and a novel mechanism of duplicate gene retention. *Development* **129,** 2339-2354.

McKay, I. J., Muchamore, I., Krumlauf, R., Maden, M., Lumsden, A., and Lewis, J. (1994). The kreisler mouse: a hindbrain segmentation mutant that lacks two rhombomeres. *Development* **120,** 2199-2211.

Mechta-Grigoriou, F., Garel, S., and Charnay, P. (2000). Nab proteins mediate a negative feedback loop controlling Krox-20 activity in the developing hindbrain. *Development* **127,** 119-28.

Moens, C. B., Cordes, S. P., Giorgianni, M. W., Barsh, G. S., and Kimmel, C. B. (1998). Equivalence in the genetic control of hindbrain segmentation in fish and mouse. *Development* **125,** 381-391.

Moens, C. B., Yan, Y.-L., Appel, B., Force, A. G., and Kimmel, C. B. (1996). valentino: a zebrafish gene required for normal hindbrain segmentation. *Development* **122,** 3981-3990.

Mori, H., Miyazaki, Y., Morita, T., Nitta, H., and Mishina, M. (1994). Different spatio-temporal expressions of three otx homeoprotein transcripts during zebrafish embryogenesis. *Brain Res Mol Brain Res* **27,** 221-31.

Nonchev, S., Vesque, C., Maconochie, M., Seitanidou, T., Ariza-McNaughton, L., Frain, M., Marshall, H., Sham, M. H., Krumlauf, R., and Charnay, P. (1996). Segmental expression of Hoxa-2 in the hindbrain is directly regulated by Krox-20. *Development* **122,** 543-554.

Oates, A. C., Lackmann, M., Power, M. A., Brennan, C., Down, L. M., Do, C., Evans, B., Holder, N., and Boyd, A. W. (1999). An early developmental role for eph-ephrin interaction during vertebrate gastrulation. *Mech Dev* **83,** 77-94.

Oxtoby, E., and Jowett, T. (1993). Cloning of the zebrafish krox-20 gene (*krx20*) and its expression during development. *Nucl. Acids Res.* **21,** 1087-1095.

Philipsen, S., and Suske, G. (1999). A tale of three fingers: the family of mammalian Sp/XKLF transcription factors. *Nucleic Acids Res* **27,** 2991-3000.

Prince, V. E., Joly, L., Ekker, M., and Ho, R. K. (1998a). Zebrafish hox genes: genomic organization and modified colinear expression patterns in the trunk. *Development* **125,** 407-420.

Prince, V. E., Moens, C. B., Kimmel, C. B., and Ho, R. K. (1998b). Zebrafish hox genes:expression in the hindbrain region of wild-type and mutants of the segmentation gene valentino. *Development* **125,** 393-406.

Reifers, F., Bohli, H., Walsh, E. C., Crossley, P. H., Stainier, D. Y., and Brand, M. (1998). Fgf8 is mutated in zebrafish acerebellar (ace) mutants and is required for maintenance of midbrain-hindbrain boundary development and somitogenesis. *Development* **125,** 2381-95.

Rossel, M., and Capecchi, M. R. (1999). Mice mutant for both Hoxa1 and Hoxb1 show extensive remodeling of the hindbrain and defects in craniofacial development. *Development* **126,** 5027-40.

Sagerström, C. G., Grinblat, Y., and Sive, H. (1996). Anteroposterior patterning in the zebrafish, Danio rerio: an explant assay reveals inductive and suppressive cell interactions. *Development* **122,** 1873-1883.

Sagerstrom, C. G., Kao, B. A., Lane, M. E., and Sive, H. (2001). Isolation and characterization of posteriorly restricted genes in the zebrafish gastrula. *Dev Dyn* **220,** 402-8.

Schneider-Maunoury, S., Seitanidou, T., Charnay, P., and Lumsden, A. (1997). Segmental and neuronal architecture of the hindbrain of Krox-20 mouse mutants. *Development* **124,** 1215-26.

Schulte-Merker, S., Ho, R. K., Herrmann, B. G., and Nusslein-Volhard, C. (1992). The protein product of the zebrafish homologue of the mouse T gene is expressed in nuclei of the germ ring and the notochord of the early embryo. *Development* **116,** 1021-1032.

Seitanidou, T., Schneider-Maunoury, S., Desmarquet, C., Wilkinson, D. G., and Charnay, P. (1997). Krox-20 is a key regulator of rhombomere-specific gene expression in the developing hindbrain. *Mech Dev* **65,** 31-42.

Sham, M. H., Vesque, C., Nonchev, S., Marshall, H., Frain, M., Gupta, R. D., Whiting, J., Wilkinson, D., Charnay, P., and Krumlauf, R. (1993). The zinc finger gene Krox20 regulates HoxB2 (Hox2.8) during hindbrain segmentation. *Cell* **72,** 183-196.

Studer, M., Gavalas, A., Marshall, H., Ariza-McNaughton, L., Rijli, F. M., Chambon, P., and Krumlauf, R. (1998). Genetic interactions between Hoxa1 and Hoxb1 reveal new roles in regulation of early hindbrain patterning. *Development* **125,** 1025-36.

Studer, M., Lumsden, A., Ariza-McNaughton, L., Bradley, A., and Krumlauf, R. (1996). Altered segmental identity and abnormal migration of motor neurons in mice lacking Hoxb-1. *Nature* **384,** 630-634.

Sun, Z., and Hopkins, N. (2001). vhnf1, the MODY5 and familial GCKD-associated gene, regulates regional specification of the zebrafish gut, pronephros, and hindbrain. *Genes Dev* **15,** 3217-29.

Theil, T., Ariza-McNaughton, L., Manzanares, M., Brodie, J., Krumlauf, R., and Wilkinson, D. G. (2002). Requirement for downregulation of kreisler during late patterning of the hindbrain. *Development* **129,** 1477-85.

Theil, T., Frain, M., Gilardi-Hebenstreit, P., Flenniken, A., Charnay, P., and Wilkinson, D. G. (1998). Segmental expression of the EphA4 (Sek-1) receptor tyrosine kinase in the hindbrain is under direct transcriptional control of Krox-20. *Development* **125,** 443-452.

Vlachakis, N., Choe, S. K., and Sagerstrom, C. G. (2001). Meis3 synergizes with Pbx4 and Hoxb1b in promoting hindbrain fates in the zebrafish. *Development* **128,** 1299-312.

Weinberg, E. S., Allende, M. L., Kelly, C. S., Abdelhamid, A., Murakami, T., Andermann, P., Doerre, O. G., Grunwald, D. J., and Riggleman, B. (1996).

Developmental regulation of zebrafish *MyoD* in wild-type, *no tail* and *spadetail* embryos. *Development* **122,** 271-280.

Xu, Q., Alldus, G., Holder, N., and Wilkinson, D. G. (1995). Expression of truncated Sek-1 receptor tyrosine kinase disrupts the segmental restriction of gene expression in the Xenopus and zebrafish hindbrain. *Development* **121,** 4005-16.

Xu, Q., Alldus, G., Macdonald, R., Wilkinson, D. G., and Holder, N. (1996). Function of the Eph-related kinase rtk1 in patterning of the zebrafish forebrain. *Nature* **381,** 319-22.

Xu, Q., Holder, N., Patient, R., and Wilson, S. W. (1994). Spatially regulated expression of three receptor tyrosine kinase genes during gastrulation in the zebrafish. *Development* **120,** 287-99.

Xu, Q., Mellitzer, G., Robinson, V., and Wilkinson, D. G. (1999). In vivo cell sorting in complementary segmental domains mediated by Eph receptors and ephrins. *Nature* **399,** 267-71.

Zhang, M., Kim, H.-J., Marshall, H., Gendron-Maguire, M., Lucas, A. D., Baron, A., Gudas, L. J., Gridley, T., Krumlauf, R., and Grippo, J. F. (1994). Ectopic Hoxa-1 induces rhombomere transformation in mouse hindbrain. *Development* **120,** 2431-2442.

**Table 1. Misexpression of *nlz* affects rostral hindbrain gene expression [a]**

| Gene [b] | Embryos Affected (%) [c] | |
|---|---|---|
| | *nlz* | *βgal* |
| *krox20* (r3) | 64.9 (640/986) | 4.3 (18/414) |
| *krox20* (r3; 24 hpf) | 56.3 (117/208) | 1.5 (3/206) |
| *ephA4* (r3) | 62.4 (121/194) | 2.3 (4/175) |
| *ephA4* (r3; 24hpf) | 63.6 (75/118) | 1.4 (1/73) |
| *hoxb1a* (r4) | 41.1 (411/999) | 1.1 (15/1345) |
| *hoxb1a* (r4; 24 hpf) | 27.9 (58/208) | 0.5 (1/206) |
| *ephrinB2a* (r4) | 44.9 (70/156) | 0.7 (1/140) |
| *hoxa2* (r2/3) | 45.4 (149/328) | 1.3 (2/157) |
| *ephB4a* (r2/3) | 40.2 (66/164) | 1.0 (1/103) |
| *gbx1* (r1-r3; 8-9 hpf) | 51.6 (141/273) | 4.5 (8/177) |
| *iro1* (r1-r3; 8-9 hpf) | 0.7 (1/149) | 1.1 (1/90) |
| *mariposa* (r1-r4 boundaries) | 37.9 (11/29) | 1.1 (1/88) |
| *otx2* (forebrain) | 1.1 (1/87) | 1.6 (1/63) |
| *pax2.1* (MHB) | 0.3 (2/601) | 0.7 (4/537) |
| *ephrinA2* (midbrain) | 2.6 (1/39) | 2.8 (1/36) |
| *hoxb3* (r5/r6) | 0.8 (1/122) | 1.4 (1/74) |
| *hoxd4* (r7) | 1.7 (6/358) | 0.9 (4/457) |
| *valentino* (r5/r6) | 0.6 (1/169) | 1.7 (4/229) |
| *caudal* (caudal domain) | 1.4 (1/69) | 2.2 (1/46) |

| | | |
|---|---|---|
| *myoD* (somites) | 1.1 (1/87) | 1.5 (1/67) |
| *ntl* (notochord) | 4.2 (21/503) | 2.2 (20/887) |

a) 1 to 2 cell stage embryos were injected with 400 pg of *nlz* or *βgal* mRNA, fixed at the 10 to 14 somite stages (except where indicated), analyzed by in situ hybridization with the markers listed and flat mounted.

b) Injected embryos were scored for the expression of genes in the areas indicated.

c) The percent of embryos showing changes in expression of the listed genes. Reduction in expression was seen for all genes except for *hoxb1a* and *ephrinB2a*, wherein expansion of gene expression was observed.

**Table 2. Competition analysis of Nlz versus dominant negative Nlz.**

| mRNA Injected [a] | Embryos Affected [b] |
|---|---|
| *nlz* (300 pg) + *βgal* (300 pg) | 21.6 (65/301) |
| *nlz* (300 pg) + *nlzΔ385-460* (300 pg) | 2.1 (6/289) |
| *βgal* (600 pg) | 1.3 (1/80) |

a) 1 to 2 cell stage embryos were injected with mRNA of the genes listed, fixed at the 10 to 14 somite stages and analyzed by in situ hybridization with *krox20* and *hoxb1a* probes.

b) The percent of embryos exhibiting loss of r3 and expansion of r4 gene expression.

**Figure 1. *nlz* is dynamically expressed during early midbrain and hindbrain development.**

Embryos were processed for double in situ hybridization with *nlz* (blue stain) together with *krox20* (red stain) in panels A–E,G,I,K, or with *nlz* (blue stain) together with *pax2.1* (red stain) in panels F,H,J,L,M. All embryos were flat-mounted and are shown in dorsal views with anterior to the top at 20X magnification, except that B and D are at 40X magnifications of the left side of panels A and C, respectively. A-E,G,I,K,M show the entire hindbrain and mhb, while F,H,J,L show only the mhb. In situ probe combination is shown at the bottom left-hand corner and embryonic stage is shown at the bottom right-hand corner. Abbreviations: mhb, midbrain-hindbrain boundary; r, rhombomere; hpf, hours post fertilization; s, somites.

**Figure 1**

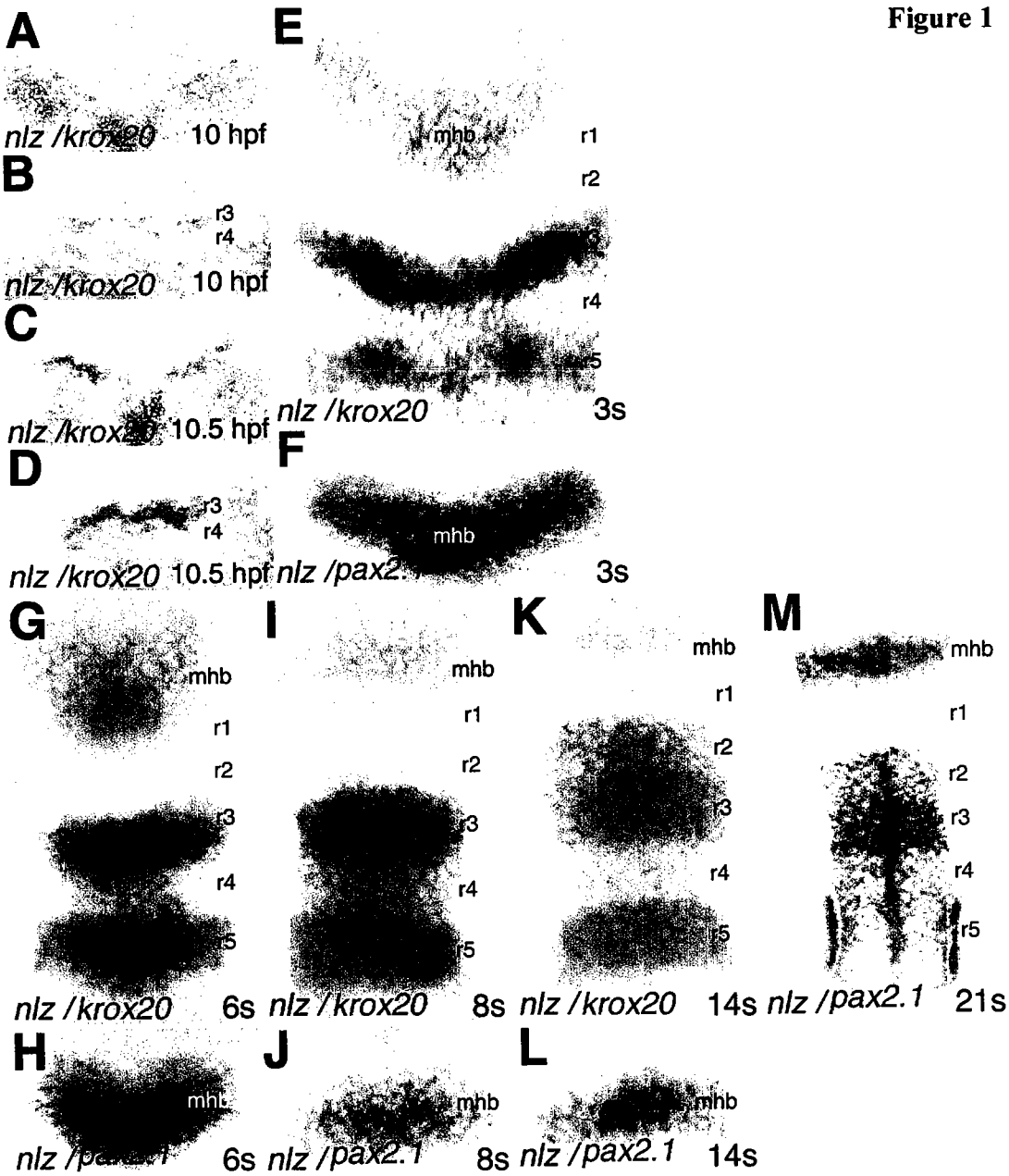
A
nlz /krox20 10 hpf
B
r3
r4
nlz /krox20 10 hpf
C
nlz /krox20 10.5 hpf
D
r3
r4
nlz /krox20 10.5 hpf
E
mhb
r1
r2
r4
r5
nlz /krox20 3s
F
mhb
nlz /pax2.1 3s
G
mhb
r1
r2
r3
r4
r5
nlz /krox20 6s
I
mhb
r1
r2
r3
r4
r5
nlz /krox20 8s
K
mhb
r1
r2
r3
r4
r5
nlz /krox20 14s
M
mhb
r1
r2
r3
r4
r5
nlz /pax2.1 21s
H
mhb
6s
J
mhb
nlz /pax2.1 8s
L
mhb
nlz /pax2.1 14s

**Figure 2. Misexpression of *nlz* causes a disruption in rostral hindbrain patterning.** Embryos were injected with 400 pg of *nlz* (A,C,E,G,I,K,M,O,Q,S,U,W) or *βgal* (B,D,F,H,J,L,N,P,R,T,V,X) mRNA with the exception of K,L in which 100 pg of *βgal* mRNA was additionally co-injected. Embryos were processed for in situ hybridization for *krox20* (detected in blue; A,B,K,L or in red; E,F,M,N,S-V), *ephA4* (detected in blue; C,D,W,X), *ntl* (detected in blue; C,D,S,T), *hoxa2* (detected in blue; E-H), *hoxb1a* (detected in red; G,H or in blue; M,N,S,T), *pax2.1* (detected in red; G,H), *ephB4a* (detected in blue; I,J), *ephrinB2a* (detected in red; I,J or in blue; U,V), *gbx1* (detected in blue; O,P), and *mariposa* (detected in blue; Q,R) and additionally processed for X-gal staining (K,L). All embryos were flat mounted at the 10-14s stage (14-16 hpf) with the exception of M,N (1 to 2 somite stage, 11 hpf); O,P (whole-mounts, 8-9 hpf); Q,R,W,X (prim-5 stage, 24 hpf); and are shown in dorsal views with anterior to the top. Markers are shown at the bottom left-hand corner and injected RNA is shown at the bottom right-hand corner. Arrows indicate loss of gene expression. Asterisks indicate expansion of gene expression from its normal domain with the exception in panel Q, where they indicate mispositioned rhombomeres. Arrowheads in Q,R indicates rhombomere boundaries. The variable signal detected for *ntl* in C,D,S,T is due to slight variations in the focal plane. Abbreviations: mhb, midbrain-hindbrain boundary; r, rhombomere.

Figure 2A-L

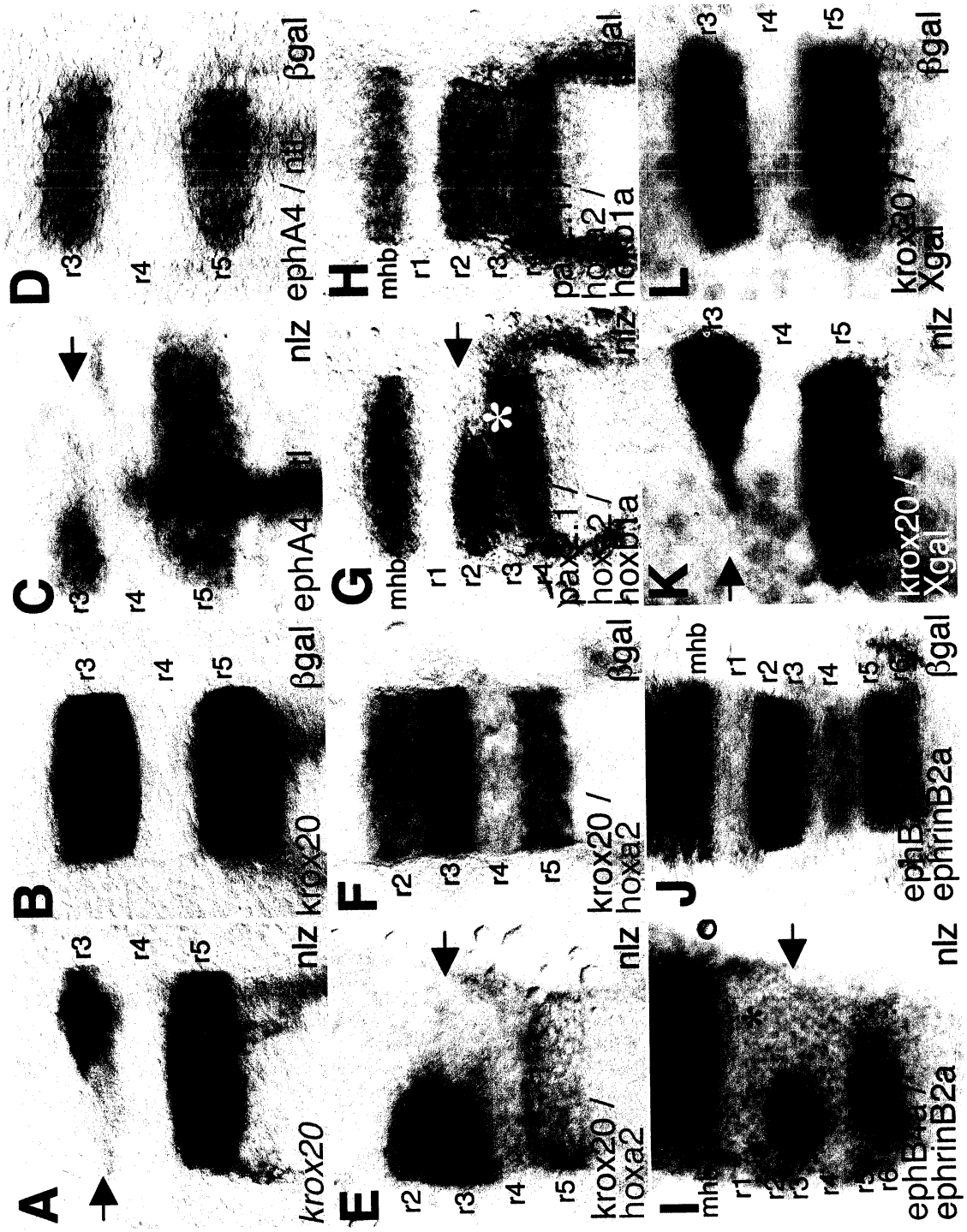
A
krox20
r3
r4
r5
nlz
B
krox20
βgal
C
ephA4
D
ephA4 / nlz
βgal
E
krox20 / hoxa2
F
krox20 / hoxa2
βgal
G
pax2.1 / hoxb1a
mhb
r1
r2
r3
r4
r5
H
pax2.1 / hoxb1a
βgal
I
ephB2a / ephrinB2a
r6
J
ephB2a / ephrinB2a
K
krox20 / Xgal
L
krox20 / Xgal
βgal

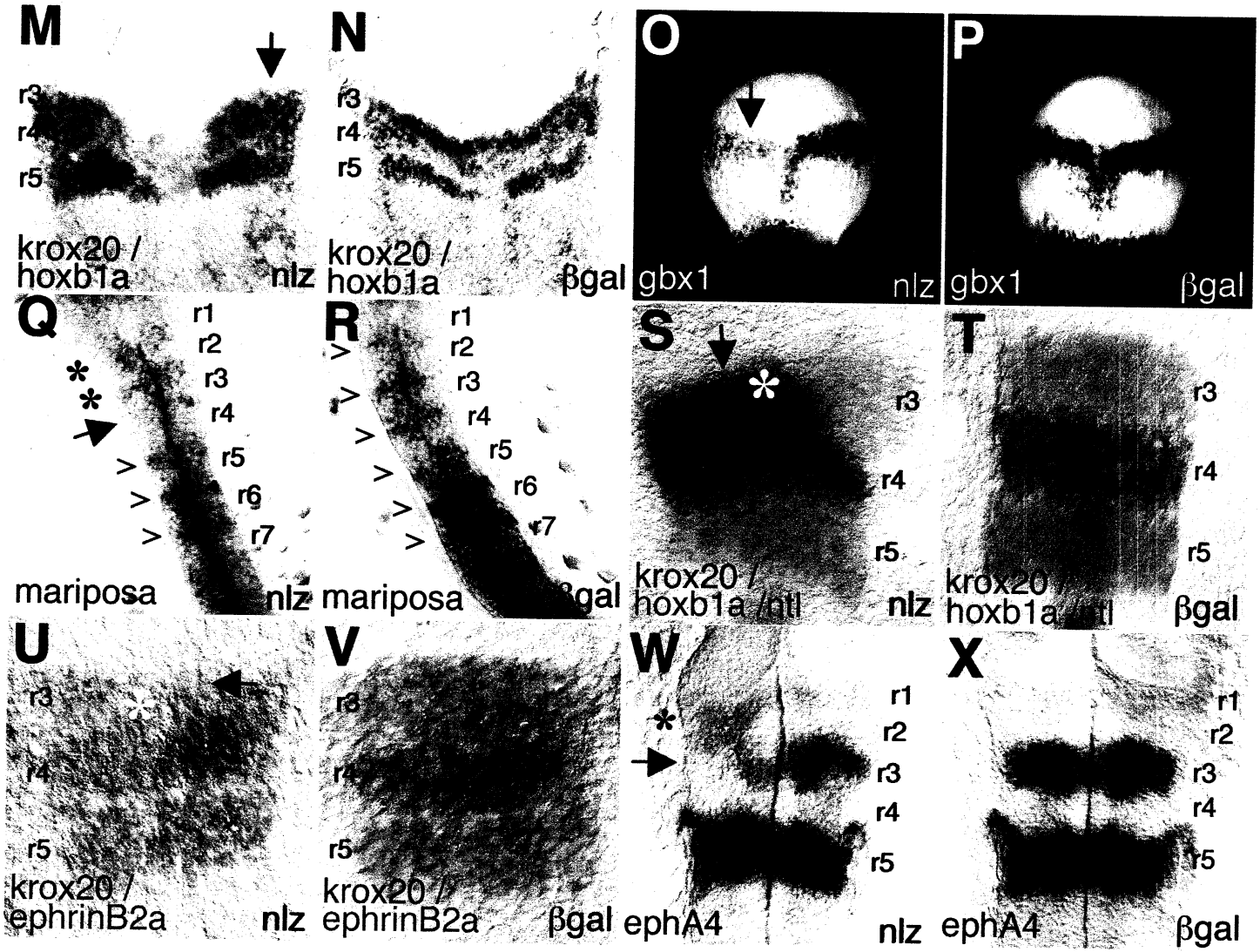
M
r3
r4
r5
krox20 /
hoxb1a
nlz
N
r3
r4
r5
krox20 /
hoxb1a
βgal
O
gbx1
nlz
P
gbx1
βgal
Q
r1
r2
r3
r4
r5
r6
r7
mariposa
nlz
R
r1
r2
r3
r4
r5
r6
r7
mariposa
βgal
S
r3
r4
r5
krox20 /
hoxb1a /ntl
nlz
T
r3
r4
r5
krox20 /
hoxb1a /ntl
βgal
U
r3
r4
r5
krox20 /
ephrinB2a
nlz
V
r3
r4
r5
krox20 /
ephrinB2a
βgal
W
r1
r2
r3
r4
r5
ephA4
nlz
X
r1
r2
r3
r4
r5
ephA4
βgal

Figure 2M-X

**Figure 3. Nlz is a nuclear protein and interacts with the co-repressor Groucho.** (A-C). Nlz is nuclearly localized. Embryos were injected with 800 pg of *mycnlz* mRNA and fixed at 5 hpf. All embryos were flat-mounted and shown in animal pole views at 40X magnification. The embryos were immunostained with anti-c Myc and treated with DAPI. Panel A shows anti-c Myc staining (green), panel B shows DAPI staining of panel A (purple) and panel C shows a merged image of panels A and B (light blue indicates merged green and purple). The signals visualized are indicated at the bottom right-hand corner. (D). GST pull-down assays. Purified GST-Groucho fusion or GST were immobilized on glutathione-sepharose beads and incubated with $^{35}$S-labeled Nlz or Nlz deletion constructs. After washing of the beads, bound proteins were separated by SDS-PAGE and visualized by autoradiography. Aliquots containing 10% of the total amount of $^{35}$S-labeled protein used in the assay are shown (10% load). Nlz binds strongly to the GST-Groucho fusion protein whereas MTnlzΔ385-460, MTnlzΔ408-460 and MTnlzΔ173C exhibit very weak binding. GST alone does not significantly bind to the various Nlz constructs. (E) Nlz constructs. Nlz deletion constructs are shown schematically. Column at right indicates co-repressor binding (+ = strong Groucho interaction; - = weak Groucho interaction). Nlz is shown in blue except for a region shared with the Sp1 family of transcription factors (SP, gray), $C_2HC$ or $CHC_2$ zinc finger motif (Z1, green) and $C_2H_2$ zinc finger (Z2, red). Numbers indicate amino acid position. Line brackets indicate deleted regions. (F). All Nlz constructs are expressed at comparable levels in vivo. Embryos were injected at the 1-2 cell stage with 800 pg mRNA encoding Myc tagged constructs as indicated at the top of each lane. Embryos

were lysed at 5 hpf, resolved on a 10% SDS-PAGE gel, western blotted and probed with an anti-Myc antibody.

**Figure 3**


A
FITC
B
DAPI
C
Merged

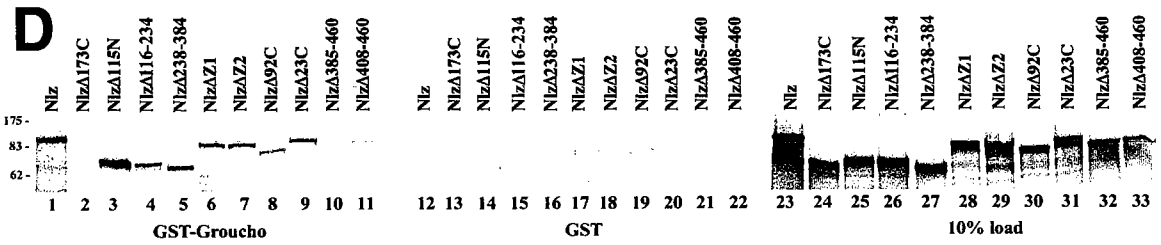
D
Nlz
NlzΔ173C
NlzΔ115N
NlzΔ116-234
NlzΔ238-384
NlzΔZ1
NlzΔZ2
NlzΔ92C
NlzΔ23C
NlzΔ385-460
NlzΔ408-460
175 -
83 -
62 -
1 2 3 4 5 6 7 8 9 10 11
12 13 14 15 16 17 18 19 20 21 22
23 24 25 26 27 28 29 30 31 32 33
GST-Groucho
GST
10% load

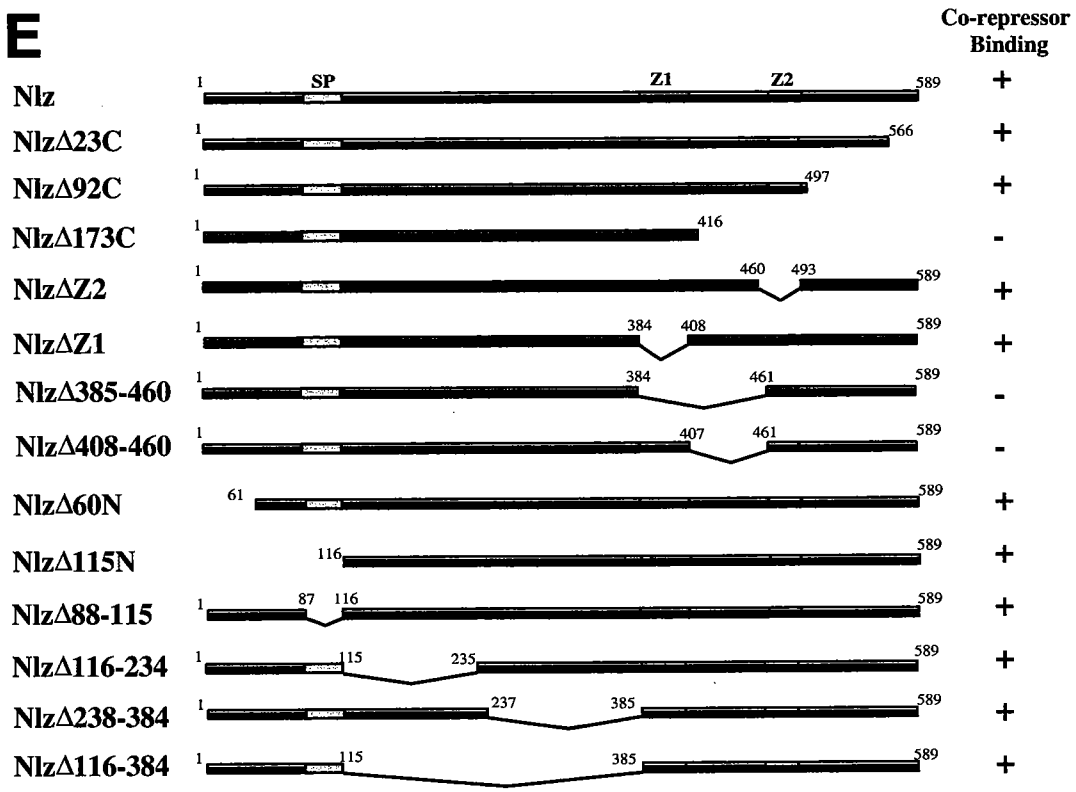
E
Co-repressor Binding
Nlz
SP
Z1
Z2
1
589
+
NlzΔ23C
566
+
NlzΔ92C
497
+
NlzΔ173C
416
-
NlzΔZ2
460
493
589
+
NlzΔZ1
384
408
589
+
NlzΔ385-460
384
461
589
-
NlzΔ408-460
407
461
589
-
NlzΔ60N
61
589
+
NlzΔ115N
116
589
+
NlzΔ88-115
87
116
589
+
NlzΔ116-234
115
235
589
+
NlzΔ238-384
237
385
589
+
NlzΔ116-384
115
385
589
+

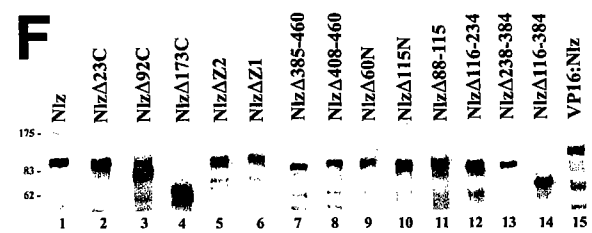
F
Nlz
NlzΔ23C
NlzΔ92C
NlzΔ173C
NlzΔZ2
NlzΔZ1
NlzΔ385-460
NlzΔ408-460
NlzΔ60N
NlzΔ115N
NlzΔ88-115
NlzΔ116-234
NlzΔ238-384
NlzΔ116-384
VP16:Nlz
175 -
83 -
62 -
1 2 3 4 5 6 7 8 9 10 11 12 13 14 15

**Figure 4. Dominant negative form of Nlz induces overlapping gene expression domains in the hindbrain.**

Embryos were injected with either 400 pg of *dnNlz* (*MTnlzΔ385-460*) (A-D,G,I), 25 pg of *VP16Nlz* (E) or 400 pg of *βgal* (F,H,J) mRNA and processed for in situ hybridization for *krox20* (detected in red; A-J), *hoxb1a* (detected in blue; A-J), *ntl* (detected in blue; G-J) and *otx* (detected in blue; I-J). All embryos were fixed at 14-16 hpf, flat mounted (A-H) or whole mounted (I-J), and shown in dorsal views with anterior at the top. Dashed lines in A-E encircle overlap in *krox20* and *hoxb1a* expression. The variable signal detected for *ntl* in G-J is due to slight variations in the focal plane.

**Figure 4**

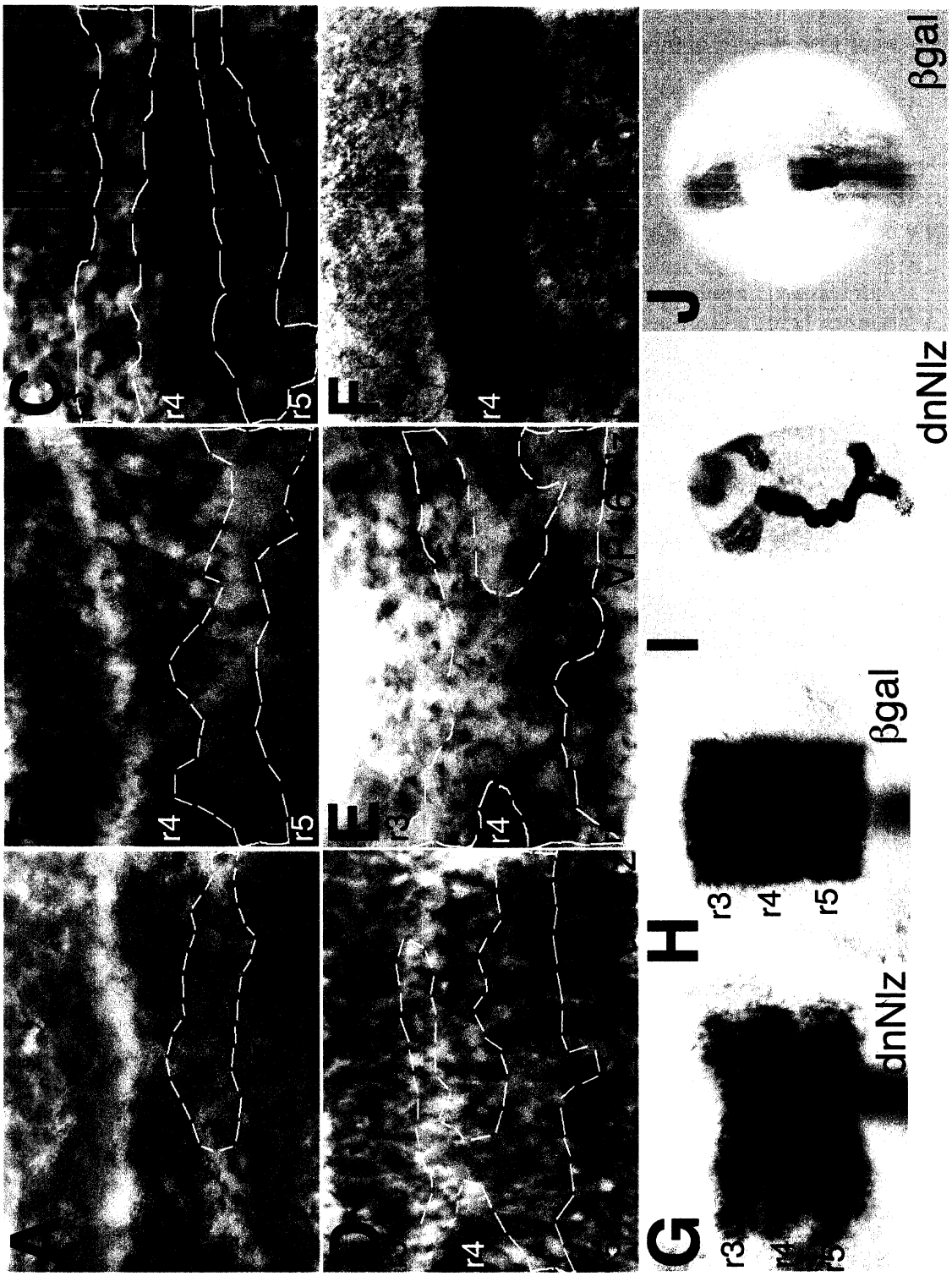
A
r4
r5
C
r4
r5
E
r3
r4
r4
G
r3
r4
r5
dnNlz
H
r3
r4
r5
βgal
I
dnNlz
J
βgal

**Figure 5. Nlz belongs to a novel family of zinc-finger proteins.**

(A). Sequence comparison of conserved domains. Nlz is shown in blue except for a region shared with the Sp1 family of transcription factors (SP, gray), $C_2HC$ or $CHC_2$ zinc-finger motif (Z1, green) and the $C_2H_2$ zinc-finger (Z2, red). Percentiles represent percent identity of each domain to Nlz, as determined using the Jotun Hein method with PAM250 residue weight table. Numbers indicate amino acid position. The family includes two zebrafish proteins, Nlz (AAK73547) and Nlz2 (sequence compiled from EST contigs wz1906.2 and wz1906.1); two *Drosophila* proteins, NocA (A55929) and Elbow (AAM48283); two hypothetical human proteins, FLJ14299 and MGC2555; and two hypothetical mouse proteins, NM_145459 and XM_146263. Abbreviations: Dr, *Danio rerio*; Dm, *Drosophila melanogaster*; Hs, *Homo sapiens*; Mm, *Mus musculus*; ND, not determined. (B). Phylogenetic tree of aligned Nlz-related proteins using the Clustal method with PAM250 residue weight table.

**A**

**Figure 5**


| | | | |
|---|---|---|---|
| **Dr Nlz** | | | |
| **Dr Nlz2** | **100%** | **69.2%** | **82.4%** |
| **Dm NocA** | **66.7%** | **35.7%** | **55.9%** |
| **Dm Elbow** | **65.5%** | **39.3%** | **52.9%** |
| **Hs FLJ14299** | **100%** | **75.9%** | **85.3%** |
| **Hs MGC2555** | **96.7%** | **64.3%** | **88.2%** |
| **Mm NM_145459** | **96.7%** | **64.3%** | **88.2%** |
| **Mm XM_146263** | **100%** | **75.9%** | **ND** |

**B**

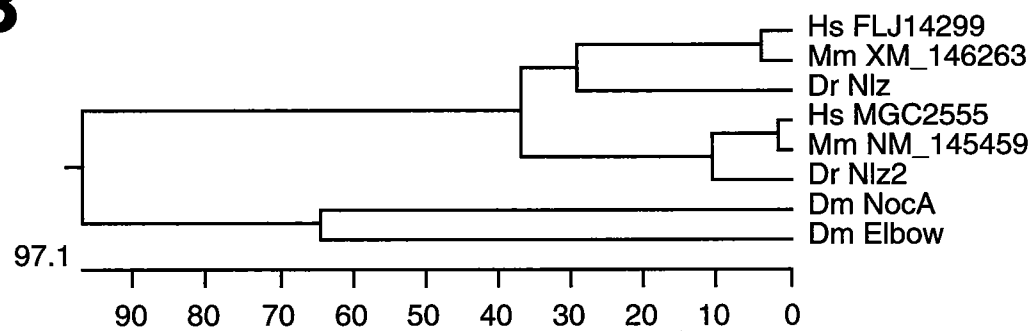

## CHAPTER II

# ISOLATION OF NLZ2 AND CHARACTERIZATION OF ESSENTIAL DOMAINS IN NLZ-FAMILY PROTEINS

Alexander P. Runko and Charles G. Sagerström*
Department of Biochemistry and Molecular Pharmacology, and Program in Neuroscience, University of Massachusetts Medical School, Worcester, MA

*To whom correspondence should be addressed:
Department of Biochemistry and Molecular Pharmacology
364 Plantation Street/LRB 822
Worcester MA 01605
Phone: (508) 856 8006
Fax: (508) 856 8007
Email: charles.sagerstrom@umassmed.edu

Runko, A.P., and Sagerström, C.G. (2003). *J Biol Chem*, submitted.

## Summary

In this study we clone and characterize *nlz2*, a second zebrafish member of the *nlz*-related zinc-finger family. *nlz2* is expressed together with *nlz* in a broad posterior domain during gastrula stages, as well as at the midbrain-hindbrain boundary (MHB) and in the hindbrain caudal to rhombomere (r) 4 during segmentation. *nlz2* is also expressed in distinct regions from *nlz*, notably in the forebrain, midbrain, and trunk. We find that misexpression of *nlz2* represses gene expression in the rostral hindbrain, similar to misexpression of *nlz*. We next compare *nlz* and *nlz2* sequences to identify and characterize conserved domains. We find a conserved C-terminal domain required for nuclear localization and two conserved domains (the Sp motif and a putative $C_2H_2$ zinc finger) required for repressor function. We also demonstrate that Nlz self-associates via its C-terminus, interacts with Nlz2 and binds to histone deacetylases. We find two forms of Nlz generated from alternative translation initiation sites in vivo. These have distinct activities, apparently due to differential activity of the N-terminal Sp motif. We conclude that Nlz2 functions as a transcriptional repressor, similar to Nlz, and that Nlz family proteins possess distinct domains involved in the mediation of nuclear localization, self-association, corepressor binding and repression.



Keywords: Corepressor; Groucho; Hindbrain; Histone deacetylases; Nlz; Rhombomere; Sp1 proteins; Transcription; Zebrafish; Zinc-finger.

## Introduction

We recently identified *nlz* as a member of a novel sub-family of zinc-finger proteins (1). We find that Nlz functions to control segmental gene expression in the zebrafish hindbrain and likely represses transcription by recruiting the corepressor Groucho (1). Sequence similarities between members of this zinc-finger sub-family suggest that the functions of these proteins are evolutionarily conserved. Indeed, the Nlz-related proteins NocA, Elbow and TLP-1 have been found to play a role in morphogenesis of embryonic structures in *Drosophila* (2,3) and *C. elegans* (4). Homozygous *elbow* and *nocA* mutants exhibit defects in tracheal development, particularly stalled and aberrant migration of the dorsal branch and lateral trunks of the trachea (3). Conversely, misexpression of *elbow* in the trachea results in the repression of genes expressed in the visceral branch and dorsal trunk while the number of cells forming the dorsal branch increase (3). Homozygous *nocA* mutants also display brain anomalies such as protrusion of the embryonic supraesophageal ganglion and a reduction of ocelli (photosensory cells) (2). Mutations in *tlp-1* affect specification of asymmetric cell fates and cell fusion resulting in abnormal tail morphogenesis in *C. elegans* (4). This sub-family also includes two hypothetical proteins each in the mouse and human, which have not yet been functionally characterized (1,3,5).

The Nlz sub-family of zinc-finger proteins is related to the vertebrate Sp1-like family of transcription factors (1,4). Members of both families are expressed in developing embryos. However, while *nlz*-related genes have restricted expression patterns, *sp1*-related genes are more ubiquitously expressed. Sp1-like proteins have been

found to function both as transcriptional activators or repressors, depending on context (6), but to date Nlz-related proteins have only been shown to mediate transcriptional repression (1,3). Several domains are common to both families, including the Sp motif, the Buttonhead (Btd) box and the $C_2H_2$ zinc-finger domain as well as serine/theorine- and glutamine-rich regions. While some of these domains are essential for Sp1 function, their specific roles are not known and it is not clear what role they may play in Nlz family proteins.

We recently reported the existence of a second zebrafish gene in this family, *nlz2*, in the EST database (1). We have now cloned *nlz2* and find high homology between *nlz* and *nlz2*. In particular, the Sp motif, a domain resembling the Btd box and a putative $C_2H_2$ zinc finger are all conserved. We find that *nlz2* is expressed similarly to *nlz* during gastrula stages. Specifically, *nlz2* is expressed together with *nlz* in a broad dorsoposterior domain during gastrula stages. During the segmentation period, *nlz* and *nlz2* are co-expressed at the midbrain-hindbrain boundary (MHB), but the *nlz2* expression pattern also diverges from *nlz*. In particular, although *nlz* and *nlz2* are both expressed in the caudal hindbrain, *nlz2* expression never expands rostral to the rhombomere (r) 5 segment while *nlz* expression encompasses most of the hindbrain up to the r2 segment. Additionally, *nlz2* is expressed in the forebrain, where *nlz* expression is never observed. We find that misexpression of *nlz2*, similar to *nlz*, results in a loss of r3 gene expression, suggesting that *nlz2* and *nlz* function similarly as repressors. We next tested the function of domains conserved among members of the Nlz family. We find that nuclear localization of both Nlz2 and Nlz depends on an intact C-terminus and that nuclear

localization is required for *nlz* function. We also discovered that Nlz binds histone deacetylases (HDACs), self-associates and binds to Nlz2, but Nlz self-association does not appear essential for function. Western blot analysis of endogenous Nlz revealed two forms of Nlz, apparently generated by the use of alternative translation start sites. Further analyses determined that the two forms of Nlz have distinct activities in vivo and demonstrated that a domain located in the N-terminus, shared among the Sp1 family of transcription factors, may regulate Nlz-mediated repression independently of Groucho and HDAC binding.

## Experimental Procedures

*RT-PCR and Cloning*

RNA was extracted from 10-hour stage embryos using the ToTally RNA Isolation Kit (Ambion). cDNA was synthesized with Superscript II Reverse Transcriptase (Gibco BRL) according to the manufacturer's instructions. The coding region of *nlz2* was amplified with primers 5'-CCGCTCGAGAGATCTATGATCACATCGCCCTC-3' and 5'-TGCTCTAGACAATCACTGGTATCCAAGCG-3' from cDNA using the Expand High Fidelity PCR System (Roche) according to the manufacturer's instructions. The amplified *nlz2* product was purified using the QIAquick PCR Purification Kit (Qiagen), digested with *Xho*I and *Xba*I and subcloned into the same sites of pCS2+MT. The sequence of *nlz2* was submitted to Genbank as accession# AY371081. The *nlz2* construct was then digested with *Hind*III and *Xba*I and the coding region (including the myc epitope tags) was subcloned into the same sites of hsp70+NLS+MT. The hsp70*:nlz* construct was generated by excising the *nlz* coding region (including the myc epitope tags) with *Hind*III and *Not*I and subcloned by utilizing the same sites in hsp70+NLS+MT. Nlz deletions constructs were generated as described previously (1) or by standard molecular biology cloning techniques into the pCS2+, pCS2+MT or pCS2+NLS+MT vectors. The N-terminus of *grg3* (nucleotides# 1-795 of the open reading frame) was amplified with primers 5'-TAGAATTCAATGTATCCGCAGGGCCGGCAT-3' and 5'-

GAAGGCCTCTCGTTGGACACATCCACCAC-3' from cDNA, digested with *Eco*RI and *Stu*I and subcloned into the same sites in pCS2+.

*In situ hybridization and immunostaining*

Whole- and flat-mount in situ hybridizations using digoxigenin- or fluorescein-labeled antisense RNA probes was performed as described (1,7) including a probe containing 1149 nucleotides of the *nlz2* coding region (synthesized from the EST fc59b07.y1, whose sequence was cloned into the *Not*I and *Sal*I sites of the pSPORT1 vector). Fluorescent immunostaining was performed as described (1,8).

*Embryo injections*

Synthesis and injection of capped mRNA encoding for the *nlz* deletion constructs were performed as described (1). Embryos were also injected with the following DNA constructs: hsp70:*nlz2*, hsp70:*nlz* or hsp70:*GFP*, whose coding region is under the control of a heat shock-inducible promoter, at the 1-2 cell stage, heat-shocked at 70% epiboly (~7.5 hpf) for one hour at 37°C and fixed at the 10-somite stage (14 hpf).

*GST pull-down and Western analysis*

GST:Nlz was constructed by excising the *nlz* coding region from pCS2+MT:*nlz* with *Eco*RI and *Not*I and subcloned into the pGEX-6P-3 vector (Pharmacia) by utilizing the same restriction sites. The GST:Nlz fusion protein was expressed in BL21 cells (Pharmacia) for 16 hours at room temperature by the addition of 0.5 mM IPTG. The

bacteria was lysed and GST:Nlz protein was purified using a GST Purification Module (Pharmacia) according to the manufactor's instructions. Nlz constructs were in vitro labeled with $^{35}$S-methionine using the TnT SP6 Coupled Reticulocyte Lysate System (Promega). GST pull-downs were performed as described (1).

Anti-Nlz antiserum was derived from rabbits immunized with purified Nlz protein (Research Genetics, Inc.). Western blot analyses confirm that prebleed serum did not give any signal and the anti-Nlz antiserum specifically recognized Nlz protein. For Western blot analysis, lysates of three gastrula-stage embryos or protein in vitro synthesized from the TnT SP6 Coupled Reticulocyte Lysate System (Promega) were used per lane. Samples were resolved on a 10% polyacrylamide gel by SDS-PAGE, Western blotted, probed with a 1:5000 dilution of the anti-Nlz antiserum and a 1:5000 dilution of anti-rabbit Ig, Horseradish Peroxidase linked whole antibody (from donkey) (Amersham Biosciences), and detected using chemiluminescence.

## Results

### Nlz2 is related to and functions similarly to Nlz

*Nlz2 and Nlz share conserved domains*

We have previously reported that an *nlz*-related sequence, *nlz2*, can be assembled from a series of ESTs (1). However, since none of these ESTs contains the entire *nlz2* open reading frame, we cloned *nlz2* from mid-gastrula zebrafish cDNA (see methods). Sequence analysis demonstrates that Nlz2 exhibits 55.3% identity to the Nlz protein. Nlz and Nlz2 share several highly conserved regions (Fig. 1). These include the Sp motif (a short N-terminal region shared among the vertebrate Sp1-like family of transcription factors) (1,4), the Buttonhead (Btd) box (an eight- to eleven-amino acid motif that mediates transcriptional activity) (9), a putative $C_2H_2$ zinc-finger (which may participate in nucleic acid or protein binding) (10-12), and serine/threonine-rich regions (which may govern transcriptional activation) (13). This homology suggests that Nlz2 may have similar activity to Nlz.

*nlz2 is co-expressed with nlz at gastrulation stages, but expression diverges by segmentation stages*

In situ hybridization analysis on zebrafish embryos reveals *nlz2* mRNA early and throughout the blastomeres (Fig. 2A,B) suggesting that it is maternally deposited. We find that at early gastrula stages, *nlz2* appears to be co-expressed with *nlz* near the

blastoderm margin with a gap in the dorsal midline (Fig. 2C) that is eventually enclosed at mid-gastrula stages (Fig. 2D). At late-gastrula stages, *nlz2* is expressed in a broad posterior domain (Fig. 2E), similarly to *nlz* (1). At early segmentation stages (11 hpf), *nlz2* is expressed in the forebrain, the posterior hindbrain caudal to rhombomere (r) 4 (Fig. 2F,K) and expression extends throughout the whole length of the trunk (not shown). By the 3-somite stage (12 hpf), *nlz2* expression is initiated in the midbrain-hindbrain boundary (MHB), as delineated by *nlz* (Fig. 2G) and *pax2.1* (Fig. 2L) expression in the MHB. Also, at this stage, expression of *nlz2* in the forebrain appears to expand (Fig. 2G,L). At the 10-somite stage (14 hpf), *nlz2* expression is maintained in the forebrain, the caudal hindbrain and the trunk, with expression in the MHB broadening anteriorly to encompass the midbrain (Fig. 2H). By the 14-somite stage (16 hpf), *nlz2* expression in the midbrain is reduced and expression in the forebrain extends to the optic primordium (Fig. 2I). At the 22-somite stage (20 hpf), *nlz2* expression persists in above-mentioned regions including the optic stalk (Fig. 2J). In conclusion, we find that *nlz2* is expressed similar to *nlz* in the caudal hindbrain (although *nlz2* never extends rostrally to r5) and the MHB, however it is also expressed in the forebrain, midbrain and trunk.

*nlz2 has similar activity to nlz*

We have proposed that Nlz acts as a repressor of transcription and reported that misexpression of full-length *nlz* causes loss of gene expression in the rostral hindbrain of zebrafish embryos (1). We next sought to determine if *nlz2* has a similar function. We found that injecting *nlz2* mRNA into embryos did not give a high level expression of

Nlz2 protein, likely due to the mRNA being unstable (not shown). We instead turned our efforts to misexpressing *nlz2* under the control of a heat shock-inducible promoter (hsp70). Embryos were injected at the 1- to 2-cell-stage with either hsp70:*nlz2*, hsp70:*nlz* or hsp70:*GFP*, heat-shocked at 70% epiboly (~7.5 hpf) for one hour at 37°C and fixed at the 10-somite stage (14 hpf). This leads to efficient induction as seen by hsp70:*GFP* (Fig. 3A). We then assayed for defects in the rostral hindbrain by in situ analysis for *krox20* expression (a marker for r3 and r5 (14)). We find that misexpressing *nlz* under control of the heat shock-inducible promoter represses *krox20* in r3, but not in r5 (Fig. 3C, Table 1). This phenotype is identical to that observed upon the injection of *nlz* mRNA (1), demonstrating that the heat shock-inducible construct work as well as mRNA injections. We also find that misexpressing *nlz2* under the control of a heat shock-inducible promoter results in a similar phenotype (Fig. 3D, Table 1). We conclude that ectopic expression of *nlz2*, similar to *nlz*, disrupts gene expression in the rostral hindbrain.

**In vivo structure-function analysis reveals domains essential for Nlz function**

Our sequence alignment in Figure 1 defined several domains conserved between Nlz and Nlz2, and we next set out to define the importance of these domains for *nlz* function. We elected to perform much of our structure-function analysis in zebrafish embryos since this provides a physiologically relevant environment and the functional analysis can be done rapidly (embryos can be assayed at 5-14 hours after mRNA injection).

*Nlz functions primarily in the nucleus and its localization is governed by the C-terminus*

We have previously shown that Nlz is a nuclear protein (1), but Nlz does not contain a consensus nuclear localization signal (NLS). In order to begin to understand how Nlz translocates to the nucleus, we set out to define the domain essential for nuclear localization. To this end, we determined the subcellular distribution of a panel of Nlz deletion constructs (summarized in Fig. 4). Embryos were injected with 800 pg mRNA encoding Myc epitope-tagged Nlz deletion constructs at the 1- to 2-cell stage, flat-mounted at early gastrula stage (~5 hpf) and examined for distribution of the Myc-tagged protein by fluorescent immunohistochemistry (Fig. 4). We find that Nlz constructs with C-terminal deletions (NlzΔ92C and NlzΔ173C) reside primarily in the cytoplasm (not shown and Fig. 5B) instead of the nucleus, while N-terminal or internal deletions (e.g. NlzΔ60N, NlzΔ115N, NlzΔ116-234, NlzΔ238-384 and NlzΔ116-384) do not affect nuclear localization (not shown and Fig. 4). Specifically, the fact that NlzΔ92C is cytoplasmic, but NlzΔ23C is nuclear, indicates that amino acids# 498-566 are important for the nuclear localization of Nlz. Since Nlz2 shares high homology to Nlz, we reasoned that the Nlz2 C-terminus might also govern nuclear localization. We find that Nlz2 is indeed a nuclear protein (Fig. 5C) and nuclear localization is dependent on an intact C-terminus since an Nlz2Δ180C construct is primarily cytoplasmic (Fig. 5D).

To determine if Nlz function is dependent on nuclear localization, we then expressed truncated constructs that localizes primarily to the cytoplasm and assayed for Nlz function by quantifying the number of injected embryos affected (not shown and Fig.

4). Embryos were injected at the 1- to 2-cell-stage with 400 pg mRNA encoding each construct, fixed at the 10-somite stage (14 hpf) and assayed for defects in the rostral hindbrain by in situ hybridization analysis. We find that NlzΔ92C has a reduced activity (Fig. 4, 19.7% of injected embryos affected vs. 64.9% for wild-type Nlz). However, upon addition of a NLS to NlzΔ92C, the frequency of affected embryos becomes comparable to full-length Nlz (Fig. 4, 79.4% vs. 64.9%, respectively). This suggests that Nlz must reside in the nucleus to be fully active. We also find that NlzΔ173C is likewise inactive (Fig. 4, 6.4%) and localizes primarily to the cytoplasm (Fig. 5B). Interestingly, NlzΔ173C remains inactive even with the addition of a NLS (Fig. 4, <5%), suggesting that other regions (amino acids# 417-497) are necessary for Nlz function. Accordingly, we find that a construct lacking the $C_2H_2$ zinc finger (amino acids# 461-492, NlzΔZF) is less active than full-length Nlz (Fig. 4, 19.7% vs. 69.4%, respectively), although it localizes to the nucleus (not shown and Fig. 4) and interacts efficiently with Groucho (1). We conclude that the C-terminus is required both for nuclear localization (via amino acids# 498-566) and for function (via $C_2H_2$ zinc-finger).

*nlz is co-expressed with a groucho-related gene and associates with class I histone deacetylases*

We have demonstrated that Nlz associates with the Groucho corepressor in vitro and that *nlz* represses gene expression in the hindbrain (1). We next tested if *groucho*-related genes are co-expressed with *nlz* in the rostral hindbrain. To this end, we performed in situ analysis at the 10-somite stage (14 hpf) with a probe for *grg3* (the only

zebrafish member of the *groucho* family isolated to date) (15,16) together with *nlz* (Fig. 6A) or markers for the hindbrain (r3 and r5) and the midbrain-hindbrain boundary (Fig. 6B). We find that *grg3* is expressed in the anterior region of the embryo, encompassing the forebrain, the midbrain, and extending into the rostral hindbrain at least to r4 (Fig. 6A,B). This suggests that *groucho*-related genes might mediate repression by *nlz* in the rostral hindbrain and raises the possibility that Nlz interacts with other corepressors further caudally.

We next tested if Nlz bind histone deacetylases (HDACs), corepressors that function by removing acetyl groups from core histones and maintain a transcriptionally silenced chromatin state (17,18). Utilizing GST pull-down assays, we find that Nlz associates with two class I HDACs (HDAC1 and 2) (Fig. 6C, lane 1 and not shown). To determine the region of Nlz required for this interaction, we utilized our panel of Nlz deletion constructs and tested them for HDAC2 binding in the GST pull-down assay (Fig. 6C). We find that Nlz constructs lacking the C-terminal 173 amino acids exhibits significantly weaker binding with HDAC2 (Fig. 6C, lane 2). We also find that deletions within the C-terminal 206 amino acids (Fig. 6C, lanes 4-7) or the internal region (amino acids # 116-384, not shown) were not essential for HDAC2 binding. Instead, deletions of the region between the Btd box and the $C_2H_2$ zinc finger (Fig. 6C, lanes 8,9) severely affected HDAC2 binding, indicating that this region is required for HDAC2 association. We note that this region is also involved in Groucho binding (1) and since Groucho mediates repression by recruiting HDACs (17,18), this might point to a synergistic effect between Nlz, Groucho and HDACs in mediating transcriptional repression.

*Nlz self-associates and binds to Nlz2*

Since the Nlz-related protein Elbow was found to associate with itself (3), we tested if Nlz can self-associate by using GST pull-down assays (Fig. 7A). We find that indeed, Nlz interacts efficiently with itself (Fig. 7A, lane 1). In order to determine the domain of Nlz required for this association, we utilized our panel of Nlz deletion constructs (summarized in Fig. 4) and tested them for Nlz interaction in the GST pull-down assay (Fig. 7A, lanes 2 to 10). We find that the Nlz interactions are dependent on an intact C-terminus – deletions within the N-terminus of Nlz has no effect on Nlz association (Fig. 7A, lanes 2 and 3; NlzΔ115N and NlzΔ116-234), while deletions within the C-terminus exhibit weaker binding (Fig. 7A, lanes 4,5,6,9 and 10; NlzΔ238-384, NlzΔ385-460, NlzΔ408-460, NlzΔ92C and NlzΔ173C) except for NlzΔ23C (not shown). Deletion of either the Btd box or the $C_2H_2$ zinc finger alone did not significantly decrease Nlz interaction (Fig. 7A, lanes 7 and 8). Taken together, the data in Fig. 7A suggest that there are multiple regions required for self-association located within the C-terminal half of Nlz (amino acids# 238-566).

To determine if Nlz self-association plays a role in *nlz* function, we misexpressed Nlz deletion constructs that exhibit weaker Nlz association (NlzΔ238-384, NlzΔ385-460, NlzΔ408-460, NlzΔ92C and NlzΔ173C) and assayed their activity (summarized in Fig. 4). Some of these truncated *nlz* constructs are equally active to full-length Nlz (Fig. 4, e.g. NlzΔ238-384, 41.6%), suggesting that self-association is not essential for Nlz-function. Although some other constructs display a pronounced reduction in activity

compared to full-length *nlz* (Fig. 4, e.g. NlzΔ408-460, 25.7%; NlzΔ92C, 19.7%; NlzΔ173C, 6.4% and NlzΔ385-460, <5%), this can be explained by the lack of other essential domains (such as the $C_2H_2$ zinc-finger) in those constructs. Thus, we do not find a correlation between self-association and function suggesting that self-association is not necessary for Nlz function.

We next examined if Nlz2 is capable of interacting with Nlz. Utilizing GST pull-down assays, we find that that Nlz2 and Nlz do indeed form complexes (Fig. 7B, lane 1). Since Elbow and Noc are thought to function as a complex in repressing the expression of target genes (3), this indicates that a Nlz/Nlz2 complex may function in the caudal hindbrain or at the MHB, where *nlz* and *nlz2* are co-expressed.

**Two forms of Nlz with distinct N-termini and disparate activities are present in vivo**

*Two forms of Nlz are present in vivo*

Western analysis using polyclonal rabbit antisera raised against full-length Nlz revealed two major bands in lysates from gastrula stage embryos (Fig. 8A, lane 1) - a 72 kDa form, which is close to the predicted size for Nlz, and a small molecular weight form (62 kDa). We find that these two forms are detected in embryo lysates from the 50% epiboly stage (5 hpf) to at least the 10-somite stage (14 hpf) (not shown). We also find that in vitro translation of a plasmid containing the *nlz* cDNA yields the same two forms, but with the smaller 62 kDa form predominating (Fig. 8A, lane 2). We conclude that two

forms of Nlz are present in vivo and that both forms can be generated from the same cDNA.

*Alternative translation initiation sites generate the two forms of Nlz*

We reasoned that the two forms of Nlz might be the result of translation initiating from two distinct start sites in the *nlz* transcript. In support of this idea, a downstream AUG is present at residue# 61 and translation from this site would generate a 62 kDa protein. Surveys of eukaryotic mRNAs have defined a consensus sequence (Kozak sequence) for initiation codons (5'-GCC GCC $^{A}/_{G}$CC AUG G$^{A}/_{C}$U-3') with the most important positions for efficient translation being a purine at position –3 and a G at position +4 (with the A of the AUG codon defined as position +1) (19,20). Significantly, the initiation codons present in endogenous *nlz* (5'-CCG AUC CAG AUG AGC-3') or in the *nlz* plasmid (5'-CCG AAU UCA AUG AGC-3') lack the conserved nucleotides at positions –3 and +4 (bases that match the Kozak sequence are underlined) and two protein forms are detected for these transcripts (Fig. 8A, lanes 1 and 2, respectively). Thus, inefficient recognition of the upstream initiation site may result in a portion of the translation machinery complex continuing to scan and initiating at the downstream site, a process known as leaky scanning (21,22). Notably, the downstream initiation site located at amino acid# 61 (5'-AUU CUC AAA AUG UUG-3') has the conserved nucleotide at position –3.

The leaky scanning hypothesis was tested by generating two new constructs. In the first (*kozak:nlz*), we placed an improved Kozak sequence upstream of the Nlz start

codon (5'-GCC GCC ACC AUG AGC-3') in the *nlz* plasmid. In the second (*nlz*$^{Met->GlyPro}$), we mutated the downstream initiation site from methionine to glycine and proline (5'-AUU CUC AAA CCC GGG-3'). In vitro translation from the *kozak:nlz* plasmid (Fig. 8B, lane 3) yielded both the full-length and the smaller Nlz protein. However, the protein levels were reproducibly reversed relative to translation from the *nlz* plasmid (Fig. 8B, lane 1), consistent with translation now being initiated more efficiently at the upstream AUG. In vitro translation of *nlz*$^{Met->GlyPro}$ yielded the full-length Nlz protein, but the smaller 62 kDa form was not present (Fig. 8B, lane 2), consistent with initiation at the downstream AUG site being eliminated. In this lane an even smaller Nlz form was apparent, perhaps due to initiation at a site even further downstream (e.g. 5'-ACC ACC CAC AUG GAC-3' at amino acid # 231). We conclude that the two forms of Nlz can be generated by translation from two initiation sites in the *nlz* transcript.

We note that in vitro translation from a plasmid containing a cDNA encoding the Myc-tagged Nlz protein (Myc:Nlz) yields a single protein of 90 kDa (Fig. 8B, lane 4). This size closely corresponds to the large form (full-length) of Nlz plus the Myc tags, suggesting that introduction of a Myc tag at the N-terminus prevents generation of the smaller form of Nlz, perhaps by favoring translation from the initiation codon contributed by the Myc tags. Indeed, the *myc:nlz* plasmid has an initiator codon (5'-UUU AAA GCU AUG GAG-3') that is more similar to the consensus Kozak sequence.

*The two forms of Nlz have distinct activities*

Since we detect two forms of Nlz in the embryo, we next examined if the two forms have the same activity in vivo. To this end, we generated a construct (*myc:nlzΔ60N*, with the first 60 amino acids deleted) that encodes only the small form of Nlz (Fig. 8B, lane 5) and compared it to Myc:Nlz, which generates only the full-length form (Fig. 8B, lane 4). To examine the effect of these constructs, we microinjected 400 pg mRNA encoding each construct into 1- to 2-cell-stage zebrafish embryos and assayed for defects in the rostral hindbrain. We find that Myc:NlzΔ60N is expressed at similar levels to Myc:Nlz (1) and induces a loss of r3 gene expression comparable to Myc:Nlz when misexpressed (Fig. 4, 49.3% vs. 64.9%, respectively). However, about half of the *myc:nlzΔ60N*-injected embryos (Fig. 4, 46.6%) exhibit an extensive overlap in r4- and r5-specific gene expression with occasional lateral expansion of rhombomere-specific gene expression and defective notochords (not shown). This observed effect is similar to the phenotypes associated with misexpression of a dominant negative Nlz (dnNlz) construct, generated by disrupting the Groucho binding site in Nlz (1). We conclude that Myc:NlzΔ60N can function similar to Myc:Nlz, but it may also be able to block Nlz function under some circumstances.

*An N-terminal motif is important for Nlz-mediated repression*

Although the short form of Nlz (*myc:nlzΔ60N*) has dominant negative activity similar to dnNlz (Fig. 4), it still binds Groucho (not shown) while dnNlz does not (1). This suggests that the N-terminus of Nlz may contain an additional domain required for repression. To test this, we utilized our panel of *nlz* deletion constructs to define this

essential N-terminal domain (summarized in Fig. 4). Zebrafish embryos were injected at 1- to 2-cell-stage with mRNA encoding each Myc-tagged construct and assayed for their phenotype by in situ analysis (not shown, Fig. 4). We find that removal of a small domain (amino acids # 88-115), which is found in the vertebrate Sp1-like family of transcription factors (that we named the Sp motif), is sufficient to induce the dominant negative phenotype (Fig. 4, 37.7% of *nlzΔ88-115* injected embryos). Since this construct does not disrupt co-repressor binding (1), we conclude that the Sp motif represents a domain required for Nlz function.

We note that N-terminal truncations that remove the Sp motif (*nlzΔ88-115* and *nlzΔ115N*) give rise to only the dominant negative phenotype (Fig. 4, 37.7% and 41.9%, respectively). In contrast, N-terminal truncations that remove domains situated in close proximity to the Sp motif (*nlzΔ60N* and *nlzΔ116-234*) retain activity associated with wild-type Nlz (Fig. 4, 49.3% and 32.2%, respectively) while also exhibiting the dominant negative phenotype (Fig. 4, 46.6% and 46.2%, respectively). One exception may be NlzΔ116-384, although this construct posses a large deletion (~50% of the protein). We suggest that removal of adjacent sequences may partially interfere with the Sp motif to generate forms of Nlz that have both activities (albeit at reduced frequencies). While we have no evidence suggesting that generation of the short form is regulated in vivo, its presence may modulate Nlz function in the developing embryo.

## Discussion

In this study we show that *nlz2* and *nlz* share conserved domains, are co-expressed during hindbrain development and are both able to repress gene expression in the rostral hindbrain. We use structure-function analysis to determine that nuclear localization of Nlz2 and Nlz is governed by their respective C-termini and that Nlz function is enhanced when residing in the nucleus. We find that Nlz associates with itself, as well as with Nlz2, although self-association does not appear to be essential for tested Nlz activities. We have previously shown that Nlz binds Groucho, but here find that *nlz* is not always co-expressed with a *groucho*-related gene (*grg3*), and instead may associate directly with histone deacetylases in some regions of the embryo. Two forms of Nlz, resulting from translation initiating at two distinct start sites in the *nlz* transcript, were detected in vivo. These forms possess distinct functions as a result of differential activity of the Sp1 domain, an N-terminal domain required for Nlz-mediated repression. We conclude that *nlz* genes regulate development of the zebrafish hindbrain, though the usage of conserved domains and the interaction with corepressors.

### *Nlz family zinc-finger proteins behave as transcriptional repressors*

It is likely that members of the Nlz zinc-finger family regulate various aspects of embryological development through the transcriptional repression of target genes (1-3). We have shown that the misexpression of *nlz* in zebrafish embryos results in the loss of genes expressed in r2 and r3, concomitant with a partial expansion of genes expressed in

r4 into r3 and interference with endogenous *nlz* function leads to an expansion of r5-specific gene expression into r4 (1). Here we show that misexpression of *nlz2* also results in loss of r3 gene expression (Fig. 2D and Table 1). Parallel to these results in zebrafish, related genes in *Drosophila* and *C.elegans* may have similar activities (2-4). Homozygous mutants display expanded expression of tracheal-specific genes and defects in embryonic brain and head structures while the misexpression of either *nocA* or *elbow* results in visceral branch migration defects (2,3). While *tlp-1* mutants in *C.elegans* exhibit abnormal tail morphology due to defects in cell fusions and changes in cell polarity, it is not clear if TLP-1 is involved in transcriptional repression or activation (4). The function of the Nlz-related genes in the mouse and human also have not been elucidated (1). We conclude that the biological activities of *elbow* and *nocA* in the trachea, and *nlz* and *nlz2* in the rostral hindbrain, are consistent with a role in repression of transcription.

Repressors are expected to function in the nucleus and consistent with this, Elbow (3), TLP-1 (4), Nlz (1) and Nlz2 (Fig. 5C) localize to the nucleus. Additionally, we have determined that Nlz function is dependent on nuclear localization (Fig. 4), suggesting that Nlz-related proteins must reside in the nucleus in order to exert their full activity. Nlz family proteins appear to mediate repression by associating with corepressors. Both Elbow (3) and Nlz (1) associates with the corepressor Groucho and we have also determined that Nlz binds class I histone deacetylases (Fig. 6C). *grg3* expression is present in the zebrafish rostral hindbrain (Fig. 6A,B), while HDAC1 is expressed ubiquitously (Zchut & Sagerström, unpublished results) suggesting that Nlz may bind

different corepressors in different regions of the embryo. Lastly, a truncated *nlz* construct lacking the corepressor interaction domain, disrupts endogenous Nlz function (1). This collectively suggests that Nlz-related proteins repress the transcription of genes by recruiting corepressors.

It is not known if Nlz-related proteins can bind to DNA since DNA-binding proteins often contain several $C_2H_2$ zinc fingers (12) and Nlz-related proteins only contain one such motif (Fig. 1). We have determined that the putative $C_2H_2$ zinc finger is important for Nlz function since removal of this domain resulted in a reduced number of affected embryos in our ectopic expression assay (Fig. 4). The association of two Nlz-related proteins, as a functional complex, would provide a suitable number of $C_2H_2$ zinc fingers necessary for DNA binding (1). Elbow was found to homodimerize, in addition to heterodimerize with NocA, and suggested to function as a complex to repress dorsal trunk genes in the dorsal branch and visceral branch genes in the lateral trunks (3). Though we find that Nlz can self-associate (Fig. 7A), as well as interact with Nlz2 (Fig. 7B), our misexpression analyses of *nlz* deletion constructs suggest that self-association is not necessary for Nlz-mediated repression (Fig. 4). Though the zinc finger domain of the Nlz-related proteins closely resembles the consensus $C_2H_2$ sequence (4), important differences remain. Structural analyses have determined that the amino acids at positions −1, 3 and 6 of the consensus are required to make base-pair contacts with the primary DNA strand whereas the amino acid at position 2 makes contact with the complementary strand of DNA (23). The zinc finger domain of the Nlz-related proteins only share conserved residues at positions 2 and 3 (not shown), suggesting that this domain is not

capable of binding DNA. In addition, residues that mediate phosphate contacts at positions –5, 7 and 15 (23) are conserved with the Nlz-related proteins at only one position (not shown). This suggests that the $C_2H_2$ zinc finger of Nlz-related proteins has insufficient characteristics to be considered a DNA binding motif. Although we cannot exclude the possibility that residues flanking the zinc-finger domain might be involved in DNA recognition (24,25), we favor the possibility that the single zinc finger of the Nlz-related proteins may instead mediate protein-protein interactions, as reported for other $C_2H_2$ zinc finger proteins (26-28).

*Nlz proteins are broadly related to the Sp1 family of transcription factors*

We have deduced that a domain located at the N-terminus of Nlz (Sp motif) is required for function (Fig. 4). We find that this region (amino acids # 88-115 in Nlz) is shared among the vertebrate Sp1 family of transcription factors (named after its purification process which included Sephacryl and phosphocellulose columns) (29). The vertebrate Sp1-related proteins are broadly related to the Nlz sub-family of zinc-finger proteins (4) and are also involved in mediating embryonic development through the regulation of transcription. Homozygous mouse knockouts of the Sp1-like factors have determined that these genes are important for vitality and growth of the embryo. *sp1* knock-out mice display retarded growth and severe abnormalities during development, withstanding the fact that Sp1 has been found to activate the transcription of numerous genes (30), and mice lacking *sp3* exhibit a loss of gene products necessary for the dentin/enamel layer of the developing teeth and an impairment for proper skeletal

ossification (31,32). The *sp1*-related gene *sp4* is expressed in the central nervous system of mouse embryos and homologous recombination was used to generate mice lacking the conserved zinc-finger domains of Sp4 (33). These mutant mice exhibit low postnatal survival rates and growth, in addition to male fertility behavioral defects. *sp5* is dynamically expressed in the mouse neural tube and while mice homozygous for a *sp5* null mutation does not exhibit an overt phenotype, it has been shown to enhance the penetrance of the T mutation (null allele of *brachyury*) (34). This has been suggested to support a genetic interaction between *sp5* and *brachyury* and a role for Sp5 in regulation of transcription in the developing embryo. Taken together, *sp* knockout mice exhibit a wide range of defects, most of them severe enough to reduce viability, suggesting that Sp1-related proteins are essential for normal development. Interestingly, while Nlz-related proteins function as repressors, in part to their association with corepressors, most Sp1-like proteins mediate activation of transcription. One exception is Sp3, which contains an inhibitory domain (amino acid triplet KEE) that silences its own glutamine-rich activation domain (35). However, Sp3 has the potential to activate transcription in an in vitro assay (9,35), suggesting that the in vivo transcriptional activity of Sp1-related genes may be modulated by additional cofactors to confer activation versus repression in the developing embryo. Other vertebrate Sp1-like genes include zebrafish Bts1 (*buttonhead/Sp-related-1*), which is involved in the induction and early maintenance of *pax2.1* expression at the MHB (36). Bts1 likely functions as a transcriptional activator due to its ability to activate the expression of *collier* (*col*), a downstream target of *buttonhead* (*btd*), in *Drosophila btd* mutants. The two *Drosophila* Sp1-related proteins

(Buttonhead and D-Sp1) have also been shown to function as transcription factors important for embryonic development (segmentation of the head) (37-39). However, they do not contain a region homologous to the Sp motif and are found to be more distantly related to the Nlz and Sp1 families (4). XSPR-1, a novel Sp1-related protein in *Xenopus laevis*, was found to be expressed in the neuroectoderm (as well as the forebrain, otic vesicles and the MHB) during embryogenesis (40). However, the function of this gene has not been elucidated yet.

The vertebrate Sp1 family shares conserved domains that are important for function (13,29,38,41-43). One of these regions is the three $C_2H_2$ zinc fingers, which have been found to bind to a GC/GT boxes widely distributed in promoters and enhancers (44-48). Sp1-like factors also have multiple serine/threonine- and glutamine-rich regions, which have been determined to mediate transcriptional activation (13,43). An eleven-amino acid motif, termed the Buttonhead (Btd) box, is present in all vertebrate Sp1-like proteins and have been found to contribute to the activation of transcription (9). Lastly, an N-terminal domain (which we termed the Sp motif) is also conserved, the function of which is unknown (34,36). We point out that Nlz-related proteins share some broad characteristics with the vertebrate Sp1 family (Fig. 1) and may represent a sub-family (4). Nlz-related proteins contain only one putative $C_2H_2$ zinc finger (Fig. 1) and we have shown that this domain is important for Nlz's ability to function as a transcriptional repressor (Fig. 4). A domain that we tentatively identified as a putative zinc finger of the $C_2HC$ or $CHC_2$ class (1), may instead weakly resemble the Btd box (4). Deletion of this domain in Nlz (together with an adjacent region) reduces its affinity for the corepressors

Groucho (1) and HDACs (Fig. 5C) and instead behaves as a dominant negative (Fig. 4 and (1)). Interestingly, deletion of a small region (24 or 31 amino acids, including the Btd box) immediately adjacent to the three zinc fingers in Sp1 results in a reduction of transcriptional activation (9,41). This indicates that the Btd box plays an important role in determining protein functionality. Nlz also exhibits multiple serine/threonine-rich regions (amino acids # 112-137, 181-201, 244-289 and 425-445) and a glutamine-rich region (amino acids # 203-227) similar to the activation domains of Sp1 (Fig. 1). We note that while deletion of these regions reduces the transcriptional activity of Sp1 (41), encompassing larger deletions in Nlz resulted in a reduction of the repressor phenotype and an increase in the dominant negative phenotype (Fig. 4, e.g. NlzΔ116-234, NlzΔ116-384, NlzΔ238-384 and NlzΔ408-460). Lastly, the Sp motif is shared between both the vertebrate Sp1 and Nlz families (1,4). Deletion of N-terminal regions, including the Sp domain, has not been found to significantly dampen the transcriptional activity of Sp1 (41). However, we find that deletion of the Sp motif (or adjacent regions) is sufficient to induce dominant negative Nlz activity (Fig. 4). We propose that the Sp motif in Nlz-related proteins may mediate transcriptional repression of target genes through the association with another factor. Deletion of this region (or an adjacent region to interfere with its function) would then result in a de-repression of target genes. We have determined that deletion of the Sp motif does not interfere with corepressor interaction (Fig. 5C and (1)). Interestingly, p74 has been identified to specifically bind the N-terminus of Sp1 and inhibit Sp1-mediated transcription in vivo (49) and a similar mechanism may regulate Nlz function. Taken together, our observations indicate that

Sp1- and Nlz-family proteins utilize similar functional domains although the various family members may have different effects on transcription (activation vs. repression), perhaps as a result of interactions with different cofactors.

**Acknowledgments**

We thank members of the Sagerström lab for helpful discussions, Yasemin Gunes for assistance in cloning *nlz2* and Scott Wolfe for discussions on zinc-finger proteins. This work was supported by NIH Grants NS38183 and HD39156 (to C.G.S.).

## References


1. Runko, A. P., and Sagerström, C. G. (2003) *Dev Biol*, in press
2. Cheah, P. Y., Meng, Y. B., Yang, X., Kimbrell, D., Ashburner, M., and Chia, W. (1994) *Molecular and Cellular Biology* **14**, 1487-1499
3. Dorfman, R., Glazer, L., Weihe, U., Wernet, M. F., and Shilo, B. Z. (2002) *Development* **129**, 3585-3596
4. Zhao, X., Yang, Y., Fitch, D. H., and Herman, M. A. (2002) *Development* **129**, 1497-1508
5. Andreazzoli, M., Broccoli, V., and Dawid, I. B. (2001) *Mech Dev* **104**, 117-120.
6. Philipsen, S., and Suske, G. (1999) *Nucleic Acids Res* **27**, 2991-3000
7. Sagerström, C. G., Grinblat, Y., and Sive, H. (1996) *Development* **122**, 1873-1883
8. Hatta, K. (1992) *Neuron* **9**, 629-642
9. Athanikar, J. N., Sanchez, H. B., and Osborne, T. F. (1997) *Mol Cell Biol* **17**, 5193-5200
10. Klug, A., and Rhodes, D. (1987) *Cold Spring Harb Symp Quant Biol* **52**, 473-482
11. Berg, J. M. (1990) *J Biol Chem* **265**, 6513-6516.
12. Iuchi, S. (2001) *Cell Mol Life Sci* **58**, 625-635.
13. Pascal, E., and Tjian, R. (1991) *Genes Dev* **5**, 1646-1656
14. Oxtoby, E., and Jowett, T. (1993) *Nucl. Acids Res.* **21**, 1087-1095
15. Kobayashi, M., Nishikawa, K., Suzuki, T., and Yamamoto, M. (2001) *Dev Biol* **232**, 315-326
16. Wülbeck, C., and Campos-Ortega, J. A. (1997) *Dev. Genes Evol.* **207**, 156-166

17. Chen, G., and Courey, A. J. (2000) *Gene* **249**, 1-16.

18. Courey, A. J., and Jia, S. (2001) *Genes Dev* **15**, 2786-2796.

19. Kozak, M. (1987) *Nucleic Acids Res* **15**, 8125-8148.

20. Kozak, M. (1997) *Embo J* **16**, 2482-2492.

21. Kozak, M. (1981) *Nucleic Acids Res* **9**, 5233-5262.

22. Sedman, S. A., Gelembiuk, G. W., and Mertz, J. E. (1990) *J Virol* **64**, 453-457.

23. Wolfe, S. A., Nekludova, L., and Pabo, C. O. (2000) *Annu Rev Biophys Biomol Struct* **29**, 183-212

24. Pedone, P. V., Ghirlando, R., Clore, G. M., Gronenborn, A. M., Felsenfeld, G., and Omichinski, J. G. (1996) *Proc Natl Acad Sci U S A* **93**, 2822-2826.

25. Omichinski, J. G., Pedone, P. V., Felsenfeld, G., Gronenborn, A. M., and Clore, G. M. (1997) *Nat Struct Biol* **4**, 122-132.

26. Yang, H. Y., and Evans, T. (1992) *Mol Cell Biol* **12**, 4562-4570.

27. Gregory, R. C., Taxman, D. J., Seshasayee, D., Kensinger, M. H., Bieker, J. J., and Wojchowski, D. M. (1996) *Blood* **87**, 1793-1801

28. Merika, M., and Orkin, S. H. (1995) *Mol Cell Biol* **15**, 2437-2447

29. Kadonaga, J. T., Carner, K. R., Masiarz, F. R., and Tjian, R. (1987) *Cell* **51**, 1079-1090

30. Marin, M., Karis, A., Visser, P., Grosveld, F., and Philipsen, S. (1997) *Cell* **89**, 619-628

31. Bouwman, P., Gollner, H., Elsasser, H. P., Eckhoff, G., Karis, A., Grosveld, F., Philipsen, S., and Suske, G. (2000) *Embo J* **19**, 655-661

32. Gollner, H., Dani, C., Phillips, B., Philipsen, S., and Suske, G. (2001) *Mech Dev* **106**, 77-83

33. Supp, D. M., Witte, D. P., Branford, W. W., Smith, E. P., and Potter, S. S. (1996) *Dev Biol* **176**, 284-299

34. Harrison, S. M., Houzelstein, D., Dunwoodie, S. L., and Beddington, R. S. (2000) *Dev Biol* **227**, 358-372

35. Dennig, J., Beato, M., and Suske, G. (1996) *Embo J* **15**, 5659-5667

36. Tallafuss, A., Wilm, T. P., Crozatier, M., Pfeffer, P., Wassef, M., and Bally-Cuif, L. (2001) *Development* **128**, 4021-4034

37. Wimmer, E. A., Frommer, G., Purnell, B. A., and Jackle, H. (1996) *Mech Dev* **59**, 53-62

38. Wimmer, E. A., Jackle, H., Pfeifle, C., and Cohen, S. M. (1993) *Nature* **366**, 690-694

39. Schock, F., Purnell, B. A., Wimmer, E. A., and Jackle, H. (1999) *Mech Dev* **89**, 125-132

40. Ossipova, O., Stick, R., and Pieler, T. (2002) *Mech Dev* **115**, 117-122

41. Courey, A. J., and Tjian, R. (1988) *Cell* **55**, 887-898

42. Kadonaga, J. T., Courey, A. J., Ladika, J., and Tjian, R. (1988) *Science* **242**, 1566-1570

43. Courey, A. J., Holtzman, D. A., Jackson, S. P., and Tjian, R. (1989) *Cell* **59**, 827-836

44. Dynan, W. S., and Tjian, R. (1983) *Cell* **35**, 79-87

45. Dynan, W. S., and Tjian, R. (1983) *Cell* **32**, 669-680

46. Gidoni, D., Dynan, W. S., and Tjian, R. (1984) *Nature* **312**, 409-413

47. Gidoni, D., Kadonaga, J. T., Barrera-Saldana, H., Takahashi, K., Chambon, P., and Tjian, R. (1985) *Science* **230**, 511-517

48. Thiesen, H. J., and Bach, C. (1990) *Nucleic Acids Res* **18**, 3203-3209

49. Murata, Y., Kim, H. G., Rogers, K. T., Udvadia, A. J., and Horowitz, J. M. (1994) *J Biol Chem* **269**, 20674-20681

**Table 1**

Misexpression of *nlz2* represses r3 gene expression[a]

| Construct | Embryos affected (%)[b] |
|---|---|
| hsp70nlz2 | 52.6 (82/156) |
| hsp70nlz | 68.7 (68/99) |
| hsp70GFP | 0.0 (0/163) |

[a] One- to two-cell-stage embryos were injected with 50 pg of hsp70GFP, hsp70nlz or hsp70nlz2 DNA, heat shocked at 70% epiboly for one hour at 37°C, fixed at the 10-somite stage and analyzed by in situ hybridization for *krox20* expression.

[b] Percent of embryos (with ectopic protein expression in the hindbrain) exhibiting loss of *krox20* expression in r3.

**Figure 1.** Nlz, Nlz2 and Sp1 proteins share conserved domains. Domains of the zebrafish Nlz (AAK73547) and Nlz2 (AY371081) proteins and the human Sp1 (AAF67726) protein are shown schematically. The proteins are shown in white except for the internal start site (I, black), Sp motif (Sp, grey), serine/threonine-rich regions (S/T, blue), glutamine-rich region (Q, yellow), Buttonhead box (Btd, green), $C_2H_2$ zinc-finger (ZF, red), repressor interaction domain (RID, diagonal-hatched box) and a potential nuclear localization signal sequence (N, dot-shaded box). Numbers indicate amino acid position. Abbreviations: Dr, *Danio rerio*; Hs, *Homo sapiens*.

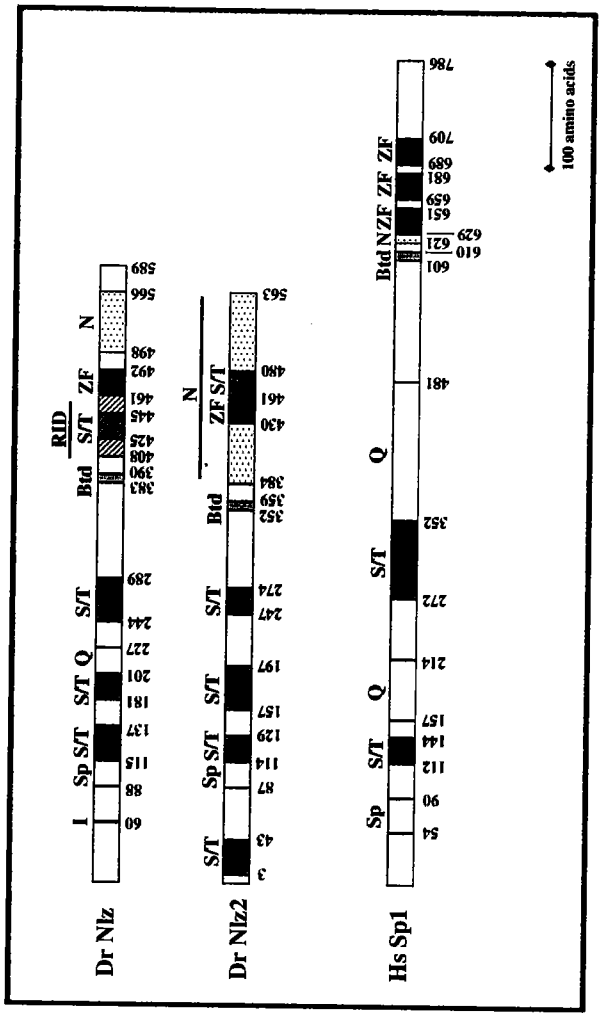
Dr Nlz
I
Sp
S/T
S/T
S/T
Q
S/T
Btd
RID
S/T
ZF
N
589
566
498
492
461
445
425
408
390
383
289
244
227
201
181
137
115
88
60
Dr Nlz2
S/T
Sp
S/T
S/T
S/T
Btd
N
ZF
S/T
563
480
461
430
384
359
352
274
247
197
157
129
114
87
43
3
Hs Sp1
Sp
S/T
Q
S/T
Q
Btd
NZF
ZF
ZF
786
709
689
681
659
651
629
621
610
601
481
352
272
214
157
144
112
90
54
100 amino acids

**Figure 1**

**Figure 2.** *nlz2* is dynamically expressed during zebrafish development. Embryos were processed for in situ hybridization for *nlz2* (detected in blue; A-L), *nlz* (detected in red; C, D, F-J), *krox20* (detected in red; K, L) and *pax2.1* (detected in red; K, L). Embryos were whole-mounted in A-E and flat-mounted in F-L and are shown in dorsal views with anterior to the top at 20X magnification. Markers are shown at bottom left-hand corner, and embryonic stage is shown at the bottom right-hand corner. Abbreviations: fb, forebrain; mhb, midbrain-hindbrain boundary; r, rhombomere; hpf, hours post-fertilization.

Figure 2


nlz2
2 hpf
4 hpf
6 hpf
8 hpf
10 hpf
F
G
H
I
J
fb
mhb
r1
r2
r3
r4
r5
r6
r7
11 hpf
12 hpf
14 hpf
nlz2/nlz
20 hpf
K
L
pax2.1
12 hpf

**Figure 3.** Misexpression of *nlz2* disrupts r3 gene expression. Embryos were injected with 50 pg of hsp70myc:GFP (A, B), hsp70myc:nlz (C) or hsp70myc:nlz2 (D) DNA, heat-shocked at 70% epiboly for one hour at 37°C and fixed at the 10-somite stage (14 hpf). Embryos were processed by in situ hybridization for *krox20* (detected in red, B-D), *nlz* (detected in blue, C) and *nlz2* (detected in blue, D) expression or immunostained with anti-c-myc (A) to detect ectopic protein. Immunostaining confirmed wide distribution of induced protein (A). Ectopic *nlz* (C) and *nlz2* (D) mRNA is detected in injected embryos (low endogenous levels were undetectable). Markers or signals visualized are shown at bottom left-hand corner, and injected DNA is shown at the bottom right-hand corner. Arrows indicate loss of r3 gene expression.

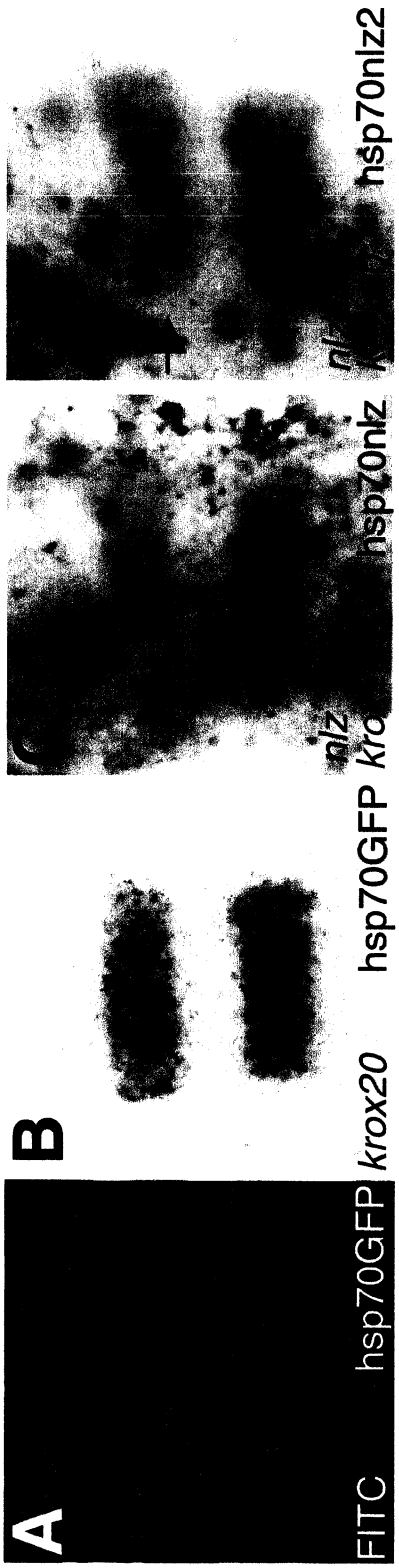
A
FITC
hsp70GFP
krox20
B
hsp70GFP
krox20
hsp70nlz
hsp70nlz2

**Figure 3**

**Figure 4.** Structure-function analysis reveals domains essential for Nlz function. Nlz deletion constructs were generated as described in experimental procedures. Thick black lines indicate Nlz protein and thin lines indicate deleted amino acid regions. Refer to Figure 1 for abbreviations used in the Nlz protein diagram. Columns at right indicate repressor activity (the percent of embryos exhibiting loss of r3 gene expression), dominant negative activity (the percent of embryos exhibiting an expansion of r5-specific gene expression into r4), cellular localization (primarily nuclear (N) or cytoplasmic (C)), self-association and HDAC binding. The number of injected embryos examined for the in situ analysis (columns 1 & 2) was >170 to <1275 for each construct (and >50 for the localization studies in column 3). The repressor and dominant negative activities for the Nlz, NlzΔ385-460 and NlzΔ408-460 constructs were reported previously (1). Abbreviations: +, strong association; +/-, insubstantial interaction; -, very weak binding; ND, not determined. Asterisk denotes NLS, nuclear localization signal sequence fused to the N-terminus of NlzΔ92C and NlzΔ173C.

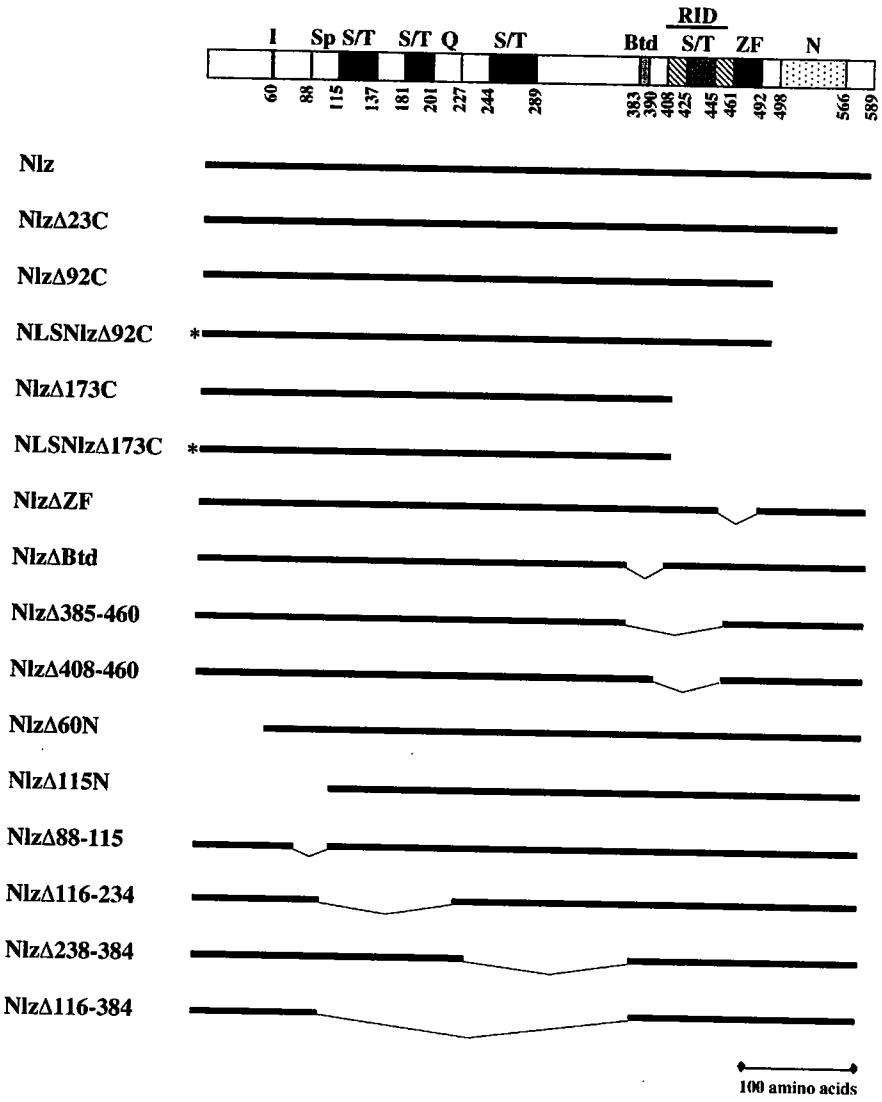


| | Repressor Activity | Dominant Negative Activity | Localization | Self-Association | HDAC Binding |
|---|---|---|---|---|---|
| Nlz | 64.9 | <5 | N | + | + |
| NlzΔ23C | 39.1 | <5 | N | + | + |
| NlzΔ92C | 19.7 | <5 | C | - | + |
| NLSNlzΔ92C | 79.4 | <5 | N | ND | ND |
| NlzΔ173C | 6.4 | <5 | C | - | - |
| NLSNlzΔ173C | <5 | <5 | N | ND | ND |
| NlzΔZF | 19.7 | <5 | N | + | + |
| NlzΔBtd | 66.4 | <5 | N | + | + |
| NlzΔ385-460 | <5 | 40.0 | N | - | - |
| NlzΔ408-460 | 25.7 | 20.9 | N | +/- | - |
| NlzΔ60N | 49.3 | 46.6 | N | + | + |
| NlzΔ115N | <5 | 41.9 | N | + | + |
| NlzΔ88-115 | <5 | 37.7 | N | + | + |
| NlzΔ116-234 | 32.2 | 46.2 | N | + | + |
| NlzΔ238-384 | 41.6 | 8.4 | N | - | + |
| NlzΔ116-384 | 6.7 | 43.9 | N | - | + |

Figure 4

**Figure 5.** Nlz and Nlz2 are nuclear proteins whose localization are dependent on their respective C-termini. Embryos were injected with 800 pg of *mycnlz* (A), *mycnlzΔ173C* (B), *mycnlz2* (C), or *mycnlz2Δ180C* (D) mRNA, fixed at 5 hpf, immunostained with anti-c-Myc, flat-mounted and shown in animal pole views at 40X magnification. (A, C) Nlz and Nlz2 localize to the nucleus. (B, D) NlzΔ173C and Nlz2Δ180C localize primarily to the cytoplasm. Injected DNA is shown at the bottom right-hand corner.

**Figure 5**

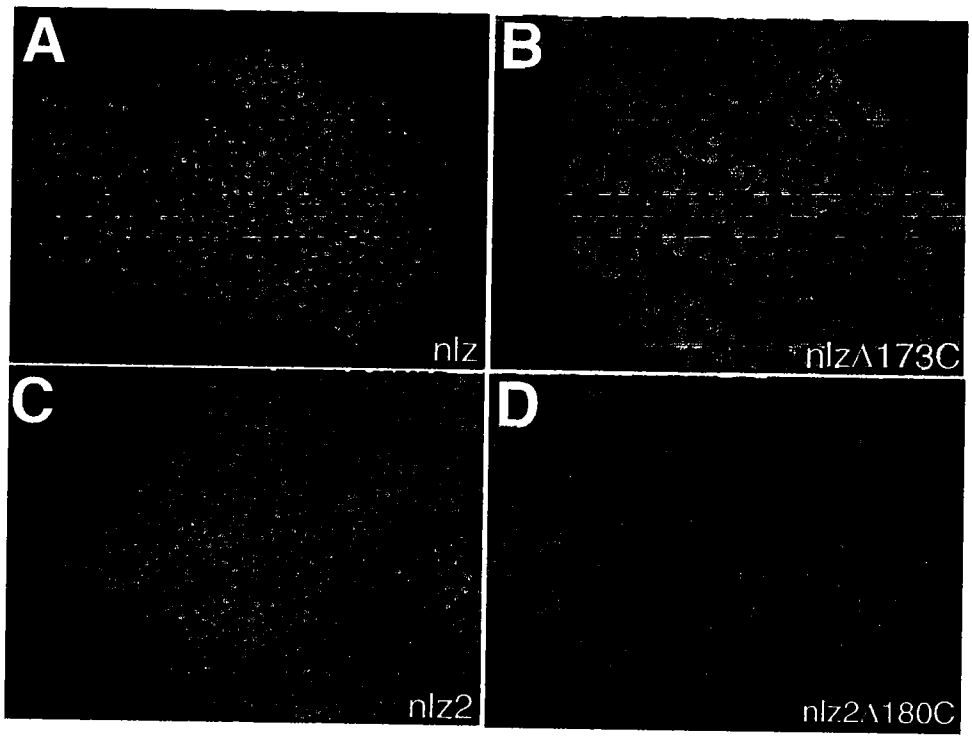

**Figure 6.** *nlz* is co-expressed with *groucho* and associates with class I histone deacetylases. (A, B) *nlz* is co-expressed with *groucho* in the rostral hindbrain. Embryos were processed for double in situ hybridization with *groucho* (detected in blue; A, B) together with *nlz* (detected in red; A) or *krox20* and *pax2.1* (both detected in red, B). Embryos were flat-mounted and are shown in dorsal views with anterior to the top at 20X magnification. Markers are shown at the bottom left-hand corner, and embryonic stage is shown at the right-hand corner. Abbreviations: fb, forebrain; mb, midbrain; mhb, midbrain-hindbrain boundary; r, rhombomere; hpf, hours post-fertilization. (C) Nlz associates with class I histone deacetylases. Purified GST-HDAC2 fusion or GST were immobilized on glutathione-sepharose beads and incubated with $^{35}$S-labeled Nlz or Nlz deletion constructs. After washing of the beads, bound proteins were separated by SDS-PAGE and visualized by autoradiography. Nlz interacts strongly with the GST-HDAC2 fusion protein, whereas NlzΔ173C, NlzΔ385-460 and NlzΔ408-460 exhibit weak binding. GST alone does not significantly bind to the Nlz deletion constructs. Aliqouts containing 10% of the total amount of $^{35}$S-labeled protein used in the assay are shown (10% load).

Figure 6


A
fb
mb
mhb
r1
r2
r3
r4
r5
14 hpf
B
fb
mb
mhb
r1
r2
r3
r4
r5
14 hpf
krox20 / pax2.1
C
175 -
83 -
62 -
1 2 3 4 5 6 7 8 9 10 11 12 13 14 15 16 17 18 19 20 21 22 23 24 25 26 27
GST-HDAC2
GST
10% load
Nlz
NlzA173C
NlzA115N
NlzAZ1
NlzAZ2
NlzA92C
NlzA23C
NlzA385-460
NlzA408-460

**Figure 7.** Nlz self-associates and binds to Nlz2. (A) Nlz self-association requires an intact C-terminus. Purified GST-Nlz fusion or GST were immobilized on glutathione-sepharose beads and incubated with $^{35}$S-labeled Nlz or Nlz deletion constructs. After washing of the beads, bound proteins were separated by SDS-PAGE and visualized by autoradiography. Nlz interacts strongly with the GST-Nlz fusion protein, whereas NlzΔ238-384, NlzΔ385-460, NlzΔ408-460, NlzΔ92C and NlzΔ173C exhibit weak binding. GST alone does not significantly bind to the Nlz deletion constructs. Aliqouts containing 10% of the total amount of $^{35}$S-labeled protein used in the assay are shown (10% load). (B) Nlz2 interacts with Nlz. Nlz2 interacts strongly with the GST-Nlz fusion protein and does not significantly bind to GST alone.

Figure 7

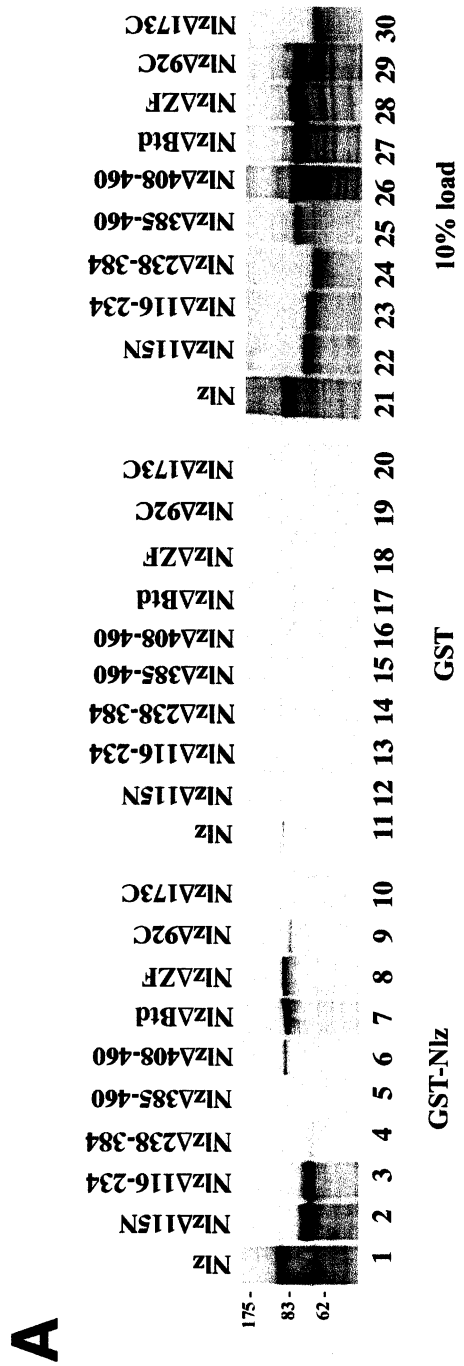
A
175-
83-
62-
1 2 3 4 5 6 7 8 9 10 11 12 13 14 15 16 17 18 19 20 21 22 23 24 25 26 27 28 29 30
Nlz
NlzA115N
NlzA116-234
NlzA238-384
NlzA385-460
NlzA408-460
NlzABtd
NlzAZF
NlzA92C
NlzA173C
GST-Nlz
GST
10% load
B
175-
83-
62-
GST-Nlz
GST
10% load
Nlz2
Nlz2
Nlz2

**Figure 8.** Nlz exists in two forms that are generated by the use of two translation start sites. (A) Two forms of Nlz are detected in vivo and in vitro. Lysate of three uninjected embryos (lane 1), 1 ul of in vitro translated Nlz (lane 2) and 1 ul of a mock in vitro translation reaction (lane 3) were resolved on a 10% polyacrylamide gel by SDS-PAGE, Western-blotted, probed with anti-Nlz antiserum and detected using chemiluminescence. (B) The short form of Nlz is generated from a downstream initiation site at position 61 of Nlz. 5 ul of $^{35}$S-labeled in vitro translated Nlz (lane 1), Nlz$^{Met->GlyPro}$ (lane 2), Kozak:Nlz (lane 3), Myc:Nlz (lane 4) and Myc:NlzΔ60N (lane 5) were separated by SDS-PAGE and visualized by autoradiography.

Figure 8

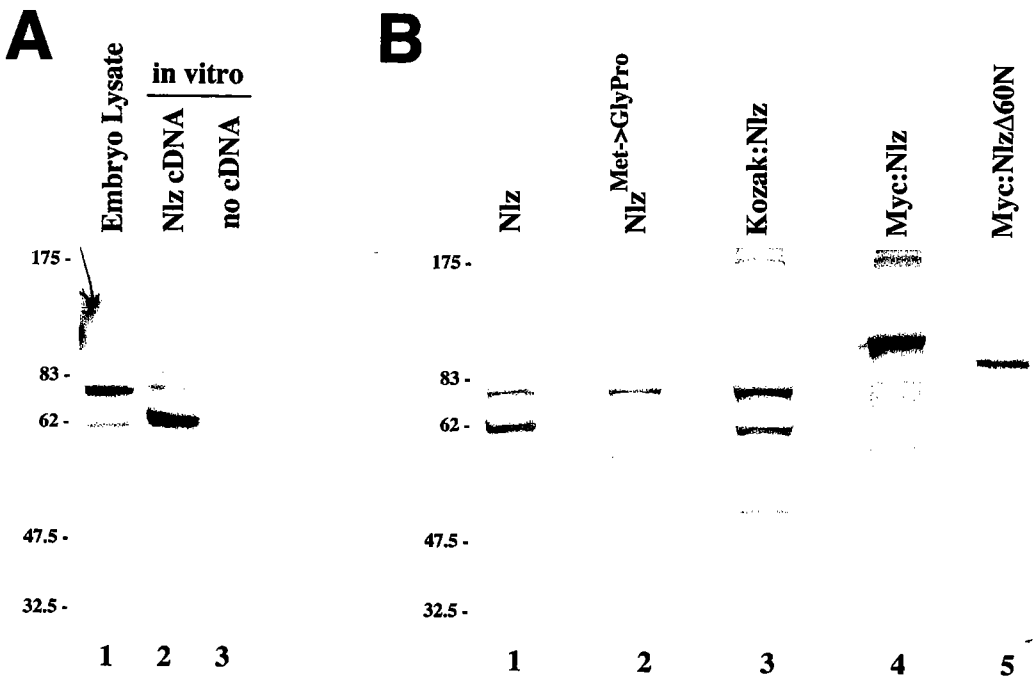
A
Embryo Lysate
in vitro
Nlz cDNA
no cDNA
175 -
83 -
62 -
47.5 -
32.5 -
1
2
3
B
Nlz
Met->GlyPro Nlz
Kozak:Nlz
Myc:Nlz
Myc:NlzΔ60N
175 -
83 -
62 -
47.5 -
32.5 -
1
2
3
4
5

# CONCLUSION

The zebrafish hindbrain arises from seven segments, termed rhombomeres, which form within the neuroectoderm. Rhombomeric identity is characterized by the stereotypical arrangement of reticulospinal neurons and cranial nerves that underlie the formation of these specialized compartments. Patterning of the rhombomeres is a highly regulated process that involves the establishment of distinct domains, the conferment of specific identities upon each segment and the formation of boundaries between individual rhombomeres. In Chapter I, I have discussed the role of a candidate hindbrain patterning gene, *nlz*, in the regulation of segmental gene expression in the rostral hindbrain and suggest that it functions as a transcriptional repressor. In Chapter II, I have discussed that another *nlz*-related gene, *nlz2*, is also expressed in the hindbrain and has similar functions as *nlz*. I have also identified conserved domains shared among the Nlz-related genes and members of Sp1 family that gave insight to which regions of Nlz are important for activity and how it may function in transcription. In summary, the work completed in this thesis identifies *nlz* as a hindbrain patterning gene involved in the regulation of gene expression in the rostral hindbrain and proper formation of rhombomere boundaries.

## Approaches for determining the role of Nlz in development

In this thesis, I have employed the use of several techniques to explore the function of Nlz. Gain of function analysis ('forward' approach) was performed by the microinjection of mRNA into zebrafish embryos. This approach is well-suited to examine the effects of an ectopically expressed gene since the mRNA is synthesized in vitro and is translated by the host embryo after injection. The zebrafish organism offers significant advantages as a model system due to the accessibility of a large collection of embryos from the pairing of an adult male and female, the relative swift time course of embryological development that allows a brief time for development of the hindbrain to occur and the translucency of the embryo that allows for straightforward phenotypical analysis. Misexpression of *nlz* in the developing embryo was found to disrupt rostral hindbrain gene expression, more specifically, the loss of gene expression in r2/r3, concomitant with an expansion of r4 gene expression into r3 (Chapter I). Conversely, loss of function analysis ('reverse' approach), through the inhibition of gene function, was performed by utilizing dominant negative constructs. Nlz constructs without the corepressor (Groucho and the class I histone deacetylases) interaction domain were found to disrupt endogenous Nlz function and interfere with the ability of Nlz to behave as a repressor. In particular, embryos injected with the dominant negative exhibited an expansion of r5-specific gene expression into r4 (Chapter I). Taken together, both the ectopic expression and inhibition of gene function provided conclusive results to indicate that Nlz mediates the proper segmental gene expression and segregation of the r4 domain.

*Loss of function analysis reveals a potential new role for Nlz*

Another approach employed to down-regulate the expression of a particular gene is the injection of antisense oligonucleotides. These oligos were designed as a small fragment of DNA (20-25 bases) that specifically form DNA-RNA hybrids with the targeted mRNA and recruits RNase H to cleave and subsequently degrade the target mRNA (Cazenave et al., 1989). However, the oligos were found to generate non-specific toxic side effects (Stein, 1999), limiting the applicability of this approach. Recently, a new antisense strategy has been employed that utilizes 'morpholino' oligonucleotides (MO) (Summerton, 1999; Summerton and Weller, 1997). These oligos, synthesized from DNA analogs, are chemically modified to enable resistance to nucleases, thus increasing biological stability. MOs are designed to target and bind a small area (18 to 25 bases) between the 5' cap of an mRNA and its start codon, thus inhibiting translation by preventing the initiation complex from assembling into a full ribosome at the start site and initiate translation of the mRNA. MO injections have been shown to mimic the phenotypes of known mutants (Lele et al., 2001; Nasevicius and Ekker, 2000), proving the penetrance of MOs for an efficient loss of function analysis.

In addition to the injection of dominant negative constructs, another viable option for the loss of Nlz function approach is the employment of Nlz MO injections. One- to two-cell stage zebrafish embryos were injected with one of two MOs targeted to the Nlz start site (MO1, oligo designed to target the –10 to +14 bases of the Nlz start site with the A of the AUG codon defined as position +1; MO2, oligo designed to target the +1 to +25

bases of the Nlz start site). These MO-injected embryos were then fixed at the 10-somite stage (14 hpf) in order to assay for defects in the embryo by in situ analysis. Even though high doses (injected with 3 ng MO1 or MO2) proved lethal and a significant percentage of embryos injected with intermediate doses (1.5 to 2.25 ng MO1 or MO2) did not survive (>50 %), the remaining surviving embryos displayed gastrulation defects (stalling or abnormal migration of cells involuting to form the germ ring, converging to form the embryonic shield or extending to form the primary embryonic axis), in addition to an arrest of development during late gastrula stages (7 to 10 hpf) (not shown). Due to the severity of the Nlz MO phenotype, analysis of potential hindbrain effects was not feasible. Embryos injected with a control MO at the same concentration(s) did not exhibit any similar phenotypes, suggesting that the gastrulation defects displayed by Nlz MOs are specific and that Nlz may be required for a role in early development. The processes that are expected to be constrained would occur when *nlz* is first expressed. Indeed, the expression of *nlz* is detected surrounding the blastoderm margin at early gastrula stages (5-6 hpf) (Sagerstrom et al., 2001) and Nlz MOs effect embryos at gastrula stages. This suggests that *nlz* may be required for the morphogenetic movements of involution, convergence and extension that occur during gastrulation and are responsible for defining the primary embryonic axis. Additionally, the interference of *nlz* function through the injection of dominant negative constructs yielded embryos with gastrulaton defects (lateral widening of hindbrain gene expression domains and misshaped or shortened notochords) and cell sorting defects at rhombomere boundaries (expansion of r5-specific gene expression into r4) (Chapter I). Thus, loss of function analyses through the injection

of dominant negative constructs or MOs indicates that *nlz* may govern processes that occur during gastrulation.

The effectiveness of *nlz* inhibition by injected MO was tested by detecting the amount of Nlz protein present in Nlz MO-injected embryos. Lysates of the Nlz MO-injected embryos were resolved by SDS-PAGE, Western-blotted, probed with anti-Nlz antiserum and the proteins were detected using chemiluminescence (Fig. 1A). None of the Nlz MO-injected embryos exhibited a loss of Nlz protein (neither full-length Nlz or short-form protein levels were significantly reduced) (Fig. 1A, lanes 2-4), suggesting that the Nlz MOs may not specifically target *nlz* and inhibit mRNA translation at a detectable level. Furthermore, quantification of the Nlz protein levels for inhibition of function may not be discernable in a developing embryo. Translation overall may be only partially inhibited by the MOs, but still effective for preventing the precise amount of *nlz* mRNA that is needed to be translated for function during gastrula stages. It remains plausible that the inhibition of *nlz* mRNA translation in the MO-injected embryo is sufficient to induce a localized effect, such as defects in gastrulation processes, but remain undetectable when quantifying the complete amount of Nlz protein synthesized. Indeed, in vitro synthesized Nlz protein is inhibited by Nlz MOs at high concentrations (8.2 μM) (Fig. 1B, lanes 3,5,7), albeit at high doses that may be too toxic for an embryo, indicating that the Nlz MOs has the capacity to block translation of *nlz* transcripts in an in vitro assay. Interestingly, while *hox* MO-injected embryos display increasing frequencies and severities of defects from the 0.8 to 4 ng MO range, in vitro translation of *hox* mRNA is inhibited by the MO concentration of 40 μM (Hunter and Prince, 2002). This

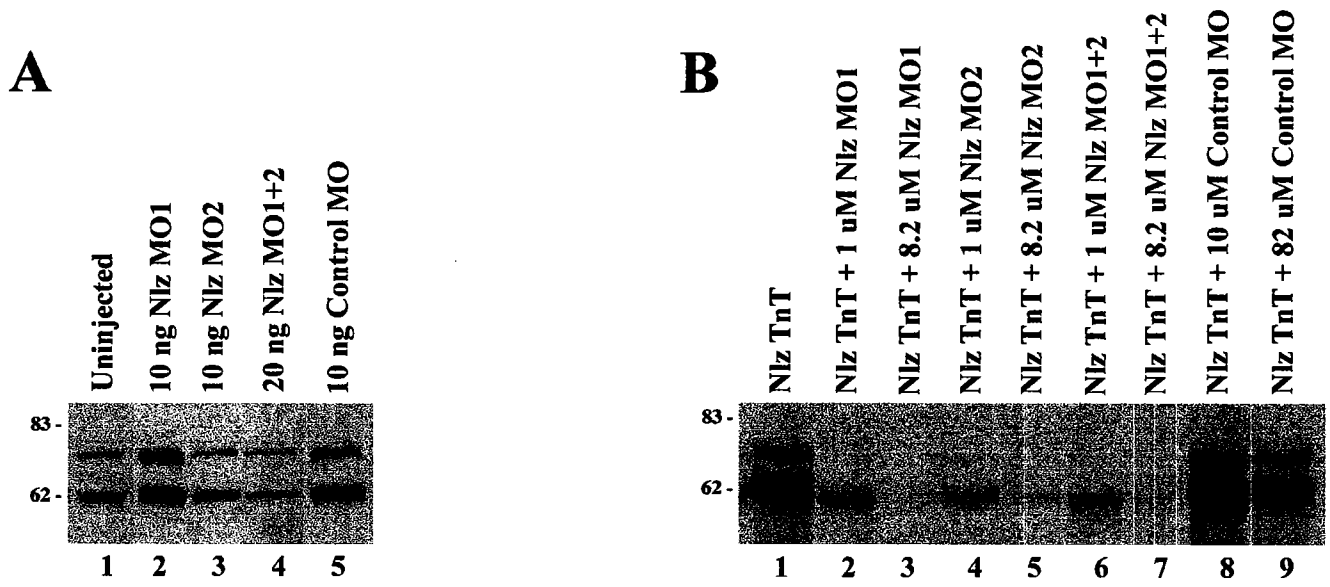


**Figure 1.** Morpholino-targeted inhibition of Nlz translation. (A) Embryos injected with Nlz MO1 or 2 do not exhibit 'knockdown' of *nlz* mRNA translation. Lysate of five embryos that were not injected (lane 1), or injected with 10 ng of Nlz MO1 (lane 2), 10 ng of Nlz MO2 (lane 3), 20 ng of Nlz MO1+2 (lane 4) and 10 ng of control MO (lane 5) were resolved on a 10% polyacrylamide gel by SDS-PAGE, Western-blotted, probed with anti-Nlz antiserum and detected using chemiluminescence. (B) In vitro synthesized Nlz protein is inhibited by Nlz Morpholinos. Nlz protein were in vitro labeled with $^{35}$S-methionine and synthesized using the TnT SP6 Coupled Reticulocyte Lysate System (Promega) in the absence (lane 1) or presence of 1 uM Nlz MO1 (lane 2), 8.2 uM Nlz MO1 (lane 3), 1 uM Nlz MO2 (lane 4), 8.2 uM Nlz MO2 (lane 5), 1 uM Nlz MO1+2 (lane 6), 8.2 uM Nlz MO1+2 (lane 7), 10 uM Control MO (lane 8) or 82 uM Control MO (lane 9). Proteins were separated by SDS-PAGE and visualized by autoradiography. Molecular weight markers (in kDa) are indicated at the left of gels. Abbreviations: MO, morpholino; ng, nanogram; uM, microMolar.

demonstrates that the effectiveness of MOs is dependent on concentration and context of experimental environment conditions (embryo vs. in vitro). Nevertheless, Nlz MO-targeted gene 'knockdown' may be only partially effective in determining early functions of *nlz* in the developing embryo. Utilization of Nlz MOs does not eliminate the possibility that other factors may compensate for the inhibition of *nlz* function. One possibility is the short form of Nlz, which is present at the same time as full-length Nlz in the developing embryo and is found to possess both repressor (*nlz*-mediated) and interfering (inhibition of *nlz* function) activities (Chapter II). Another factor is *nlz2*, which is expressed in the caudal hindbrain and is found to function similarly to *nlz* when overexpressed (Chapter II). This indicates that the function of Nlz-related genes may only be elucidated with the inhibition of mRNA translation for all *nlz*-related genes in the developing embryo, which may be technically challenging to the constraints of toxicity associated with increasing MO-concentrations. Retrospectively, loss of Nlz function analyses with MO and dominant negative injections, and the loss of function phenotypes of the Nlz-related proteins NocA (Cheah et al., 1994; Dorfman et al., 2002), Elbow (Dorfman et al., 2002), TLP-1 (Zhao et al., 2002) and the vertebrate Sp1-factors (summarized in Chapter II), all suggest that Nlz-related proteins play prominent roles for early embryonic development.

## Mechanism of Nlz function

The elucidation of *nlz* function was determined by employing misexpression analyses of full-length *nlz* (gain of function) and dominant negative constructs (loss of function) in Chapter I and utilizing a deletion panel of *nlz* constructs in Chapter II to uncover important domains necessary for Nlz-mediated repression. However, it is not known how *nlz* exactly functions in the developing embryo. In this section, I will discuss that the biological activities associated with Nlz-related proteins, such as transcriptional repression, nuclear localization and corepressor binding, involves specific protein-protein interactions.

### *The $C_2H_2$ zinc-finger mediates transcriptional activity*

It is likely that Nlz-related proteins are involved in transcriptional repression, however it is not known how Nlz mediates this activity. Nlz may function in binding to target DNA sites, through its $C_2H_2$ zinc-finger, to exert repression or recruit other factors that function as corepressors to govern transcriptional repression. In Chapter I, I have discussed the possibility that the association of two Nlz-related proteins may provide the minimum number of zinc fingers necessary for DNA binding. In Chapter II, I have discussed that the presence of this $C_2H_2$ zinc-finger is important for Nlz-mediated repression, however Nlz self-association was found not to be required for Nlz-mediated transcriptional repression. With the finding that the Nlz zinc-finger lacks essential

residues important for DNA binding, suggests that Nlz-related proteins are unable to bind to DNA through its zinc-finger domain and may instead utilize other regions for DNA association. One method of determining if Nlz-related proteins are capable of recognizing DNA is to employ a 'selective amplification and binding' assay (Blackwell and Weintraub, 1990). This method utilizes labeled double-stranded oligonucleotides containing random nucleotides flanked by known primer sequences (with restriction sites to allow cloning of desirable individual templates) incubated with the Nlz protein. The bound templates are isolated by EMSA (electrophoretic mobility shift assay), amplified by PCR (polymerase chain reaction), subjected to multiple rounds of re-selection and re-amplification to increase stringency of specific binding and then cloned and sequenced. To confirm that the isolated DNA template is indeed a binding site for the Nlz protein, a reporter plasmid could be constructed (with the luciferase gene under the control of the actin promoter and the potential Nlz DNA binding region) and co-injected with mRNA encoding *nlz* into zebrafish embryos. Luciferase levels would then be quantified in the presence or absence of *nlz* mRNA to determine if Nlz binds DNA and mediates repression of luciferase activity. This method would identify potential DNA binding motifs within Nlz and the generation of Nlz deletion constructs could be utilized to determine if these DNA binding motifs are essential for Nlz-mediated transcriptional repression.

Though Nlz-related proteins likely do not bind DNA, they may instead utilize different domains to mediate interactions with other proteins in order to elicit transcriptional activity. One candidate region is the putative $C_2H_2$ zinc-finger (as

discussed in Chapter II) and transcription factors with a single zinc-finger have been reported to be suitable to interact with another protein and permit transcriptional activity (Merika and Orkin, 1995; Yang and Evans, 1992). To this end, a yeast two-hybrid system analysis (employing a zebrafish library) could be utilized to identify proteins that interact with the Nlz $C_2H_2$ zinc-finger and mediate transcriptional repression.

*Corepressor binding governs Nlz-mediated repression*

Nlz-related proteins may exert transcriptional repression by virtue of their association with known corepressors that include Groucho (Chapter I) and histone deacetylases (Chapter II). The assembly of a multi-protein complex that synergizes to repress transcription of specific genes involves interactions between repressors, corepressors and numerous basal machinery components. Since Nlz-related proteins may not bind DNA directly, other interacting proteins (as yet unidentified) may function in directing Nlz to the target DNA site. In Chapters I and II, I have demonstrated that Nlz proteins interact with both Groucho and HDACs. However, while some HDACs are ubiquitously expressed, Groucho is only expressed in the rostral hindbrain, suggesting that other *groucho*-related genes that may participate in recruiting HDAC activity are present in other regions of the embryo. While the recruitment of HDACs to modulate chromatin structure involves Groucho interaction to mediate repression, other factors may also participate to work directly upon the general transcriptional machinery (Chen and Courey, 2000; Courey and Jia, 2001). This includes corepressors that function to prevent activators from binding to a given promoter, thus resulting in repression of

transcriptional activity (Criqui-Filipe et al., 1999; Zhang et al., 2001). Thus, it remains plausible that Nlz may govern repression by either associating with Groucho to recruit HDACs and create a repressed chromatin state or by displacing and preventing activators from participating in forming a cooperative assembly of proteins that function as a transcriptional complex. Nonetheless, this suggests that Nlz may interact with numerous proteins involved in interfering with the general transcriptional machinery and the proper structure of chromatin in order to facilitate repression of transcription.

*Specific protein interactions may be necessary for Nlz nuclear localization and activity via the Sp motif*

In Chapter II, I have discussed that Nlz deletion constructs that do not reside in the nucleus (C-terminal deletions encompassing amino acids # 498 to 566) exhibit a reduced number of affected embryos exhibiting repressor activity when misexpressed. Since sequence analysis indicates that Nlz does not contain a nuclear localization signal sequence (NLS), this suggests that an accessory protein may bind to and shuttle Nlz to the nucleus. In order to identify proteins that potentially interact with the Nlz region important for nuclear localization, a yeast two-hybrid system could be employed.

Embryos injected with a construct without the Sp motif exhibited a reduction in the repressor phenotype, suggesting that the Sp motif in Nlz-related proteins may regulate transcriptional activity through the interaction with other cofactors (excluding Groucho or HDAC) (Chapter II). It has been reported that the nuclear protein p74 binds to the Sp1 protein via the N-terminus (which encompasses the Sp motif) and this interaction

correlates with a substantial reduction of transcriptional activity in vivo (Murata et al., 1994). The Sp motif may also function as a docking region for factors responsible for targeting Nlz to the template since Nlz does not appear to possess a DNA binding domain. To this end, a yeast two-hybrid system could be utilized to identify proteins that interact with the Sp motif. These isolated factors could then be characterized to determine if they do indeed function as DNA binding proteins that direct Nlz to the target template and repress transcription.

## Restriction of *nlz* gene expression in the rostral hindbrain controls segmental identity

The establishment of individual segmental identities within the hindbrain involves tightly coupled processes that include the initiation of genes expressed in the presumptive hindbrain and their subsequent regulation. In the introduction of this thesis, I have discussed the known mechanisms that are involved in these processes. In this section, I will mention how *nlz* is involved in the specification and regulation of rhombomere identity in the rostral hindbrain.

### *Mutual exclusion of specific gene expression governs rostral hindbrain gene expression*

The expression of *nlz* is dynamic within the prospective hindbrain during embryonic development. In Chapter I, I have shown that during late gastrula stages, *nlz* is

expressed from the caudal (posterior) end of the embryo to the rhombomere (r) 3/r4 boundary in the hindbrain. By segmentation stages, *nlz* expression begins to expand rostrally (anteriorly) into r3 (between 10.5 to 11 hpf) and r2 (by 16 hpf) and persist in these regions even at later stages (20 hpf). The ectopic expression of *nlz* results in a distinct disruption of genes expressed in the rostral hindbrain (Chapter I). Examinations of *nlz*-injected embryos at late gastrula stages indicate that genes expressed in the r1-r3 domains of the hindbrain are no longer present. Additionally, analysis of *nlz*-injected embryos at segmentation stages reveal that there is a disruption of genes expressed in r2 and r3, with r4-gene expression appearing to expand anteriorly into r3. This indicates that the ectopic presence of *nlz* in the rostral hindbrain at early stages (late gastrula) appears to be mutually exclusive with the initiation of gene expression within r2 and r3. Similarly, this regulation of initial rhombomere identity due to the mutual exclusion of genes expressed in particular domains has been previously documented (Barrow et al., 2000). The expression of *krox20* within r5 is only apparent after the retreat of *hoxa1* and *hoxb1* expression from this region (Barrow et al., 2000) and *hoxa1/hoxb1* double mutants exhibit *krox20* expression in r4 and r5 due to the absence of *hoxa1* and *hoxb1* expression in these rhombomeres (Rossel and Capecchi, 1999). These results suggest that r5 possess the intrinsic ability to express *krox20*, however initiation of *krox20* expression in r5 is only apparent with the absence of *hoxa1* and *hoxb1* signals (Barrow et al., 2000). Likewise, the initiation of gene expression in r2 and r3 may be exclusive with the premature presence of *nlz* during gastrula stages. This suggests that normally during

gastrula stages, *nlz* is only expressed at an anterior limit to the r3/r4 boundary, perhaps allowing for the initiation of genes expressed in r2 and r3.

The mechanism that regulates the restrictive expression limits of *nlz* is unknown. However, it is possible that *hox* genes from paralogue group 1 (*hoxa1* and *hoxb1*) may mediate this restrictive expression, since similarly to *nlz*, the anterior limits of expression for both *hoxb1* and *hoxa1* coincide at the r3/r4 presumptive boundary during late gastrula stages (Prince et al., 1998). Additionally, the ectopic expression of the *hox* paralogue group 1 genes results in a transformation of the r2 region to a r4 state (Alexandre et al., 1996; Bell et al., 1999; McClintock et al., 2001; Zhang et al., 1994). As discussed in Chapter I, gene expression within r4 is also disrupted – *nlz*-injected embryos appear to have a partial expansion of r4-gene expression into the region where r3 gene expression was lost. However, this was only apparent at late segmentation stages. Analysis of *nlz*-injected embryos at gastrula stages (10.5-11 hpf) indicate that only r3 gene expression is affected, suggesting that maintenance of *nlz* expression at caudal regions of the embryo does not prominently depend on activities of *hox* genes from paralogue group 1. Nonetheless, *nlz* appears to function during gastrula stages to restrict the expression of non-r4 (r2 and r3) genes in the caudal hindbrain.

After initiation of r2 and r3 gene expression, *nlz* expression expands anteriorly into these rostral regions, perhaps functioning in the down-regulation of r2- and r3-gene expression proliferation. An analogous mechanism occurs with the expression of *krox20* in r3 and r5, which is mediated by the corepressors NAB1 and NAB2 in a negative feedback loop (Mechta-Grigoriou et al., 2000). The ectopic expression of *nab1* or *nab2*

results in reduced and irregularly-shaped r3 and r5 domains, with expanded r4 expression domains (Mechta-Grigoriou et al., 2000). This phenotype is similar to the misexpression of *nlz*, indicating that *nlz* may participate in a negative feedback regulatory loop to control gene expression within the r2 and r3 domains. This regulation may ensure that non-r4 (r2 and r3) genes are not expressed in the r4 domain and the rostral hindbrain is properly segmented during initiation of gene expression. Thus, the mutual exclusion that exists between *nlz* and genes expressed in the presumptive rostral hindbrain during late gastrula stages, and the regulatory cascade that is present between *nlz* and genes expressed in r2 and r3 during segmentation, suggest that *nlz* controls the initial regionalization of the rostral hindbrain and maintenance of rhombomere identity.

## Model of *nlz* function

Insights into *nlz* function and its mechanism of action was elucidated by the detailed analysis of *nlz* expression during early neural development, gain of function studies, misexpression of dominant negative *nlz* constructs, misexpression of the short form of *nlz* and corepressor binding assays (Chapters I and II). The results obtained from these experiments suggest that *nlz* participates in the mediation of transcriptional repression and this is governed by interactions with corepressors. The data that are presented and discussed in this thesis suggests that *nlz* is required for the proper formation of r4 by repressing non-r4 (r2 and r3) gene expression during morphogenesis

of the segmental hindbrain and this is illustrated in the model of *nlz* function (Figs. 2 and 3).

In a gastrula-staged embryo, *nlz* is expressed with an anterior limit at the r3/r4 boundary in the presumptive hindbrain. Since it is not known if Nlz is capable of binding DNA and Nlz does not posses any domains that resemble DNA binding motifs, the model proposes that Nlz binds to DNA via association with a DNA binding protein (DBP). Once Nlz is targeted to the template (directly or indirectly), it then recruits the corepressors Groucho and HDACs to mediate transcriptional repression. Thus, Nlz functions to repress the expression of r2 and r3 (non-r4) genes in the presumptive r4 domain (Fig. 2A). Throughout the segmentation period, r2 and r3 gene expression is initiated and maintained in their respective presumptive rhombomeres by specific initiation factors (Fig. 2A,B). During later segmentation stages, *nlz* expression expands anteriorly to the r2 and r3 regions, perhaps functioning in the regulation of r2 and r3 genes in their particular domains through a negative feedback loop (Fig. 2B). It is plausible that this may occur through the association with different cofactors (DBP or corepressors) in r2 and r3. The repression of r2- and r3-gene expression in r4 may also be fortified by the presence of *hox* genes from paralogue group 1 (due to mutual exclusion, see above section).

The misexpression of *nlz* in developing embryos results in the ectopic expression of *nlz* in the rostral hindbrain, where *nlz* is not yet normally present, such as in r2 and r3 (Fig. 3A). Within this region, ectopic *nlz* may function in employing the same repressor complex components in r4 (DBP and the corepressors Groucho and HDAC) to repress

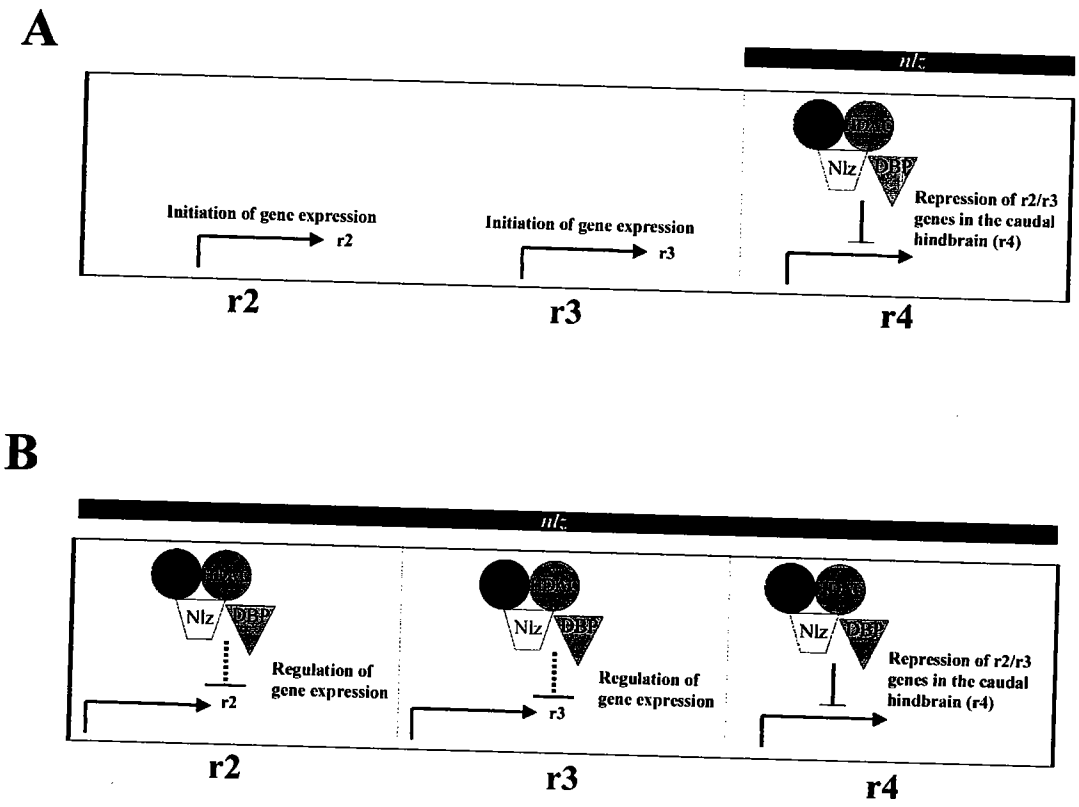


**Figure 2.** Model of Nlz function in the developing zebrafish hindbrain. (A) Nlz functions to repress non-r4 (r2 and r3) gene expression in the caudal hindbrain during gastrula stages. r2 and r3 gene expression is initiated in their prospective rhombomeres by specific factors. (B) Nlz functions to regulate gene expression in the rostral hindbrain (r2 + r3) during segmentation stages. Schematic of hindbrain is shown with anterior to the left (only r2-4 is depicted). Arrow indicates activation of gene expression. Black line indicates repression. Black box represents *nlz* expression domain. Nlz is shown as a yellow trapezoid, DBP as a green triangle, Gro as a red circle and HDAC as a blue circle. Abbreviations: r2-4, rhombomeres 2-4; DBP, DNA-binding protein; Gro, Groucho corepressor; HDAC, histone deacetylases.

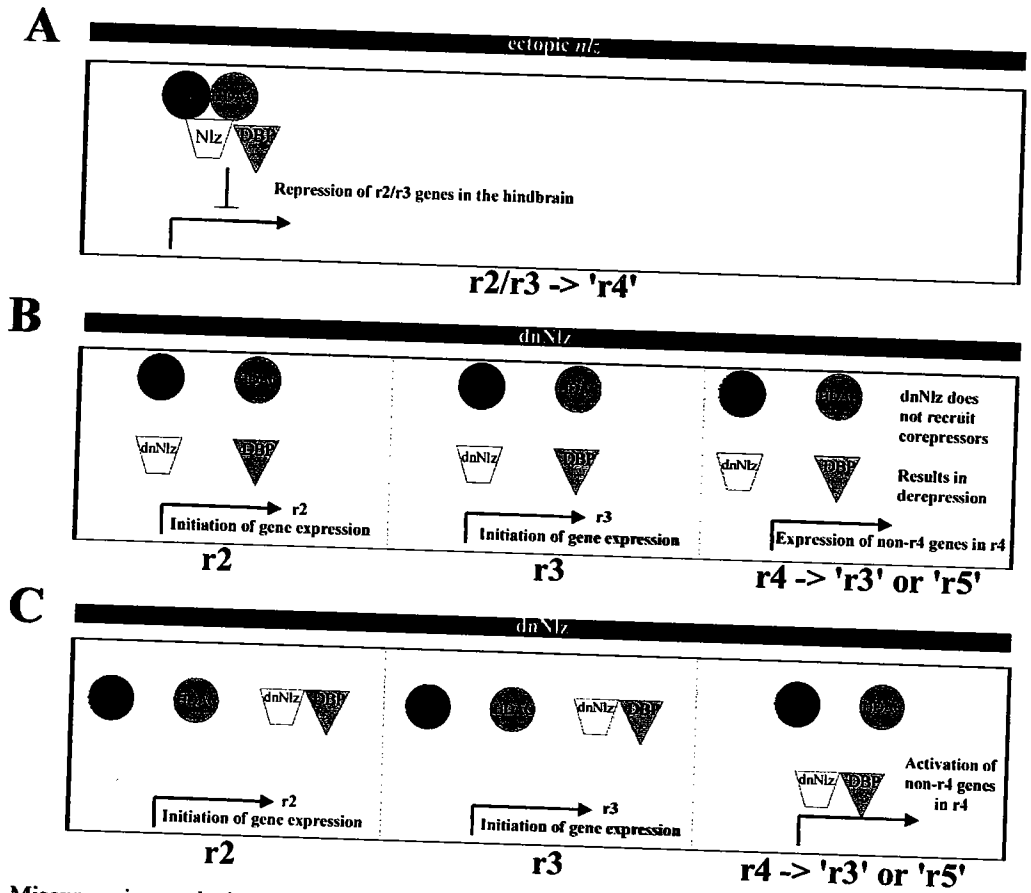


**Figure 3.** Misexpression analysis reveals a functional role for Nlz in the hindbrain. (A) Misexpression of *nlz* results in loss of r2 and r3 gene expression and an expansion of r4 gene expression. (B,C) Misexpression of dominant negative Nlz (dnNlz). (B) Misexpression of dnNlz results in the derepression of non-r4 (r3 or r5) genes since dnNlz cannot recruit the corepressors Groucho and HDACs. (C) Misexpression of dnNlz results in the activation of non-r4 (r3 or r5) genes in r4, perhaps through the association with a DBP. Schematic of hindbrain is shown with anterior to the left (only r2-4 is depicted). Arrow indicates activation of gene expression. Black line indicates repression. Black box represents ectopic *nlz* (A) or dnNlz (B,C) expression. Nlz is shown as a yellow trapezoid, DBP as a green triangle, Gro as a red circle, HDAC as a blue circle and dnNlz as a grey trapezoid. Abbreviations: r2-4, rhombomeres 2-4; DBP, DNA-binding protein; Gro, Groucho corepressor; HDAC, histone deacetylases; dnNlz, dominant negative Nlz.

genes expressed in r2 and r3, resulting in an anterior expansion of r4 gene expression (Fig. 3A). The misexpression of dominant negative *nlz* constructs (dnNlz) generates a phenotype associated with the interference of Nlz-mediated repression. Since dnNlz cannot recruit corepressors, this may alleviate Nlz-mediated gene repression in r4 by the derepression of genes (non-r4) normally targeted by *nlz* in the rostral hindbrain (Fig. 3B). Alternatively, dnNlz could interact with a specific DBP in order to activate genes (r2, r3 or r5) normally repressed by Nlz in r4 (Fig. 3C).

In some instances, misexpression of the short form of *nlz* (*nlzΔ60N*) generates the repressor phenotype. This may occur through the association of *nlzΔ60N* with components of the *nlz* repressor complex (similar to Fig. 3A), or through interactions with other (yet unidentified) specific corepressors and DBPs. In other instances, *nlzΔ60N* generates the phenotype associated with the interference of Nlz-mediated repression. This may occur through the interaction of *nlzΔ60N* with endogenous *nlz*, thus preventing *nlz* from associating with components of the transcription repressor complex, resulting in the de-repression of *nlz*-targeted genes. Alternatively, *nlzΔ60N* may instead bind to DBPs in order to activate non-r4 (r2, r3 or r5) genes in r4 (similar to Fig. 3C). In all, this model demonstrates that *nlz* mediates repressor activity through the association with corepressors in a dynamic fashion during development in order to properly segment the rostral hindbrain.

## Additional roles of *nlz* in development

The dynamic expression of *nlz* during the initiation and specification of rhombomeric identity at late gastrula to segmentation stages indicates that *nlz* functions to regionalize the zebrafish hindbrain. The model of *nlz* function proposes that *nlz* mediates transcriptional repression through interaction with corepressors (Groucho and histone deacetylases) in order to repress non-r4 (r2 and r3) gene expression in r4 and properly segment the rostral hindbrain. In addition to morphogenesis of the hindbrain, the pattern and period of *nlz* expression suggests that this candidate segmentation gene may have additional functional roles in early development and the subsequent growth of embryonic structures.

### *Functions of nlz during gastrulation*

The expression of *nlz* is first detected as a ring near the blastoderm margin with a gap in the dorsal midline of early gastrula stage zebrafish embryos (Sagerstrom et al., 2001). By mid-gastrula stages, *nlz* expression in the dorsal midline increases and by late gastrula stages, *nlz* is expressed in a broad posterior domain (Sagerstrom et al., 2001). The expression of *nlz* during the initial gastrulation stages suggests that *nlz* may participate in early functions associated with this period. At the onset of gastrulation, the initiation and specification of particular embryonic fates take place and the morphogenetic movements of involution, convergence and extension arranges the three distinctive germ layers (ectoderm, mesoderm and endoderm) in an orderly manner,

defining the primary embryonic axis. Nlz may function in regulating the cellular movements associated with epiboly, when cells of the blastodisc begin to thin and spread out over the yolk sac, thus contributing to the proper establishment of the rudiment embryonic body plan.

While the gain of function approach (through misexpression analysis) revealed a role for *nlz* in segmentation of the hindbrain, the loss of function approach (through the expression of dominant negative *nlz* constructs or anti-sense *nlz* morpholino oligos) indicated that *nlz* might govern processes that occur during gastrulation (not shown and Chapter I). Interference of *nlz* function resulted in embryos displaying a general disorganization of embryonic structures which included the lateral widening and broadening of midbrain and hindbrain regions, twisted and shortened notochords, and the absence of cell sorting at rhombomere boundaries. These results are consistent with defects in cell migration events that occur during gastrulation such as the involution or ingression of cells during the formation of the germ ring, the convergence of cells to the dorsal midline and the extension of cells along the anterior-posterior axis of the embryo. Thus, the expression of *nlz* during the early stages of gastrulation and the morphological defects associated with interference of *nlz* function suggests that *nlz* may regulate the cellular movements that occur during gastrulation and is required for proper establishment of the embryonic body plan.

The effects that *nlz* may mediate upon gastrulation processes may be direct or indirect. It remains plausible that other *nlz*-related genes may be expressed and participates with *nlz* in governing the cellular movements associated with epiboly.

Indeed, similar to *nlz*, *nlz2* is expressed near the blastoderm margin with a gap in the dorsal midline during early gastrula stages and in a broad caudal domain by late gastrula stages (Chapter II). This expression pattern suggests that *nlz2* may function with *nlz* to jointly control the morphogenetic movements that occur during gastrulation. Evidence that *nlz2* may exhibit similar activities as *nlz* are apparent in several functional domains that are conserved among both genes and the demonstration that misexpression of *nlz2*, similar to *nlz*, represses gene expression in the rostral hindbrain at segmentation stages (Chapter II). It is likely that *nlz2* may also perform similar functions as *nlz* during early gastrula stages.

*nlz functions as an upstream regulator of segment identity genes*

In adjunction to governing processes that occur during gastrulation, *nlz* functions as a transcriptional repressor and mediates segmentation in the rostral hindbrain (Chapter I). The presence of *nlz* expression prior to the initiation of genes that are involved in the regionalization of the hindbrain and the specification of rhombomere identity suggests that *nlz* may be involved in their regulation. Signaling molecules such as FGF3 (Kiefer et al., 1996) and FGF8 (Reifers et al., 1998) and transcription factors such as *pou2* (Hauptmann and Gerster, 1995) and *vhnf1* (Sun and Hopkins, 2001) are expressed at early gastrula stages, indicating that they may not only participate with *nlz* in controlling the convergence movements that occur during gastrulation, but may also function upstream of and regulate *nlz* in order to properly form individual rhombomeres. The latter remains an unlikely scenario since analyses of *acerebellar* (*ace*) mutants, which are

defective in FGF8 (Furthauer et al., 1997; Reifers et al., 1998), and *spiel-ohne-grenzen* (*spg*) mutants, which have defects in the *pou2* gene (Belting et al., 2001), still exhibit *nlz* expression (not shown). This indicates that *nlz* functions independently from these early gastrula-stage expressed factors, however analysis of mutants defective in *vhnf1* or FGF3 signaling remains to be elucidated.

Transcription factors such as *krox20* (Oxtoby and Jowett, 1993), *valentino* (Moens et al., 1998) and the *hox* genes (Prince et al., 1998) are not expressed until late gastrula stages, indicating that *nlz* may function upstream and directly regulate the expression of these factors that are involved in hindbrain specification. Indeed, misexpression of *nlz* results in a loss of *krox20* and *hoxa2* expression in the rostral hindbrain (r2 and r3 regions) and an anterior expansion of *hoxb1a* expression from the r4 domain (Chapter I). Patterning of the hindbrain is initiated and established by the temporal expression of segmentation genes. These genes also function to regulate the expression of downstream genes that specify rhombomere identity. This includes *krox20*, which functions to regulate its own expression through the expression of its own antagonists (*nab1* and *nab2*) and regulates the expression of *hox* genes and *eph* signaling molecules (as discussed in the Introduction). In addition, *hox* genes regulate each other and synergize with other genes to control rhombomere identity (as discussed in the Introduction). It is likely that in the regulatory cascade that controls segmental gene expression in the hindbrain, *nlz* functions upstream of *krox20*, the *hox* genes and *eph-ephrin* signaling molecules in order to ensure that rostral genes (r2 and r3) are not expressed during the initiation of gene expression within the r4 domain and that

regionalization of segmental compartments (via cell sorting at rhombomere boundaries) are maintained.

Functional analyses of *nlz* that are discussed in this thesis suggest that *nlz* functions as a hindbrain-patterning gene. These genes are classified into those that are involved in the establishment of a segmental pattern (segmentation genes) and those of which are involved in the differentiation of individual segments (segment identity genes). While the loss of function of segmentation genes results in a partial or entire loss of hindbrain segments, loss of function of segment identity genes retains the segments but exhibit altered segmental identities. Additionally, gain of function of segment identity genes results in a transformation of segmental identity. Using this criteria, *nlz* may function as a segment identity gene since misexpression of *nlz* leads to a disruption of gene expression in the rostral hindbrain in which r2 and r3 gene expression is lost and r1 and r4 gene expression appear to extend into the region normally occupied by the r2- and r3-specific gene expression domains. However, both the loss and gain of function of *nlz* experiments demonstrate that a complete transformation of segmental identity does not take place – neuronal differentiation in the rostral hindbrain (branchiomotor and reticulospinal neurons) is only mildly affected (Chapter I). This demonstrates that *nlz* does not function as a segment identity gene and instead may behave primarily as a segmentation gene. This is supported by the findings that segmentation genes are expressed prior to and regulate the expression of segment identity genes (as discussed in the Introduction) and that the misexpression of a segmentation gene could inconceivably transform the identity of segments indirectly by altering the expression of segment

identity genes. *nlz* is indeed expressed at early gastrula stages, prior to the expression of segment identity genes such as *krox20* and the *hox* genes, and could function as an upstream regulator. Thus, it is likely that *nlz* functions in the regulatory cascade that controls the initial regionalization of the rostral hindbrain as a segmentation gene in order to properly control and maintain rhombomere identity.

## References


Alexandre, D., Clarke, J. D., Oxtoby, E., Yan, Y. L., Jowett, T., and Holder, N. (1996). Ectopic expression of Hoxa-1 in the zebrafish alters the fate of the mandibular arch neural crest and phenocopies a retinoic acid-induced phenotype. *Development* **122,** 735-746.

Barrow, J. R., Stadler, H. S., and Capecchi, M. R. (2000). Roles of Hoxa1 and Hoxa2 in patterning the early hindbrain of the mouse. *Development* **127,** 933-44.

Bell, E., Wingate, R. J., and Lumsden, A. (1999). Homeotic transformation of rhombomere identity after localized Hoxb1 misexpression. *Science* **284,** 2168-71.

Belting, H. G., Hauptmann, G., Meyer, D., Abdelilah-Seyfried, S., Chitnis, A., Eschbach, C., Soll, I., Thisse, C., Thisse, B., Artinger, K. B., Lunde, K., and Driever, W. (2001). spiel ohne grenzen/pou2 is required during establishment of the zebrafish midbrain-hindbrain boundary organizer. *Development* **128,** 4165-76.

Blackwell, T. K., and Weintraub, H. (1990). Differences and similarities in DNA-binding preferences of MyoD and E2A protein complexes revealed by binding site selection. *Science* **250,** 1104-10.

Cazenave, C., Stein, C. A., Loreau, N., Thuong, N. T., Neckers, L. M., Subasinghe, C., Helene, C., Cohen, J. S., and Toulme, J. J. (1989). Comparative inhibition of rabbit globin mRNA translation by modified antisense oligodeoxynucleotides. *Nucleic Acids Res* **17,** 4255-73.

Cheah, P. Y., Meng, Y. B., Yang, X., Kimbrell, D., Ashburner, M., and Chia, W. (1994). The Drosophila l(2)35Ba/nocA gene encodes a putative Zn finger protein involved in the development of the embryonic brain and the adult ocellar structures. *Molecular and Cellular Biology* **14,** 1487-1499.

Chen, G., and Courey, A. J. (2000). Groucho/TLE family proteins and transcriptional repression. *Gene* **249,** 1-16.

Courey, A. J., and Jia, S. (2001). Transcriptional repression: the long and the short of it. *Genes Dev* **15,** 2786-96.

Criqui-Filipe, P., Ducret, C., Maira, S. M., and Wasylyk, B. (1999). Net, a negative Ras-switchable TCF, contains a second inhibition domain, the CID, that mediates repression through interactions with CtBP and de-acetylation. *Embo J* **18,** 3392-403.

Dorfman, R., Glazer, L., Weihe, U., Wernet, M. F., and Shilo, B. Z. (2002). Elbow and Noc define a family of zinc finger proteins controlling morphogenesis of specific tracheal branches. *Development* **129,** 3585-96.

Furthauer, M., Thisse, C., and Thisse, B. (1997). A role for FGF-8 in the dorsoventral patterning of the zebrafish gastrula. *Development* **124,** 4253-64.

Hauptmann, G., and Gerster, T. (1995). Pou-2--a zebrafish gene active during cleavage stages and in the early hindbrain. *Mech Dev* **51,** 127-38.

Hunter, M. P., and Prince, V. E. (2002). Zebrafish hox paralogue group 2 genes function redundantly as selector genes to pattern the second pharyngeal arch. *Dev Biol* **247,** 367-89.

Kiefer, P., Strahle, U., and Dickson, C. (1996). The zebrafish Fgf-3 gene: cDNA sequence, transcript structure and genomic organization. *Gene* **168,** 211-5.

Lele, Z., Bakkers, J., and Hammerschmidt, M. (2001). Morpholino phenocopies of the swirl, snailhouse, somitabun, minifin, silberblick, and pipetail mutations. *Genesis* **30,** 190-4.

McClintock, J. M., Carlson, R., Mann, D. M., and Prince, V. E. (2001). Consequences of Hox gene duplication in the vertebrates: an investigation of the zebrafish Hox paralogue group 1 genes. *Development* **128,** 2471-84.

Mechta-Grigoriou, F., Garel, S., and Charnay, P. (2000). Nab proteins mediate a negative feedback loop controlling Krox-20 activity in the developing hindbrain. *Development* **127,** 119-28.

Merika, M., and Orkin, S. H. (1995). Functional synergy and physical interactions of the erythroid transcription factor GATA-1 with the Kruppel family proteins Sp1 and EKLF. *Mol Cell Biol* **15,** 2437-47.

Moens, C. B., Cordes, S. P., Giorgianni, M. W., Barsh, G. S., and Kimmel, C. B. (1998). Equivalence in the genetic control of hindbrain segmentation in fish and mouse. *Development* **125,** 381-391.

Murata, Y., Kim, H. G., Rogers, K. T., Udvadia, A. J., and Horowitz, J. M. (1994). Negative regulation of Sp1 trans-activation is correlated with the binding of cellular proteins to the amino terminus of the Sp1 trans-activation domain. *J Biol Chem* **269,** 20674-81.

Nasevicius, A., and Ekker, S. C. (2000). Effective targeted gene 'knockdown' in zebrafish [In Process Citation]. *Nat Genet* **26,** 216-20.

Oxtoby, E., and Jowett, T. (1993). Cloning of the zebrafish krox-20 gene (*krx20*) and its expression during development. *Nucl. Acids Res.* **21,** 1087-1095.

Prince, V. E., Moens, C. B., Kimmel, C. B., and Ho, R. K. (1998). Zebrafish hox genes:expression in the hindbrain region of wild-type and mutants of the segmentation gene valentino. *Development* **125,** 393-406.

Reifers, F., Bohli, H., Walsh, E. C., Crossley, P. H., Stainier, D. Y., and Brand, M. (1998). Fgf8 is mutated in zebrafish acerebellar (ace) mutants and is required for maintenance of midbrain-hindbrain boundary development and somitogenesis. *Development* **125,** 2381-95.

Rossel, M., and Capecchi, M. R. (1999). Mice mutant for both Hoxa1 and Hoxb1 show extensive remodeling of the hindbrain and defects in craniofacial development. *Development* **126,** 5027-40.

Sagerstrom, C. G., Kao, B. A., Lane, M. E., and Sive, H. (2001). Isolation and characterization of posteriorly restricted genes in the zebrafish gastrula. *Dev Dyn* **220,** 402-8.

Stein, C. A. (1999). Keeping the biotechnology of antisense in context. *Nat Biotechnol* **17,** 209.

Summerton, J. (1999). Morpholino antisense oligomers: the case for an RNase H-independent structural type. *Biochim Biophys Acta* **1489,** 141-58.

Summerton, J., and Weller, D. (1997). Morpholino antisense oligomers: design, preparation, and properties. *Antisense Nucleic Acid Drug Dev* **7,** 187-95.

Sun, Z., and Hopkins, N. (2001). vhnf1, the MODY5 and familial GCKD-associated gene, regulates regional specification of the zebrafish gut, pronephros, and hindbrain. *Genes Dev* **15,** 3217-29.

Yang, H. Y., and Evans, T. (1992). Distinct roles for the two cGATA-1 finger domains. *Mol Cell Biol* **12,** 4562-70.

Zhang, C. L., McKinsey, T. A., Lu, J. R., and Olson, E. N. (2001). Association of COOH-terminal-binding protein (CtBP) and MEF2-interacting transcription repressor (MITR) contributes to transcriptional repression of the MEF2 transcription factor. *J Biol Chem* **276,** 35-9.

Zhang, M., Kim, H.-J., Marshall, H., Gendron-Maguire, M., Lucas, A. D., Baron, A., Gudas, L. J., Gridley, T., Krumlauf, R., and Grippo, J. F. (1994). Ectopic Hoxa-1 induces rhombomere transformation in mouse hindbrain. *Development* **120,** 2431-2442.

Zhao, X., Yang, Y., Fitch, D. H., and Herman, M. A. (2002). TLP-1 is an asymmetric cell fate determinant that responds to Wnt signals and controls male tail tip morphogenesis in C. elegans. *Development* **129,** 1497-508.

# APPENDIX

As discussed in the introduction of this thesis, a subtractive hybridization-based screen isolated novel genes restrictedly expressed posteriorly in mid-gastrula zebrafish embryos. Through sequence and phylogenetic analyses of the isolated full-length clone (NH13), I have determined that this gene is closely related to human and mouse LMO4, a member of the nuclear LMO subfamily of LIM domain proteins. The sequence data that I have generated was incorporated into figure 1 of the following publication in this appendix. To determine the spatial and temporal distribution of *lmo4* mRNA, I processed zebrafish embryos from blastula to segmentation stages for in situ hybridization with an *lmo4* probe. At shield stage (6 hpf), *lmo4* is expressed in a broad ring in the blastoderm margin, just above the germ ring. By 75 % epiboly (8 hpf), *lmo4* is expressed in a broad dorsal region that excludes the germ ring. By bud stage (10 hpf), the expression of *lmo4* is restricted to a rostral domain within the prospective rostral hindbrain, and the anterior limit of *lmo4* expression is adjacent to the caudal border of *pax2.1* expression in the midbrain-hindbrain boundary. At this stage, *lmo4* expression was not detected in the rostral hindbrain of homozygous *acerebellar* (mutant in *fgf8*) embryos. By the 3-somite stage (11 hpf), *lmo4* expression is present in the neural plate and somites. At the 6-somite stage (12 hpf), the expression of *lmo4* becomes restricted to the anterior neural plate, while expression persists in the somites and becomes detectable in the forebrain (prospective optic primordium). Some of this *lmo4* expression data was incorporated into figures 2 and 4 of the following publication in this appendix.

# DYNAMIC EXPRESSION AND REGULATION BY FGF8 AND POU2 OF THE ZEBRAFISH LIM-ONLY GENE, LMO4

Mary Ellen Lane[1,2], Alexander P. Runko[1], Nicole M. Roy[1] and Charles G. Sagerström[1]

[1]Department of Biochemistry and Molecular Pharmacology, University of Massachusetts Medical School, 364 Plantation St/LRB822, Worcester, MA 01605

[2] Author for correspondence at current address: Department of Biochemistry and Cell Biology, Rice University, 6100 Main Street, Houston, TX 77005

melane@rice.edu

Lane, M.E., Runko, A.P., Roy, N.M., and Sagerström, C.G. (2002). *Gene Expr Patterns* **2**, 207-11.

## Abstract

We report the expression of zebrafish *lmo4* during the first 48 hours of development. Like its murine ortholog, *lmo4* is expressed in somitic mesoderm, branchial arches, otic vesicles, and limb (pectoral fin) buds. In addition, however, we report zebrafish *lmo4* expression in the developing eye, cardiovascular tissue, and the neural plate and telencephalon. We demonstrate that expression in the rostral hindbrain requires *acerebellar* (*ace/fgf8)* and *spiel ohne grenzen (spg/pou2)* activity.

**Key Words:** *lmo4*, LIM, zebrafish, neural plate, rostral hindbrain, telencephalon, optic primordia, optic vesicle, otic vesicle, olfactory bulb, retinal pigment epithelium, somite, pharyngeal arch, endocardium, zebrafish LG5, *acerebellar*, *spiel ohne grenzen*, Fgf8, Pou2.

## Materials and Methods

See figure legends.

## Results and Discussion

We previously reported cloning of several genes expressed caudally in the zebrafish gastrula (Sagerström et al., 2001). One of these is 76% identical to human and mouse *LMO4*, encoding a 167 amino acid protein with two LIM domains (Grutz et al., 1998; Kenny et al., 1998; Racevskis et al., 1999; Tse et al., 1999). LIM domains, found in functionally diverse proteins, contain tandem non-DNA binding zinc fingers (Dawid et al., 1998). LMO proteins are unique in that they lack other functional domains, and LMO proteins promote formation of multimeric transcription regulatory complexes by bridging factors such as bHLH and GATA proteins (Rabbitts, 1998). LMO proteins also function antagonistically toward LIM-Homeodomain (Lhx) proteins by competing for binding to the essential co-factor Ldb/NLI (Rabbitts, 1998). A single Drosophila LMO gene (dLMO) (Milan and Cohen, 1999; Shoresh et al., 1998; Zeng et al., 1998; Zhu et al., 1995) and four mammalian genes, LMO 1-4, have been identified (Rabbitts, 1998). Human LMO2 (Rabbitts et al., 1999) and LMO4 (Sum et al., 2002, Visvader et al., 2001) loci are targets of chromosomal translocations associated with leukemias and breast cancer, suggesting that LMO genes are also oncogenes.

We mapped zebrafish *lmo4* (AY028903) to an interval between 48.9 and 50.1 cM from the top of linkage group 5 (LG5; not shown) using a zebrafish radiation hybrid panel (Geisler et al., 1999). Several zebrafish genes located on LG5 have orthologs on Human chromosome 1 (Woods et al., 2000), where human *LMO4* resides. Sequence alignment and phylogenetic analysis (Fig. 1) support the conclusion that zebrafish *lmo4* is orthologous to human *LMO4*.

We performed a detailed analysis of zebrafish *lmo4* expression during gastrula and segmentation stages. Maternal *lmo4* mRNA is observed (Fig. 2A) but becomes undetectable by late blastula stage (Fig. 2B). During gastrulation, zygotic transcripts appear above the germ ring at shield stage (6 hpf, Fig. 2C) and become distributed broadly in the dorsal ectoderm and forerunner cells by 75% epiboly (8 hpf, Fig. 2D). By bud stage (10 hpf, Fig.2 E, F, G, J) expression is restricted to the rostral domain. Triple *in situ* hybridization with probes against *pax2.1* and *krox20* (wide and narrow red stripes, respectively in Fig. 2 F) show that bud stage *lmo4* expression is in the presumptive rostral hindbrain.

Mesendodermal expression is present during gastrula stages but more apparent as ectodermal expression decreases by the bud and early somite stage (Fig. 2 G, H arrowhead). Presomitic mesoderm and tail bud expression is observed later (Fig. 2K, S, 6-somite stage and T, 14-somite stage). Rostral somite expression is restricted to anterior epithelium and the mesenchymal core (Fig. 2U, 14-somite stage). Expression in deep cells underlying the hindbrain is visible at the 6-somite stage (arrow in Fig. 2K).

Decreased expression in the rostral hindbrain by the 3-somite stage is visible in lateral views of whole mount embryos (Fig. 2 H) though mesodermal expression in this region of the embryo is still visible. Dynamic expression in the anterior neuroepithelium begins around the 3-somite stage (Fig. 2H,I) at the anterior edge of the neural plate in the presumptive telencephalon, and persists in the dorsoanterior neural keel at the 6-somite stage (Fig. 2K, L). By the 10-somite stage (Fig. 2M), expression is visible through much of the optic vesicles and telencephalon. By the 14- and 18-somite stages (Fig. 2N,O),

optic vesicle expression is strongest in the medial areas that will form the optic stalk and retinal pigment epithelium. Expression at the 21-somite stage is restricted to the optic stalk (Fig. 2 P, Q) and the pigmented epithelium (Fig. 2R).

Expression is seen in the otic vesicle (Fig. 2V) and presumptive branchial arch region (Fig. 2W) at the 21-somite stage, as well as in the anterior sensory ganglia (Fig. 2X).

We next examined expression between the prim-5 (24 hpf) and high pec stage (48 hpf). Cardiovascular expression is observed at the prim-5 stage in the endocardium along the anteroposterior extent of the tube (Fig. 3A) and in the midline vasculature (Fig. 3B). Expression in the pharyngeal arch mesenchyme, heart and fin buds is observed at 36 hpf (Fig. 3C, D).

Telencephalic expression is a persistent aspect of *lmo4* expression. This becomes restricted to the olfactory bulb by the 21-somite stage (Fig. 2 P) and remains at least through 48 hpf (Fig. 3E). Expression in the presumptive hindbrain decreases significantly by early somitogenesis, however expression in a subset of rostral hindbrain cells is observed at 48 hpf (Fig. 3F).

While similarities in the expression zebrafish *lmo4* and that of its murine ortholog are observed (Hermanson et al., 1999; Kenny et al., 1998; Sugihara et al., 1998), we note additional aspects. In particular, expression in the rostral hindbrain during gastrula stages, which has not been described in mouse, suggests regulation by genes involved in midbrain-hindbrain boundary (MHB) formation. We examined expression in embryos mutant at the *acerebellar* (*ace*), *spiel ohne grenzen* (*spg*) and *no ishtmus* (*noi*) loci, which

encode *fgf8* (Reifers et al., 1998), *pou2* (Burgess et al., 2002; Hauptmann et al., 2002; Reim and Brand, 2002) and *pax2.1* (Brand et al., 1996), respectively. We observed normal expression of *lmo4* in embryos from *noi/pax2.1* heterozygotes at all stages and no differences in *lmo4* expression were detected prior to bud stage in embryos homozygous for *ace/fgf8* or *spg/pou2*. *spg* embryos, distinguishable by reduced *noi/pax2.1* expression, show reduced *lmo4* expression. (Fig. 4A-D, asterisks indicate *noi/pax2.1* expression, brackets in Fig. 4A, B indicate metencephalic *lmo4* expression). *ace* mutant embryos showed similarly reduced *lmo4* expression (Fig. 4E-H). Histological sections (Fig. 4 G, H) and higher magnification view (Fig. 4C, D; focal plane in the ectoderm) did not allow assignment of residual staining to a germ layer, but showed greatly reduced expression throughout.

Fgf8 signaling, detected by activation of the ERK-MAPK (Curran and Grainger, 2000; Umbhauer et al., 1995), is disrupted in the rostral hindbrain in *ace* embryos (Fig. 4I.J), *lmo4* expression may be induced by Fgf. Indeed, implantation of an bFgf-soaked Affigel bead led to ectopic *lmo4* expression (Fig. 4K, L).

## Acknowledgments

Mutant strains were kindly provided by Alex Schier, Didier Stainer, and the Tübingen stock center. We wish to thank Tatjana Piotrowski and Emily Walsh for helpful comments on the expression pattern, and Damian Dalle Nogare for assistance with sequence alignment. We thank the reviewers for helpful comments on the manuscript. Laboratory support form Hazel Sive during the initial phase of this work is acknowledged. This work was supported by NIH grant HD39156 to CGS, and MEL was supported by a Burroughs-Wellcome Postdoctoral Fellowship administered by the Life Science Research Foundation.

## References

Brand, M., Heisenberg, C. P., Jiang, Y. J., Beuchle, D., Lun, K., Furutani-Seiki, M., Granato, M., Haffter, P., Hammerschmidt, M., Kane, D. A., *et al.* (1996). Mutations in zebrafish genes affecting the formation of the boundary between midbrain and hindbrain, Development *123*, 179-90.

Burgess, S., Reim, G., Chen, W., Hopkins, N., and Brand, M. (2002). The zebrafish spiel-ohne-grenzen (spg) gene encodes the POU domain protein Pou2 related to mammalian Oct4 and is essential for formation of the midbrain and hindbrain, and for pre-gastrula morphogenesis., Development *129*, 905-16.

Curran, K. L., and Grainger, R. M. (2000). Expression of activated MAP kinase in Xenopus laevis embryos: evaluating the roles of FGF and other signaling pathways in early induction and patterning., Dev Biol *228*, 41-56.

Dawid, I. B., Breen, J. J., and Toyama, R. (1998). LIM domains: multiple roles as adapters and functional modifiers in protein interactions, Trends in Genetics *14*, 156-162.

Geisler, R., Rauch, G. J., Baier, H., van Bebber, F., Brobeta, L., Dekens, M. P., Finger, K., Fricke, C., Gates, M. A., Geiger, H., *et al.* (1999). A radiation hybrid map of the zebrafish genome, Nat Genet *23*, 86-9.

Grutz, G., Forster, A., and Rabbitts, T. H. (1998). Identification of the LMO4 gene encoding an interaction partner of the LIM-binding protein LDB1/NLI1: a candidate for displacement by LMO proteins in T cell acute leukaemia. Oncogene *17*, 2799-803.

Hermanson, O., Sugihara, T. M., and Andersen, B. (1999). Expression of LMO-4 in the central nervous system of the embryonic and adult mouse, Cell Mol Biol (Noisy-le-grand) *45*, 677-86.

Hauptmann, G., Soll, I., and Gerster, T. (2002). The early embryonic zebrafish forebrain is subdivided into molecularly distinct transverse and longitudinal domains, Brain Res Bull *57*, 371-5.

Kenny, D. A., Jurata, L. W., Saga, Y., and Gill, G. N. (1998). Identification and characterization of LMO4, an LMO gene with a novel pattern of expression during embryogenesis., Proc Natl Acad Sci U S A *95*, 11257-62.

Milan, M., and Cohen, S. M. (1999). Regulation of LIM homeodomain activity in vivo: a tetramer of dLDB and apterous confers activity and capacity for regulation by dLMO, Mol Cell Biol *4*, 267-273.

Rabbitts, T. H. (1998). LMO T-cell translocation oncogenes typify genes activated by chromosomal translocations that alter transcription and developmental processes, Genes Dev *12*, 2651-7.

Rabbitts, T. H., Bucher, K., Chung, G., Grutz, G., Warren, A., and Yamada, Y. (1999). The effect of chromosomal translocations in acute leukemias: the LMO2 paradigm in transcription and development, Cancer Res *59*, 1794s-1798s.

Racevskis, J., Dill, A., Sparano, J. A., and Ruan, H. (1999). Molecular cloning of LMO41, a new human LIM domain gene., Biochim Biophys Acta *1445*, 148-53.

Reifers, F., Bohli, H., Walsh, E. C., Crossley, P. H., Stainier, D. Y., and Brand, M. (1998). Fgf8 is mutated in zebrafish acerebellar (ace) mutants and is required for maintenance of midbrain-hindbrain boundary development and somitogenesis, Development *125*, 2381-95.

Reim, G., and Brand, M. (2002). Spiel-ohne-grenzen/pou2 mediates regional competence to respond to Fgf8 during zebrafish early neural development, Development *129*, 917-33.

Sagerström, C. G., Grinbalt, Y., Sive, H. (1996). Anteroposterior patterning in the zebrafish, Danio rerio: an explant assay reveals inductive and suppressive cell interactions, Development *122*, 1873-1883.

Sagerström, C. G., Kao, B. A., Lane, M. E., and Sive, H. L. (2001). Isolation and characterization of posteriorly restricted genes in the zebrafish gastrula, Developmental Dymanics *220*, 402-408.

Schulte-Merker, S., Ho, R. K., Herrmann, B. G., and Nusslein-Volhard, C. (1992). The protein product of the zebrafish homologue of the mouse T gene is expressed in nuclei of the germ ring and the notochord of the early embryo, Development *116*, 1021-32.

Shoresh, M., Orgad, S., Shmueli, O., Werczberger, R., Gelbaum, D., Abiri, S., and Segal, D. (1998). Overexpression Beadex mutations and loss-of-function heldup-a mutations in Drosophila affect the 3' regulatory and coding components, respectively, of the Dlmo gene, Genetics *150*, 283-99.

Sugihara, T. M., Bach, I., Kioussi, C., Rosenfeld, M. G., and Andersen, B. (1998). Mouse deformed epidermal autoregulatory factor 1 recruits a LIM domain factor, LMO-4, and CLIM coregulators, Proc Natl Acad Sci U S A *95*, 15418-23.

Sum, E. Y., Peng, B., Yu, X., Chen, J., Byrne, J., Lindeman, G. J., and Visvader, J. E. (2002). The LIM domain protein LMO4 interacts with the cofactor CtIP and the tumor suppressor BRCA1 and inhibits BRCA1 activity, J Biol Chem *277*, 7849-56.

Tse, E., Grutz, G., Garner, A. A., Ramsey, Y., Carter, N. P., Copeland, N., Gilbert, D. J., Jenkins, N. A., Agulnick, A., Forster, A., and Rabbitts, T. H. (1999). Characterization of the Lmo4 gene encoding a LIM-only protein: genomic organization and comparative chromosomal mapping, Mamm Genome *10*, 1089-94.

Umbhauer, M., Marshall, C. J., Mason, C. S., Old, R. W., and Smith, J. C. (1995). Mesoderm induction in Xenopus caused by activation of MAP kinase., Nature *376*, 58-62.

Visvader, J. E., Venter, D., Hahm, K., Santamaria, M., Sum, E. Y., O'Reilly, L., White, D., Williams, R., Armes, J., and Lindeman, G. J. (2001). The LIM domain gene LMO4 inhibits differentiation of mammary epithelial cells in vitro and is overexpressed in breast cancer, Proc Natl Acad Sci U S A *98*, 14452-7.

Woods, I. G., Kelly, P. D., Chu, F., Ngo-Hazelett, P., Yan, Y. L., Huang, H., Postlethwait, J. H., and Talbot, W. S. (2000). A comparative map of the zebrafish genome, Genome Res *10*, 1903-14.

Zeng, C., Justice, N. J., Abdelilah, S., Chan, Y. M., Jan, L. Y., and Jan, Y. N. (1998). The Drosophila LIM-only gene, dLMO, is mutated in Beadex alleles and might represent an evolutionarily conserved function in appendage development, Proc Natl Acad Sci U S A *95*, 10637-42.

Zhu, T. H., Bodem, J., Keppel, E., Paro, R., and Royer-Pokora, B. (1995). A single ancestral gene of the human LIM domain oncogene family LMO in Drosophila: characterization of the Drosophila Dlmo gene, Oncogene *11*, 1283-90.

**Figure 1. A.** Alignment of the amino acid sequence of zebrafish (Dr.) lmo4 with several members of the mouse (Mm.), human (Hs.), and zebrafish LMO family. Alignment was made using Clustal X version 1.8. HsDAT-1 is the protein in the database that gives to closest match to Mm LMO3 as published by Grutz, et al., (1998). Majority residues are shaded black. **B.** Phylogenetic analysis of LMO family members from zebrafish, mouse, human. The sequences were aligned as in A. The phylogenetic tree was constructed with Phylip 4.0, using a Jones-Taylor-Thronton Matrix and neighbor joining tree with Bootstrap values of 500. The accession numbers are: Mm LMO 1:NM057173.1, Mm LMO2: NM008505.1, Mm LMO4: NM010723.1, Hs LMO1: AJ277662.1, Hs LMO2: NM005574.2, Hs DAT: NP061110, HsLMO4: NM006769.2, Dr LMO1: AF398514.1, Dr LMO2: NM131111.1, Dr. LMO4: AY028903.

**Figure 1**

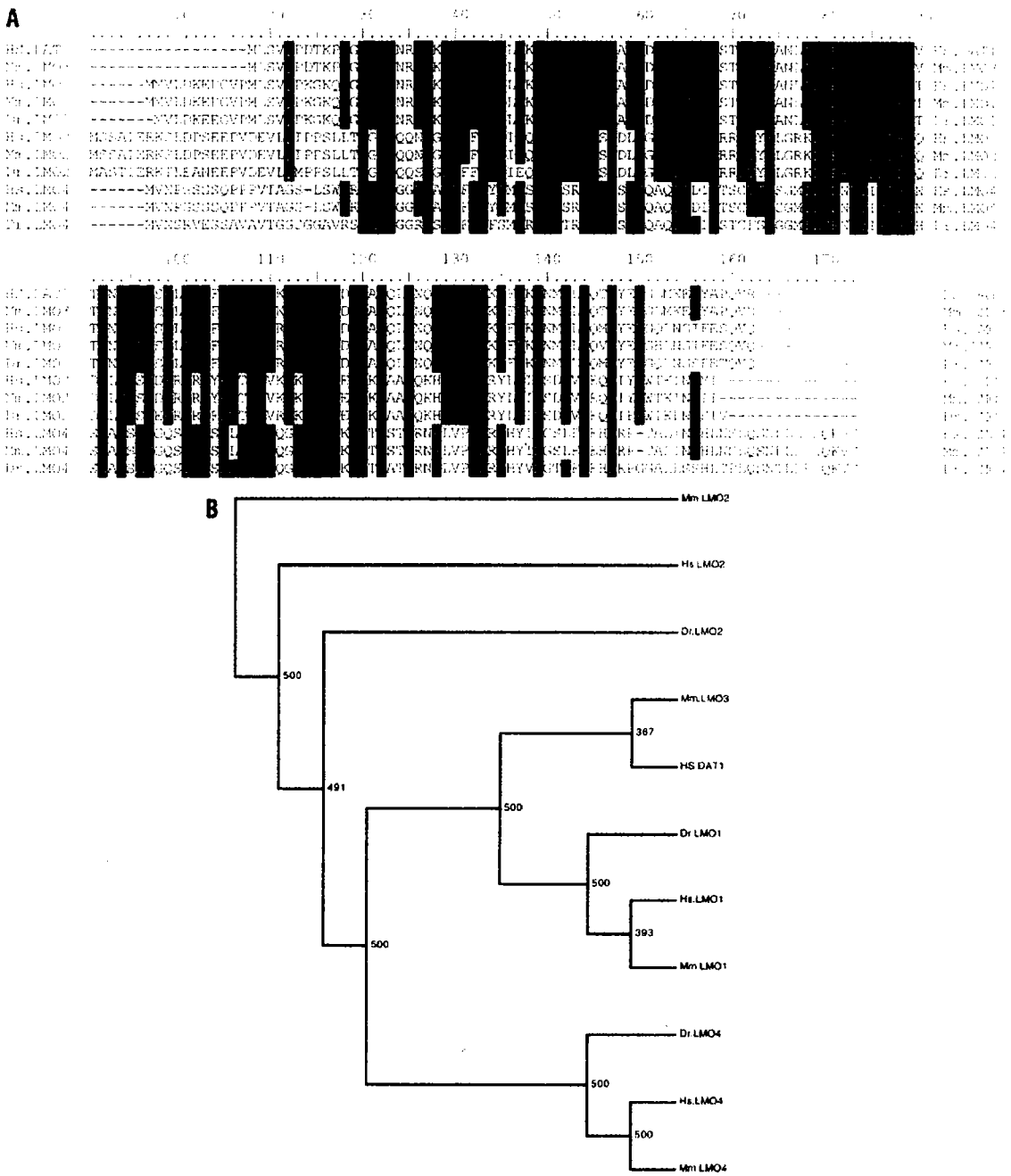
A
B
Mm LMO2
Hs LMO2
Dr LMO2
500
Mm LMO3
387
HS DAT1
491
500
Dr LMO1
500
Hs LMO1
393
Mm LMO1
500
Dr LMO4
500
Hs LMO4
500
Mm LMO4

**Figure 2. Expression of *lmo4* through the 24-somite stage.**

Whole mount in situ hybridization with an *lmo4* probe was performed as reported (Sagerström et al., 1996). **A-B**; Cleavage stages. Maternal *lmo4* expression is visible at the 2-cell stage (**A**), but is not detectable by late blastula stage (**B**). **C-G**; Gastrula stages. (**C**) Lateral view of a shield stage (6 hpf) close-up showing lmo4 expression is excluded from the margin of the shield (arrow) above the forerunner cells (arrowhead). Dorsal views of (**D**) 75% epiboly (8 hpf), (**E**) Bud stage (10 hpf), (**F**) double in situ hybridization showing *lmo4* expression in blue and *pax2.1* (upper stripe) and the rostral stripe (presumptive R3) of *krox 20* in red, in a bud stage embryo. (**G**) Lateral view of bud stage (10 hpf) embryos demonstrate that zygotic *lmo4* is restricted to the rostralmost portion of this domain by the end of gastrulation. Arrow in **G** points to mesendodermal staining. **H-I.** 3-somite stage. (**H**) Lateral view showing decreasing expression in the ectoderm at the 3-somite stage (11 hpf), expression in the somitic mesoderm (arrowhead) and low expression in the presomitic mesoderm. (**I**) Animal pole view of the embryo in (**H**), showing expression in the anterior neural plate. **J** and **J'.** Optical section through the rostral hindbrain area of a bud stage embryo and a 6-somite stage embryo, showing expression in the neural plate (np) at bud but not 6-somite stage. **K-L**; 6-somite stage. (**K**) Neural plate expression is restricted to the anterior. Mesodermal expression persists in the somites and head mesoderm (arrow) and expression in presomitic mesoderm becomes detectable. (**L**) Animal pole view of embryo in (**K**). **M-R**; Expression in the optic primordia from the 10-somite to the 21-somite stage. (**M**). 10-somite stage, expression in the telencephalon (t) and much of the optic primordia. (**N**) Expression at

the 14-somite stage is resolved to the presumptive stalk and pigmented epithelium (rpe, arrowhead). **(O)** Expression at the 18-somite stage in the optic stalk and rpe (arrowhead). **(P)** Dorsal, **(Q)** ventral and **(R)** lateral view of the optic primordia of 21-somite stage embryos. Arrowhead in R points to retinal pigment cell. **S-U**; Expression in somitic, presomitic and tail mesoderm. **(S)** Dorsal view of the tailbud presomitic mesoderm at the 6-somite stage (see also J). **(T)** Lateral view of tail mesoderm at the 14-somite stage. **(U)**. Expression in rostral somites at the 14-somite stage. **V-X**; 21-somite stage. **(V)** Dorsal view showing expression in the otic vesicle. **(W)** Same embryo as in **(V)** in a ventral focal plane, showing expression in the pharyngeal arch mesenchyme ventral to the otic vesicle. **(X)** Lateral view showing expression in the anterior sensory ganglia.

A
2-cell
B
sphere
C
shield
D
75% epiboly
E
bud
F
bud
G
bud
H
3-somite
I
J
bud
J'
3-somite
K
6-somite
L
6-somite
M
10-somite
N
14-somite
O
18-somite
P
21-somite
Q
os
R
21-somite
S
6-somite
T
14-somite
U
14-somite
V
21-somite
W
21-somite
X
21-somite

Figure 2

**Figure 3. Expression during pharyngula stages (24-48 hpf).**

**A, B**; Prim-5 stage (24 hpf). (**A**) Ventral view of the heart primordium with rostral toward the top, showing expression in the endocardium (ec). (**B**) Lateral view of trunk region (rostral to the left) showing expression in midline vasculature (arrowhead). Expression is also detectable in the ventral mesoderm (vm). **C, D**; Prim-25 stage (36 hpf). (**C**) Expression in the telencephalon (t), pharyngeal arch mesenchyme (arrowheads in **C**, **D**), and proximal fin buds (arrow in **C**). (**D**) Higher magnification ventral view of the larva in (**C**), showing expression in the pharyngeal arches (p1 and p2 and arrowhead). **E,F**; Expression in the neuroepithelium at 48 hpf. (**E**) Dorsal view with rostral toward the top, showing expression in the olfactory bulb adjacent to the nasal pits (np). (**F**) Lateral view showing expression in the rostral hindbrain, adjacent to the cerebellum (c). Abbreviations floor plate (fp), heart (h), myocardium (mc), otic vesicle (ov), notochord (n), spinal cord (sc).

Figure 3

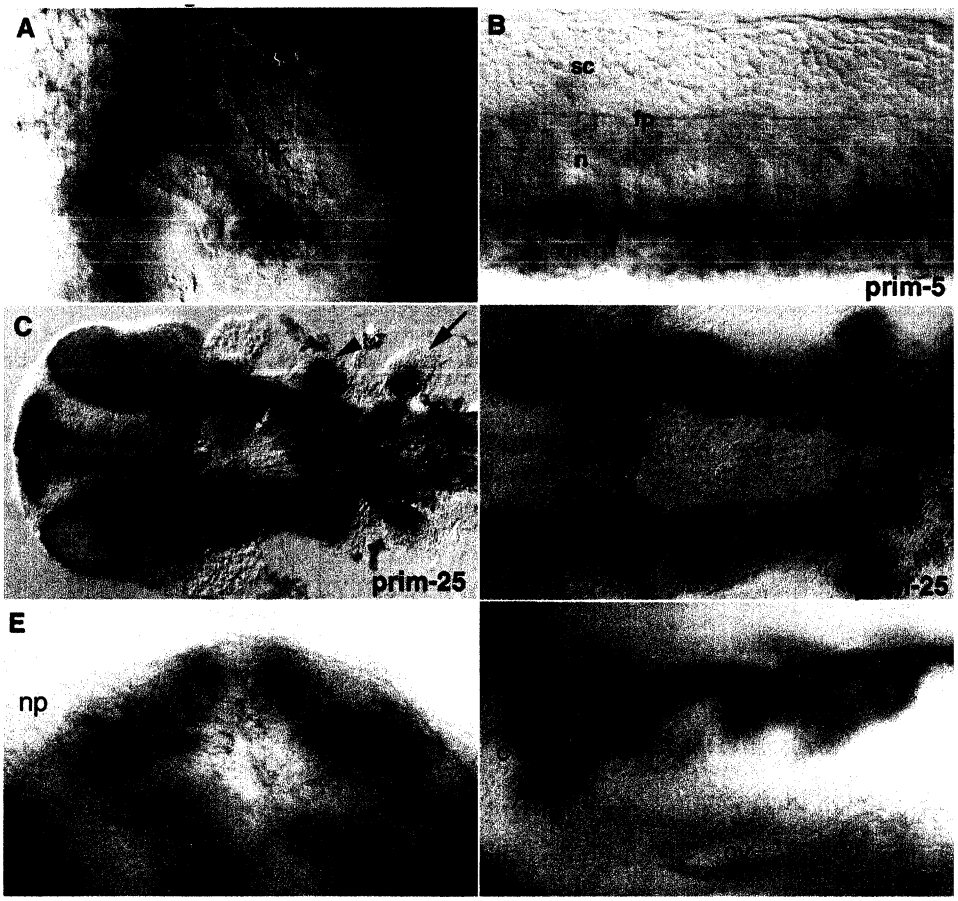

**Figure 4. Lmo4 expression in *spg/pou2* and *ace/fgf8* mutant embryos and in response to soluble Fgf.**

Embryos of various genotypes (as shown in top right corner of each panel) were analyzed with various probes (as indicated in lower right corner of each panel). In situ hybridization and immunostaining was done as reported (Sagerström et al., 2001; Schulte-Merker et al., 1992). **A, C, E, G, I, K** are wild type embryos, **B, D** are *spg* mutant embryos and **F, H, J** are *ace* mutant embryos. **K** and **L** are wild type embryos into which an Affi-Gel bead soaked in MBS (**K**) or 0.5mg/ml Fgf (**L**) was implanted at shield stage (6 hpf). **A-D** were hybridized to *noi/pax2.1* (indicated by asterisks) and *lmo4* probes (brackets in A,B). **C** and **D** are focused in the plane of the ectoderm. **E –H**, and **K-L** were hybridized to a *lmo4* probe and **I** and **J** were stained with the dP-ERK antibody (Sigma Cat. # M8159) at a dilution of 1:1000. All whole-mount embryos are dorsal views with anterior to the top. Transverse10m sections in **G** and **H** are cut through the presumptive rostral hindbrain area that shows maximal *lmo4* expression in wild type bud stage embryos. Dorsal is at the top. All embryos are at bud stage (10 hpf) except **C** and **D**, which are at the 2-somite stage.

Figure 4

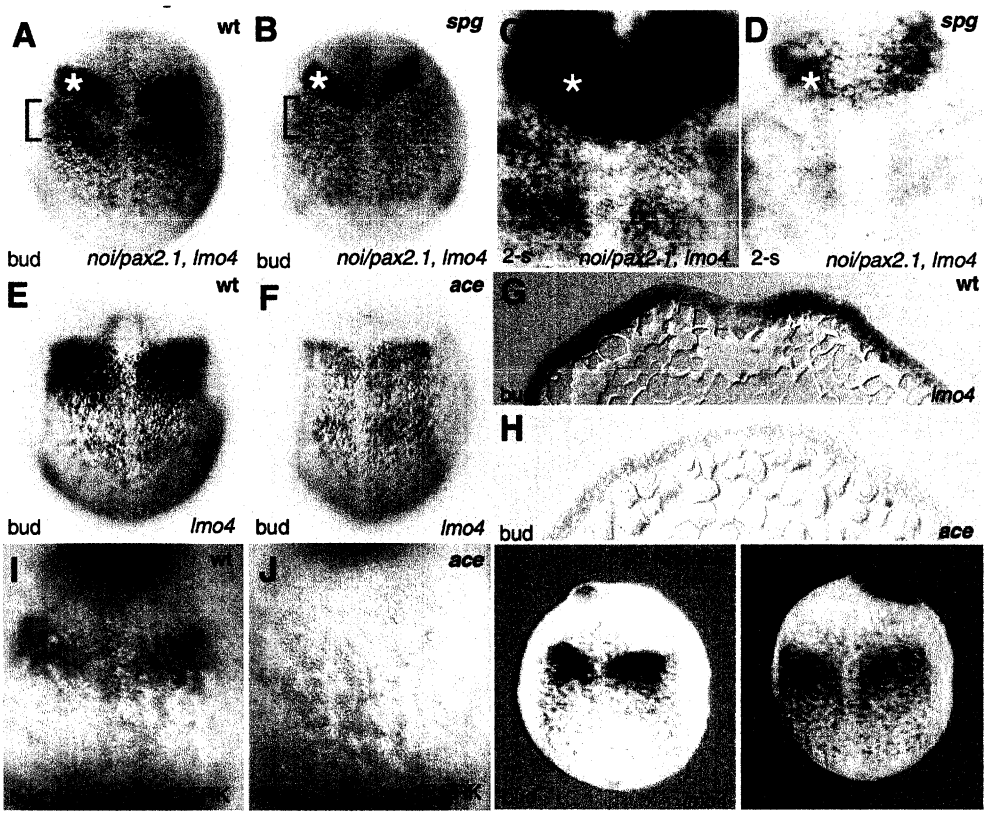
A
wt
bud
noi/pax2.1, lmo4
B
spg
bud
noi/pax2.1, lmo4
C
2-s
noi/pax2.1, lmo4
D
spg
2-s
noi/pax2.1, lmo4
E
wt
bud
lmo4
F
ace
bud
lmo4
G
wt
lmo4
H
bud
ace
I
wt
J
ace